1-1-2013

Molecular Mechanisms of Alternative Splicing Regulation: An Investigation of the Spliceosome Repressed by Hnrnp L on Cd45 Exon 4

Ni-Ting Chiou
University of Pennsylvania, nchiou0228@gmail.com

Molecular Mechanisms of Alternative Splicing Regulation: An Investigation of the Spliceosome Repressed by Hnrnp L on Cd45 Exon 4

Abstract

Alternative splicing is a key step in gene regulation and involves the differential selection of splice sites to generate different pre-mRNA transcripts. It has been shown that 90-95% of pre-mRNAs are alternatively spliced in human cells. Pre-mRNA splicing is catalyzed the spliceosome, which consists mainly of the U1, U2, U4, U5 and U6 snRNP, and about a hundred of non-snRNP proteins. Splicing regulators that bind to enhancer or silencer elements on the pre-mRNA can alter assembly of these spliceosome components. Understanding how splicing regulators control spliceosome assembly will bring insights to the prediction of splice site choices. In our lab, we used CD45 as a model gene for studying alternative splicing and spliceosome assembly. The exonic silencer sequence (ESS1) within CD45 exon 4 is bound by hnRNP L to induce its skipping. HnRNP L represses spliceosome assembly at a step after the binding of U1 and U2 snRNP on either side of the exon. My goal is to understand how hnRNP L perturbs U1 snRNP binding at the 5' splice site (5' ss) to cause the skipping of CD45 exon 4.

Using psoralen- and UV-crosslinking analysis, U1 snRNP and other protein components that associate with the sequences around the 5' ss within the hnRNP L-repressed spliceosome complexes were compared with the control complexes. These studies revealed that hnRNP L recruits hnRNP A1 to the 3' end of exon 4 to induce an extended pairing interaction between the U1 snRNA and the 5' ss. Splicing assays in vitro and in cells further demonstrated that hnRNP A1 and the U1 snRNA binding at the 3'end of exon 4 are required for hnRNP L-mediated skipping of exon 4. Further analysis of other exons repressed by hnRNP L or A1 suggests the potential for the extended U1 pairing interactions with these exons. These data imply that induction of U1 interactions with the exonic region nearby a 5' ss could be a widespread mechanism in inducing the skipping of exon. To further determine how the extended U1 binding affects the subsequent spliceosome assembly steps, hnRNP L-repressed spliceosome complexes were purified. This analysis revealed that association of U6 snRNP with the 5'ss, and recruitment of NTC components, are blocked in the hnRNP L-repressed complexes. Moreover, enhancing binding of U6 to the 5'ss overcomes the effect of the extended U1 interaction, thereby increasing the splicing of the hnRNP L-repressed substrate. These results provide the first example showing that the U1/U6 switch, a structural rearrangement during the catalytic activation of the spliceosome, is a naturally occurring point for regulating alternative splicing. This study also suggests that splicing regulators that alter U1 binding, or spliceosome components that associate with the 5' ss after U1 binding, are important factors for determining the usage of the 5'ss.

Degree Type
Dissertation

Degree Name
Doctor of Philosophy (PhD)

Graduate Group
Biochemistry & Molecular Biophysics

First Advisor
Kristen W. Lynch

Keywords
hnRNP A1, hnRNP L, spliceosome, splicing, U1 snRNP, U6 snRNP

Subject Categories
Biochemistry | Cell Biology | Molecular Biology

MOLECULAR MECHANISMS OF ALTERNATIVE SPLICING REGULATION:

AN INVESTIGATION OF THE SPLICEOSOME REPRESSED BY HNRNP L ON CD45 EXON 4

Ni-Ting Chiou

A DISSERTATION

in

Biochemistry and Molecular Biophysics

Presented to the Faculties of the University of Pennsylvania

in

Partial Fulfillment of the Requirements for the Degree of Doctor of Philosophy

2013

Supervisor of Dissertation

Signature_____

Kristen W. Lynch, Associate Professor of Biochemistry and Biophysics

Graduate Group Chairperson

Signature_____

Kathryn M. Ferguson, Associate Professor of Physiology

Dissertation Committee

Gregory D. Van Duyne, Professor of Biochemistry and Biophysics

Gideon Dreyfuss, HHMI, Professor of Biochemistry and Biophysics

Zissimos Mourelatos, Associate Professor of Pathology and Laboratory Medicine

Emmanuel Skordalakes, Associate Professor of the Wistar Institute

Sara Cherry, Associate Professor of Microbiology

Charles C. Query, Professor of Cell Biology, Albert Einstein College of Medicine

ACKNOWLEDGEMENTS

ABSTRACT

MOLECULAR MECHANISMS OF ALTERNATIVE SPLICING REGULATION:

AN INVESTIGATION OF THE SPLICEOSOME REPRESSED BY HNRNP L ON CD45 EXON 4

Ni-Ting Chiou

Kristen W. Lynch

Alternative splicing is a key step in gene regulation and involves the differential selection of splice sites to generate different pre-mRNA transcripts. It has been shown that 90-95% of pre-mRNAs are alternatively spliced in human cells. Pre-mRNA splicing is catalyzed the spliceosome, which consists mainly of the U1, U2, U4, U5 and U6 snRNP, and about a hundred of non-snRNP proteins. Splicing regulators that bind to enhancer or silencer elements on the pre-mRNA can alter assembly of these spliceosome components. Understanding how splicing regulators control spliceosome assembly will bring insights to the prediction of splice site choices. In our lab, we used CD45 as a model gene for studying alternative splicing and spliceosome assembly. The exonic silencer sequence (ESS1) within CD45 exon 4 is bound by hnRNP L to induce its skipping. HnRNP L represses spliceosome assembly at a step after the binding of U1 and U2 snRNP on either side of the exon. My goal is to understand how hnRNP L perturbs U1 snRNP binding at the 5' splice site (5' ss) to cause the skipping of CD45 exon 4.

Using psoralen- and UV-crosslinking analysis, U1 snRNP and other protein components that associate with the sequences around the 5' ss within the hnRNP L-repressed spliceosome complexes were compared with the control complexes. These studies revealed that hnRNP L recruits hnRNP A1 to the 3' end of exon 4 to induce an extended pairing interaction between the U1 snRNA and the 5' ss. Splicing assays *in*

vitro and in cells further demonstrated that hnRNP A1 and the U1 snRNA binding at the 3'end of exon 4 are required for hnRNP L-mediated skipping of exon 4. Further analysis of other exons repressed by hnRNP L or A1 suggests the potential for the extended U1 pairing interactions with these exons. These data imply that induction of U1 interactions with the exonic region nearby a 5' ss could be a widespread mechanism in inducing the skipping of exon. To further determine how the extended U1 binding affects the subsequent spliceosome assembly steps, hnRNP L-repressed spliceosome complexes were purified. This analysis revealed that association of U6 snRNP with the 5'ss, and recruitment of NTC components, are blocked in the hnRNP L-repressed complexes. Moreover, enhancing binding of U6 to the 5'ss overcomes the effect of the extended U1 interaction, thereby increasing the splicing of the hnRNP L-repressed substrate. These results provide the first example showing that the U1/U6 switch, a structural rearrangement during the catalytic activation of the spliceosome, is a naturally occurring point for regulating alternative splicing. This study also suggests that splicing regulators that alter U1 binding, or spliceosome components that associate with the 5' ss after U1 binding, are important factors for determining the usage of the 5'ss.

TABLE OF CONTENTS

LIST OF TABLES

Chapter 4

LIST OF FIGURES

Chapter 1

Introduction

In 1980, the first example of the pre-mRNA alternative splicing, the immunoglobin μ heavy chain gene, was discovered. In 2008, with the advances of the RNA sequencing techniques, it was shown that 90-95% of pre-mRNAs are alternatively spliced in the human cells (Pan et al., 2008; Wang et al., 2008). Now, alternative splicing is widely recognized as a critical step in regulating gene expression. As alternative splicing is tightly regulated by a multitude of RNA-binding proteins or RNA-protein complexes, mutations either in the splice sites, or in the splicing regulatory sequences that interfere the assembly of splicing complexes, are responsible for at least 10% of human genetic diseases (Cooper et al., 2009; Wang and Cooper, 2007). Thus, one of the important questions in the current field of RNA biology is how splicing complexes are regulated by splicing regulators to achieve alternative splicing. In this chapter, I provide an overview of alternative splicing, splicing complexes, and the model systems for studying the regulation of alternative splicing.

1.1 Regulation of alternative splicing by cis-regulatory elements

After being transcribed from a gene locus, the pre-mRNA undergoes extensive processing steps to become the mature mRNA. The properly processed mRNAs are then transported into the cytoplasm for translation. Among post-transcriptional processing steps, the three main steps are 5' capping, 3' polyadenylation and RNA splicing. The splicing step involves the removal of introns and ligation of the flanking exons to

generate the coding region of mRNA. In the alternative splicing processes, portions of the transcripts are differentially excluded or included to generate different mRNAs from a single gene (Black, 2003). When the variable region contains an exon, alternative splicing generates mRNAs that encode different protein isoforms (Figure 1.1; cassette exon). Additionally, when alternative splicing occurs within the untranslated regions (UTRs), it generates mRNAs containing different 3' or 5' UTRs, which allows the regulation of mRNA translation by 5'- or 3'-UTR-binding factors (Figure 1.1; alt 3' end and 5' end). Therefore, alternative splicing provides the opportunities for regulation or enrichment of both proteome and transcriptome.
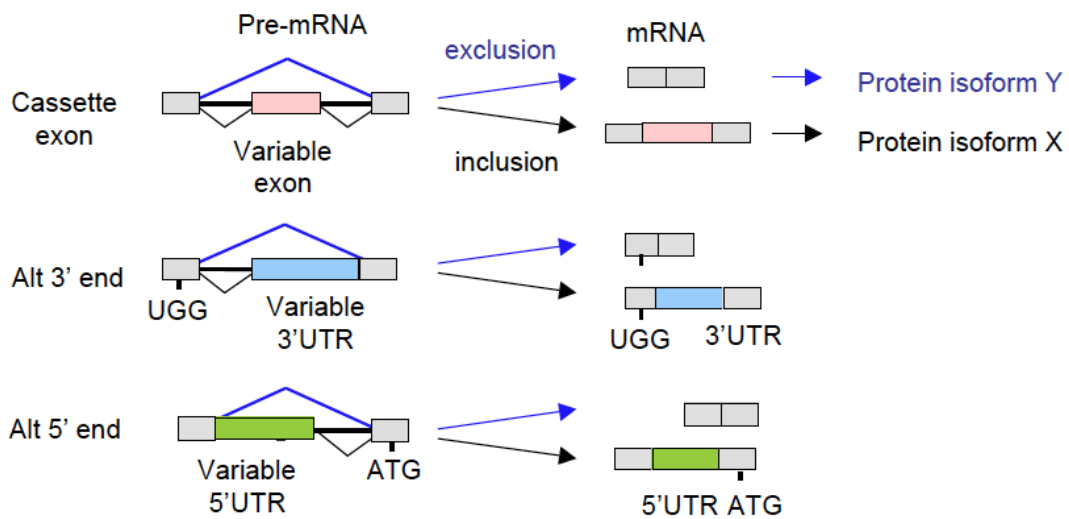
Figure 1.1 The common alternative splicing patterns. In the cassette exon pattern, the variable exon (pink box) is flanked by the constitutive exons (gray box). The alternative 3' end or 5' end splicing regulation results in generating the mRNAs that differentially exclude or include the variable 3' UTR (blue box) or 5' UTR (green box) while keeping the same constitutive UTR (gray box). Here, introns are depicted thick black lines. Blue and black lines indicate the splice sites used in the exclusion and inclusion of the variable regions, respectively.

In general, alternative splicing is regulated by the cis-regulatory elements in the pre-mRNA (Matlin et al., 2005). The exonic or intronic splicing enhancer (ESE or ISE) enhances the inclusion of the variable exon. In contrast, exonic or intronic splicing silencers (ESI or ISI) induce the skipping of the variable exon (Figure 1.2). These cis-regulatory elements are typically associated with splicing regulators to regulate the assembly of the spliceosome on the pre-mRNA to direct the pre-mRNA splicing choice. Most of these splicing regulators are subject to transcriptional or post-transcriptional regulation in response to different signal-transduction pathways (Martinez et al., 2012). In response to T-cell receptor signaling, GSK3 has been shown to phosphorylate the splicing regulator PSF to induce the skipping of CD45 exons (Heyd and Lynch, 2010). Additionally, in cancer cells, elevated production or phosphorylation status change has been observed in several splicing regulators, which contributes to alternative splicing of proto-oncogenes (David and Manley, 2010).
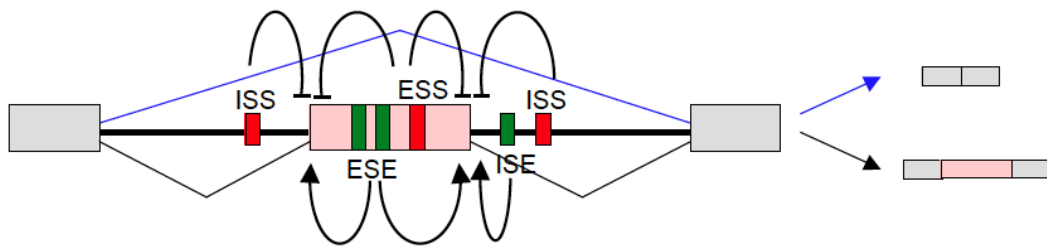
Figure 1.2 Cis-regulatory elements within the exonic and intronic regions that regulate alternative splicing. ISS and ESS (red boxes) repress the inclusion of the variable exon. In contrast, ESE and ISE (green boxes) enhance the inclusion of the variable exon. Other schematic depiction is the same as in Figure 1.1. Adapted in part from (Matlin et al., 2005).

1.2 Pre-mRNA splicing is catalyzed by the spliceosome

The pre-mRNA splicing reactions involve three reactive regions in the pre-mRNA, including the 5' splice site (5' ss), 3' splice site (3' ss) and branch point site (BPS) (Figure 1.3A). These reactive regions are all defined by short consensus sequences. In addition to these three regions, metazoan introns contain a conserved polypyrimidine tract (PPT) between the BPS and 3' ss.

The catalytic spliceosome is mainly consisted of U2, U5, and U6 small nuclear ribonucleoprotein (snRNP). Each U snRNP contain its unique snRNA and 10-20 proteins (van der Feltz et al., 2012). The catalytic spliceosome interacts and brings the splice sites together to allow the two transesterification catalytic steps to occur (Figure 1.3B). In the first catalytic step, the 5'ss is cleaved with concurrent formation of a covalent bond between the first nucleotide of the intron and an A residue at the BPS. In the following step, the catalytic spliceosome excises the lariat intron and joins the 5' and 3' exons to generate mature mRNA (Figure 1.3B, lariat intron and mRNA).

A

Pre-mRNA

AG/GURAGU
5'SS

YNYCRAY (Py)n YAG/GU
BPS   PPT   3'SS

B

Catalytc spliceosome

Catalytic step I

NTC
G
U5
U6
U2

Catalytic step II

G

mRNA

Lariat intron
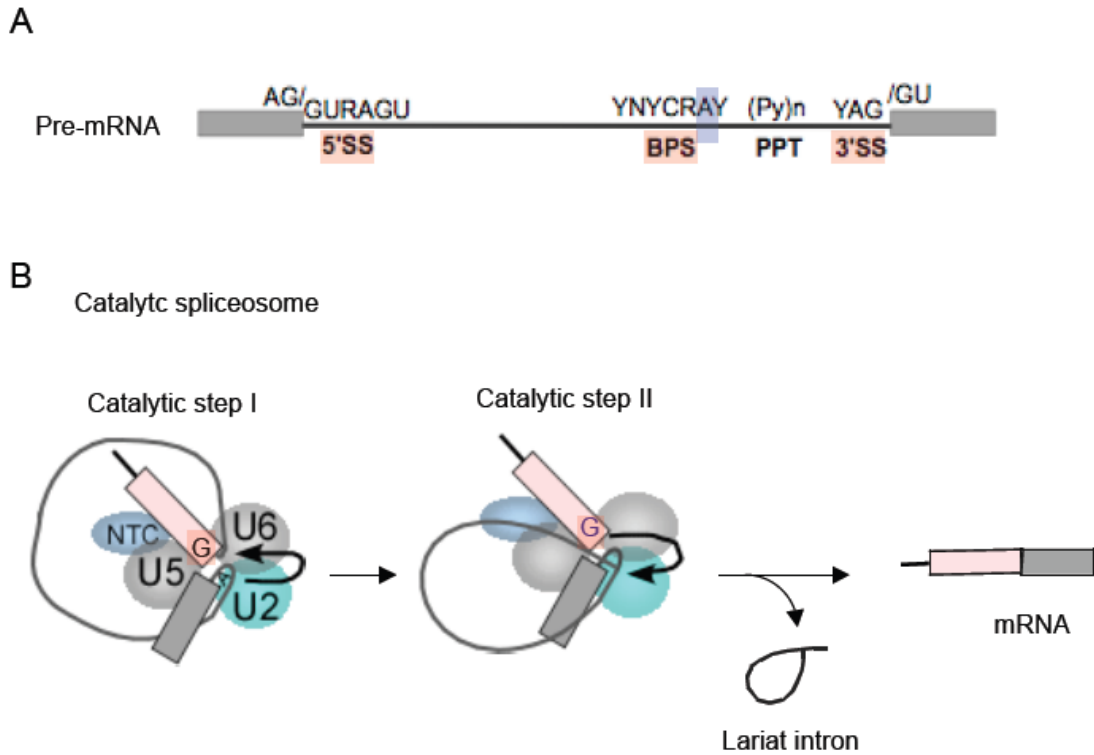
Figure 1.3 Catalysis of pre-mRNA splicing in the spliceosome. (A) The consensus sequences that define exon/intron boundaries. Consensus nucleotides are indicated above the line (Y=U or C; R=G or A), and the term for sequence is shown below. SS, splice site; PPT, polypyrimidine tract; BPS, branch point site. (B) Schematic of the two transesterification steps that occur in the catalytic spliceosome. For simplicity, only U2, U5, U6 snRNP and nineteen complex (NTC) are shown in the catalytic spliceosome. The first arrow shows the direction of the nucleolytic attack at the G nucleotide at 5'ss by the A nucleotide at BPS. The second arrow depicts that the end of the upstream exon attacks the G nucleotide at the 3'ss.

1.3 Spliceosome assembly pathways

1.3.1 Canonical intron-defined spliceosome assembly pathway

The spliceosome, the largest RNP machine in the nucleus, recognizes and positions the reactive regions in the pre-mRNA to catalyze splicing. To assemble the catalytic form of the spliceosome on the pre-mRNA, it involves five snRNPs: U1, U2, U4, U5 and U6 snRNP and additional non-snRNP associated proteins to assemble on the pre-mRNA substrate in a stepwise way. The stepwise assembly of snRNPs on the pre-mRNA forms the pre-spliceosomal E, A, B and finally, catalytic-spliceosomal C complex (Figure 1.4) (Wahl et al., 2009).

To begin the assembly of the spliceosome, U1 snRNP engages with the 5' splice site, while SF1 binds to the BPS, in an ATP-independent manner to form the pre-spliceosomal E complex (Figure 1.4; E). In metazoan systems, the 65 and 35 subunits of the U2AF protein heterodimer also bind to the PPT and 3'ss respectively during this ATP-independent step to further promote correct identification of the 3' end of the intron. In the presence of ATP, several rearrangements of the snRNPs then occur, to progress assembly from the E to A, B and C complex. The first rearrangement is that U2 snRNP displaces SF1 from the BPS to form the A complex (Figure 1.4; A). At this point, the pre-assembled U4/U6.U5 tri-snRNP and nineteen complex (NTC) are recruited to form the B complex (Figure 1.4; B). The releasing of U1 and U4 snRNP from the B complex results in the formation of the B^{act} complex (Figure 1.4; Bact) (Bessonov et al., 2010). Subsequent to the B^{act} complex formation, Prp2, a RNA helicase, triggers the formation of the covalent bond between the 5' end of the intron and the A residue, which generates the C complex (Warkocki et al., 2009) (Figure 1.4; C). In the C complex, the subsequent

second catalytic step occurs to remove the lariat-intron and ligate the flanking exons (Figure 1.3B).

During the stepwise assembly processes, multiple combinatorial interactions are generated between the spliceosomal components and the reactive regions of the substrate. Although these reactive regions have very limited conservation (see Figure 1.3A), the multiple interactions provide the spliceosome an opportunity to "check and recheck" the fidelity of interactions, thereby increasing the accuracy of site selection (Staley and Guthrie, 1998). Moreover, the transitions among these spliceosomal interactions also provide a multitude of potential points for regulating alternative splicing.
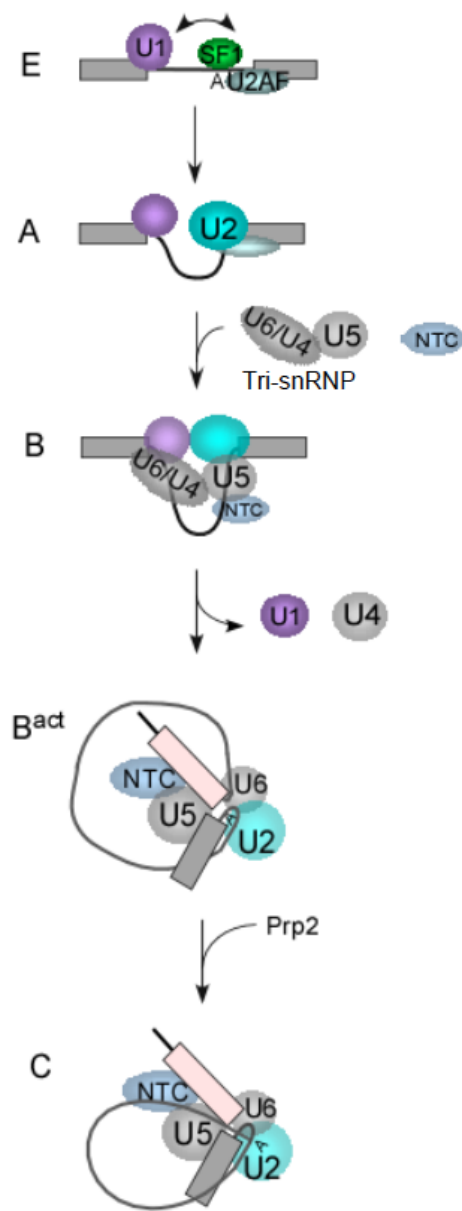
Figure 1.4. Spliceosome assembly pathway. The E complex mainly involves binding of the U1 snRNP, SF1 and U2AF at the 5' and 3' ss, respectively. U2 snRNP is then recruited to the 3'ss to form the A complex. The U1 and U2 snRNP in the A complex recruit the tri-snRNP to form the B complex. The releasing U1 and U4 snRNP from the B complex generates the B^{act} complex. Prp2 triggers the first catalytic step to occur in the B^{act} complex to generate the C complex.

1.3.2 Exon-defined spliceosome assembly pathway

The combinatorial interactions described above are built across the introns. However, the average lengths for exons and introns of human protein-coding genes are, respectively, 145 and 3364 nucleotides (Consortium, 2004). Since the exons are significantly shorter than introns, it is expected that initially identifying exons during the spliceosome assembly would help the splicing components to be deposited across the introns more precisely, and hence avoid the use of the cryptic splice sites. Thus, it is envisioned that the cross-exon interactions of the snRNPs occur first or simultaneously with the cross-intron interactions in each stage of the assembly (Figure 1.5, right column). Indeed, the U1 and U2 snRNP-containing exon-defined A complexes have been observed for several exons (Figure 1.5; A-like) (House and Lynch, 2006; Sharma et al., 2008). In addition, some exon-definition complexes have been shown to contain the tri-snRNP and the exon-bound tri-snRNP can directly interact with the upstream 5' ss to assemble the B complex across the intron (Figure 1.5; B-like) (Schneider et al., 2010b). However, despite the characterization of some exon-defined complexes, it is still unknown exactly what interactions of the RNA and protein components are involved in building the exon-defined complex, and the connection or conversion of exon-defined to intron-defined complexes.
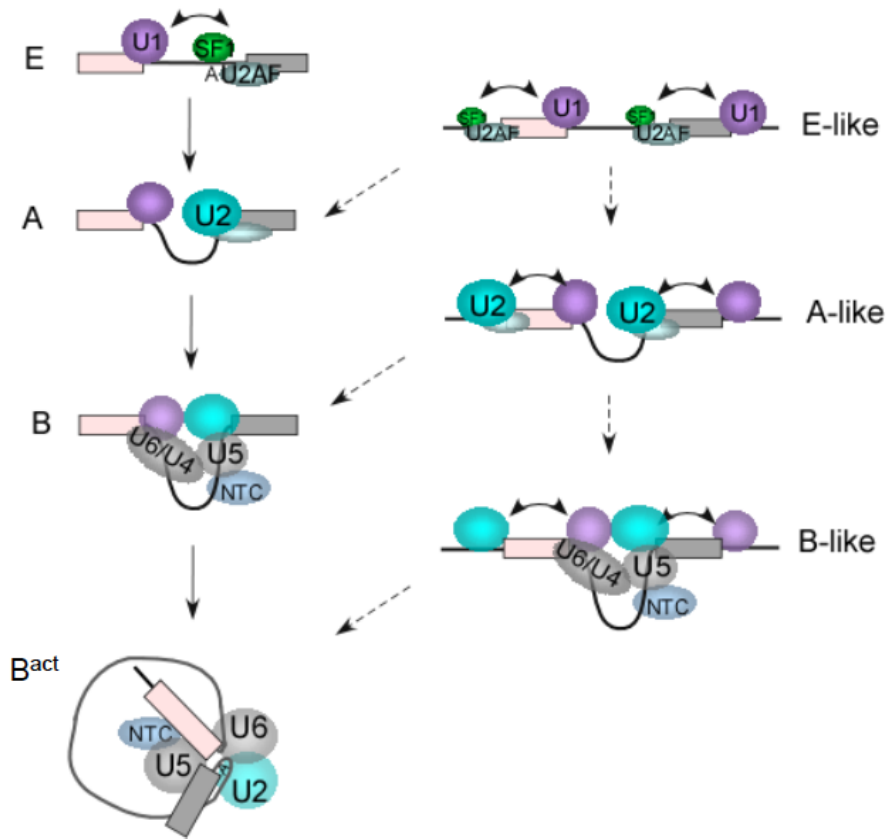
Figure 1.5 Exon-definition interactions along the spliceosome assembly pathway. Left, the canonical intron-defined orientation of spliceosome; right, the exon-defined version of each step. The cross-exon interactions can occur in any spliceosome complexes and then convert into the cross-intron interactions. The figure is adapted from (House and Lynch, 2008).

1.4 Regulation of alternative splicing by controlling splice site recognition

The best-studied mechanisms of alternative splicing regulation involve controlling the splice site recognition by regulating the association of the U1 snRNP, U2AF and the U2 snRNP with the 5' and 3' splice site, respectively (Black, 2003; Matlin et al., 2005). SR (Ser-Arg) proteins typically bind to an ESE and enhance the association of the spliceosome components to the splice sites flanking the regulated exon (Figure 1.6A) (Black, 2003). Moreover, ESEs are though to recruit SR proteins to establish a network of protein-protein interactions across the exon, thereby bridging U2 and U1 and stabilizing the exon-definied complex (Hoffman and Grabowski, 1992; Reed, 2000). The ESE-stabilized cross-exon interactions are then converted into cross-intron interactions to enhance the inclusion of the ESE-contianing exon (Figure 1.6A). In contrast, hnRNP proteins typically bind to an ESS to sterically block the ability of the spliceosomal components to bind to the splice sites, which disrupts the exon-definition interactions and represses the use of the splice sites flanking the regulated exons (Eperon et al., 2000). As a result, the use of the splice sites of the upstream and downstream exon is increased to induce the exclusion of the regulated exon (Figure 1.6B). Moreover, hnRNP proteins can compete with the SR proteins for binding to an overlapping ESE/ESS element (Zahler et al., 2004). Thus, the competition between SR and hnRNP proteins for binding to the pre-mRNA provides a combinatorial control in influencing the splice site choice. Although most of the splicing regulators are shown to effect the early spliceosome assembly steps, the later tri-snRNP recruitment steps for the B complex assembly or structural rearrangements for the C complex formation are also the potential points for regulating alternative splicing (House and Lynch, 2008).
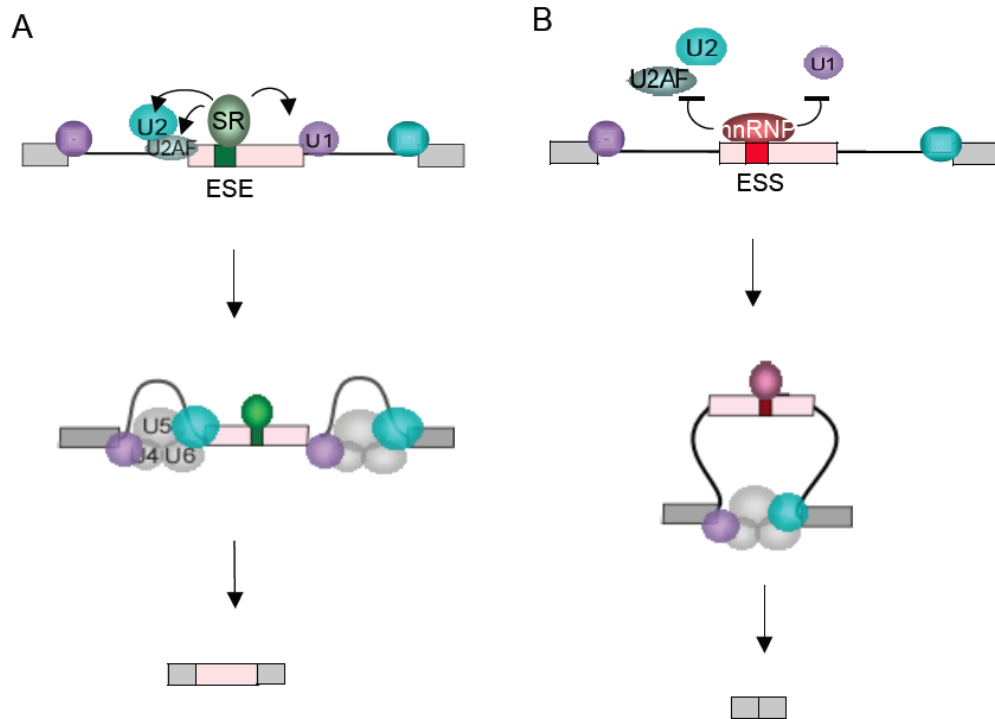
Figure 1.6 Regulation of initial splice site recognition by splicing regulators. (A) SR proteins bound to ESEs (green) recruit the U1 snRNP, U2AF and the U2 snRNP to the splice sites flanking the regulated exon via protein-protein or protein-RNA interactions, which facilitates the assembly of spliceosome on the flanking introns. (B) HnRNPs bound to ESSs (red) inhibit the recognition of splice sites by sterically blocking SR protein or U2AF interaction with the substrate, which promotes the spliceosome to assemble on the splice sites of the upstream and downstream constitutive exons to induce the exclusion of the regulated exon.

1.5 CD45, a model gene for studying alternative splicing

The CD45 gene encodes transmembrane protein tyrosine phosphatase, which is one of the most abundance proteins expressed on all hematopoetic cells and serves as an excellent model system for studying the signal-induced alternative splicing. The CD45 gene contains 33 exons, in which exon 4, 5 and 6 are variably skipped (Figure 1.7A). The extent of the skipping of CD45 variable exons has been shown to be important for modulating T-cell receptor signaling and immune responses (Hermiston et al., 2002). Misregulation of alternative splicing of the CD45 gene increased susceptibility to a number of autoimmune diseases and viral infections (Dawes et al., 2006; Lynch, 2004; Tackenberg et al., 2003). To elucidate the molecular mechanisms of alternative splicing of CD45 gene, the JSL1 cell line, which is derived from a human T-cell, was used for studying the alternative splicing of CD45 pre-mRNA. RT-PCR analysis of CD45 mRNA showed four dominant isoforms, including RABC, RBC, RC and RO isoform (Figure 1.7B) (Lynch, 2004). The skipping of all three variable exon 4, 5 and 6 generates the RO isoform of CD45 mRNA, which encodes the PTPase lacking the extra-cellular domain and having reduced phosphatase activity (Figure 1.7C) (Xu and Weiss, 2002). Importantly, the most dominant isoform in JSL1 cells is RBC (Figure 1.7B; RBC with red color), which suggests that the exon 4, 5 and 6 are not regulated together and the skipping exon 4 is mostly independent of exon 5 and 6 (Figure 1.7A; red line).
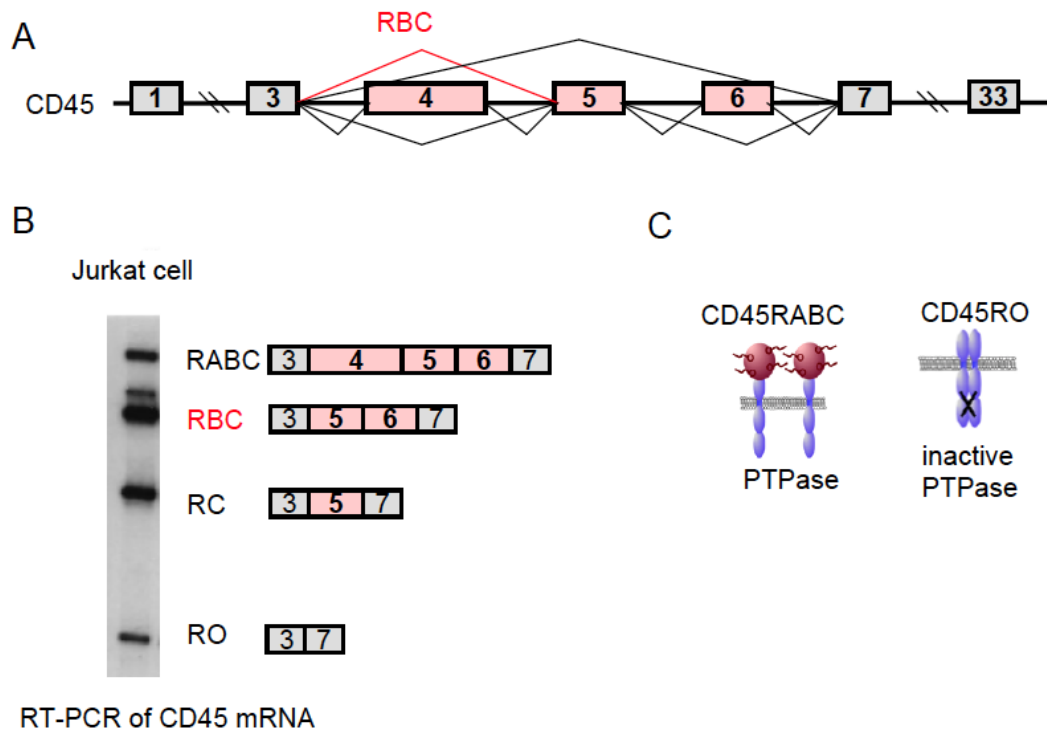
Figure 1.7 CD45 exon 4, 5, and 6 are variably skipped in human JSL1 cells. (A) Schematic of the CD45 gene. The black and red lines indicate the splice sites used in the exclusion of the variable regions. (B) Representative phosphorimaging of an RT-PCR assay. Total RNA was harvested from a Jurkat-derived cell line, JSL1 cells. Primer for reverse transcription is complementary to a smell region within the exon 7. Forward primer is within the exon 3 and labeled with ^{32}P, such that the following PCR products could be separated on a denaturing polyacrylamide gel and visualized by phosphorimager. Schematic of the RT-PCR products is shown in the left. (C) Domain structure of CD45 RABC and RO protein isoform. The variable exon 4, 5 and 6 encode a portion of the extracellular region of the protein tyrosine phosphatase (PTPase) that differs between RABC and RO isoform. Additionally, lacking the region encoded by these 3 variable exons reduces the phosphatase activity of the PTPase.

Analysis of the auxiliary sequences within the CD45 variable exons identified a 60nt silencer element, ESS1, within each of the regulated exons (Figure 1.8A; ESS1) (Lynch and Weiss, 2001; Rothrock et al., 2003; Tong et al., 2005). Sequence analysis of the ESS1 element showed that it contains a CA-rich region. Mutating the CA-rich regions of the ESS1 sequence by introducing three point mutations generates the mESS1 sequence (Figure 1.8A; mESS).

To study the regulation of the skipping of CD45 exon 4, we made the 3-exon minigene in which exon 4 was flanked by the constitutive globin exons. The exon 4 of the 3-exon minigene contains either the ESS1 or mESS sequence (Figure 1.8B). When the wild type CD45 minigene was stably integrated in JSL1 cells, PT-PCR analysis showed that approximately 4% of the minigene mRNA contains exon 4 (Figure 1.8C, left lane). Thus, the 3-exon minigene system recapitulates the skipping of CD45 exon 4 (Lynch and Weiss, 2001). By contrast, when the CD45 minigene contains the mESS sequence, the inclusion of exon 4 is increased (Figure 1.8C, right lane). It indicates that the three point mutations within the ESS1 element disrupt its splicing silencing activity. Additionally, RNA affinity purification showed that hnRNP L is the most dominant protein associated with the ESS1 but not mESS1 RNA (Figure 1.8D). Therefore, we conclude that hnRNP L is the master regulator for inducing the skipping of CD45 exon 4 by binding to ESS1 (Figure 1.8E) (Rothrock et al., 2005).

A

■ ESS1 UCCACUUUCAAGUGACCCCUUACCUACUC**ACACCACUGC**A*UU*C*U***CACCCGC**A*A*G*C*ACCU

■ mESS UCCACUUUCAAGUGACCCCUUACCUACUC**ACACCACUGG**A*UU*C*U***CACCCGG**A*A*G*A*ACCU

B 3-exon minigene

ESS1 (60nt)

mESS

C JSL1

CD45 minigene

4   80   % E4 inclusion

RT-PCR

D Biotinylated-RNA pull down

hnRNP-L
PTB
hnRNP-E2

— 116 kDa
— 97 kDa
— 66 kDa
Silver stain
— 45 kDa
— 31 kDa

E 3-exon pre-mRNA
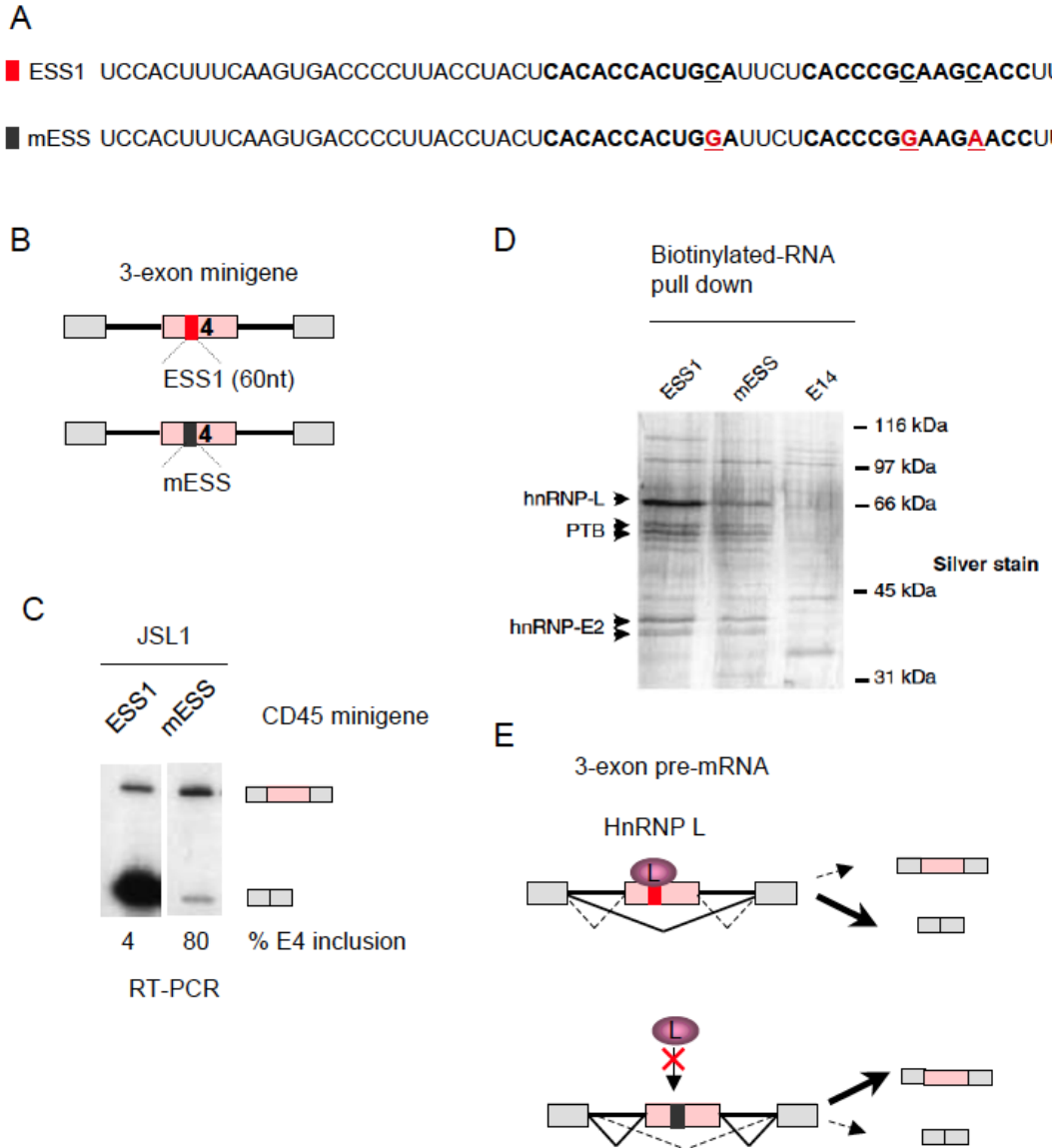
HnRNP L

Figure 1.8 HnRNP L induces the skipping of CD45 exon 4 by binding to ESS1. (A) Sequence of ESS1 and mutated ESS1 (mESS). Nucleotides shown in bold text are the CA-rich region. Three point mutations in mESS1 relative to ESS1 are within the CA-rich region and indicated by underlined red text. (B) Schematic of the 3-exon minigene in which the CD45 variable exon 4 is flanked by the constitutive globin exons. The CD45 minigene contains either ESS1 (red box) or mESS sequence (gray box) within exon 4. (C) RT-PCR analysis of the splicing of minigenes expressed in JSL1 cells using radiolabeled primer, as in Figure 1.7B. The 3-exon and 2-exon spliced RNA products are quantified by phosphorimager to calculate the percentage of the 3-exon RNA among total spliced RNA (% E4 inclusion). (D) Affinity purification of proteins associated with the ESS1 RNA. Silver-staining of proteins that were pulled down by the 5'-biotinylated ESS1, mESS or E14 RNAs from JSL1 nuclear extract. (E) The model of hnRNP L in repressing the inclusion of CD45 exon 4 by binding to ESS1.

1.6 HnRNP L induces the skipping of CD45 exon 4 by a novel mechanism

The dynamic assembly of the spliceosome suggests the regulation of splicing can occur at any of the intermediates along the spliceosome assembly pathway. Previous work used CD45 exon 4 as a model system to study the regulation of spliceosome assembly by hnRNP L. In the 3-exon minigene system, ESS1 represses the splicing of the introns flanking exon 4 to enhance the splicing of the intron flanked by the upstream and downstream constitute exon (Figure 1.9A; left). To eliminate complications from the upstream-downstream exon splicing pathway, the upstream exon was removed to generate the 2-exon pre-mRNA in which the exon 4 is flanked only by the downstream exon (Figure 1.9A; right). To characterize the mechanism of hnRNP L-mediated repression of exon 4 splicing, the splicing of the 2-exon ESS1-represssed substrate sequence is compared with a derepressed version in which the ESS1 is mutated to mESS (Figure 1.9B). The *in vitro* transcribed substrates were incubated with JSL1 nuclear extract to reconstitute the *in vitro* splicing reactions (Figure 1.9C). RT-PCR analysis of the RNA *in vitro* splicing reactions showed that in comparison to the derepressed substrate, ESS1 within the repressed substrate represses the splicing of the downstream intron (Figure 1.9D). Therefore, the splicing of the 2-exon pre-mRNA recapitulates the ESS1-mediated splicing repression of the 3-exon pre-mRNA as described in panel A (House and Lynch, 2006).
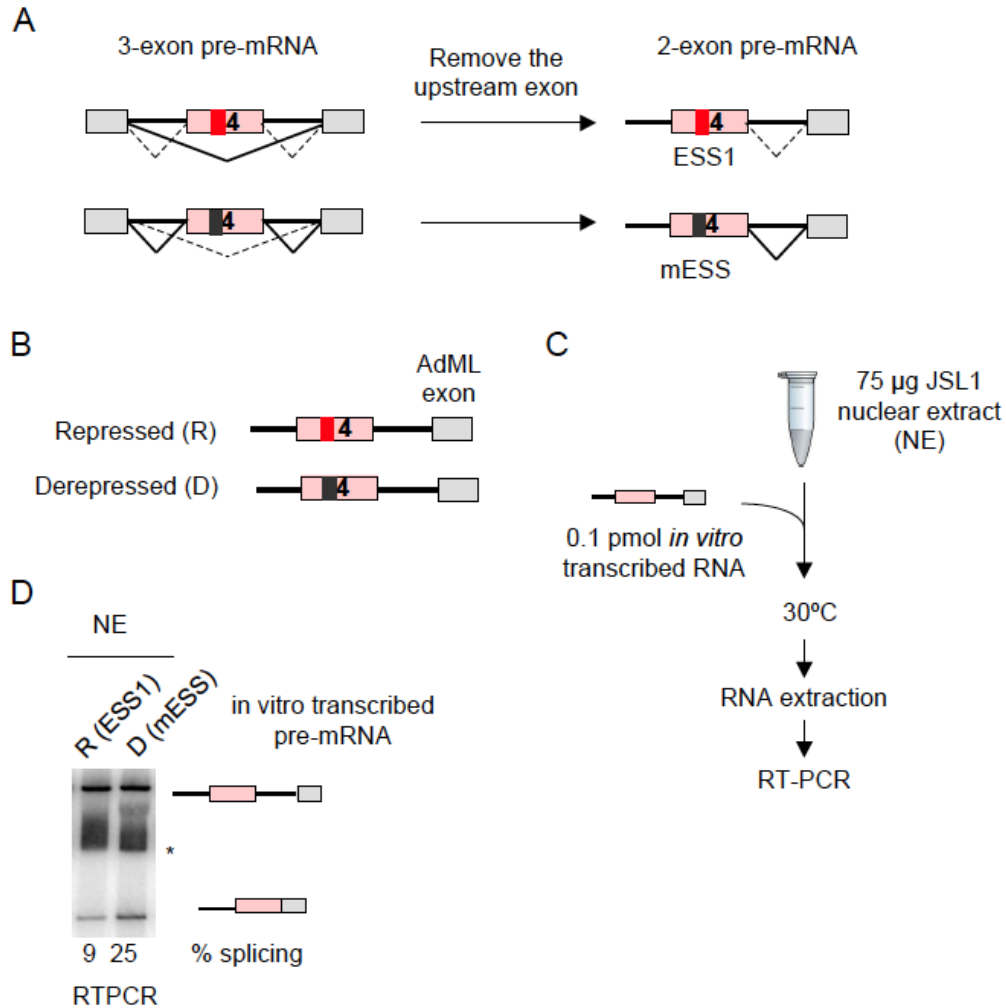
Figure 1.9 Recapitulation of ESS1-regulated splicing of CD45 exon 4 *in vitro*. (A) Comparison of the splicing regulation bewteen the 3-exon and 2-exon pre-mRNA. In the 3-exon pre-mRNA, splicing occurs not only on the introns flanking exon 4 but also on the intron between upstream and downstream exon. In the 2-exon pre-mRNA, splicing and spliceosome assembly is limited into the intron downstream of exon 4. (B) Schematic of splicing substrates. The repressed (R) construct contains the wildtype ESS1 elements (red box) within exon 4. The derepressed substrate (D) contains the mutated ESS1 in which three point mutations abolish its association with hnRNP L binding and silencing activity (dark gray box) (also see chapter 6.1). (C) Schematic of the *in vitro* splicing assay. The *in vitro* transcribed RNA substrates were incubated with JSL1 nuclear extract under splicing conditions followed by the total RNA extraction for RT-PCR analysis. (D) RT-PCR analysis of the splicing reactions using radiolabeled primer, as in Figure 1.7B. Here, pre-mRNA and spliced RNA are detected and quantified by phosphorimager to calculate the percentage of spliced RNA among total non-spliced and spliced RNA (% splicing).

The nuclear extract contains U1, U2, U4, U5 and U6 snRNP, which can be assembled on the pre-mRNA in a stepwise way to form different spliceosome intermediate complexes for splicing catalysis. To determine the spliceosome assembly steps that are altered by binding of hnRNP L to ESS1, spliceosome assembly reactions were reconstituted with nuclear extract depleted of different snRNPs. To induce the cleavage of snRNA, the oligonucleotides that are complementary to the internal region of the snRNAs were incubated with nuclear extract in the presence of RNase H (Figure 1.10A). Primer extension analysis of the oligo-treated extract showed that the snRNAs are efficiently cleaved by the oligo-directed RNase H cleavage (Figure 1.10B). In the spliceosome assembly assays, the repressed or derepressed substrates were radio-labeled so that the complexes assembled on the substrates can be visualized in a native gel by phosphorimager (Figure 1.10C). Resolution of splicing reactions containing repressed and derepressed substrate in a native gel resulted in two and three super-shifted bands, respectively (Figure 1.10D; Total). The identities of the complexes within these bands were based on their migration in a native gel and their dependence on the individual snRNPs. The middle band is assigned to be the U1-and-U2-containing A complex because the middle band was greatly reduced in the absence of the U1 or U2 snRNP (Figure 1.10D; -U1 and -U2). The top band is assigned to be the U5.U6/U4-tri-snRNP-containing B complex based on the fact that inactivation of U6 snRNP abolishes the top band (Figure 1.10D; -U6). Therefore, the progression from the A to B complex is blocked on the repressed substrate.
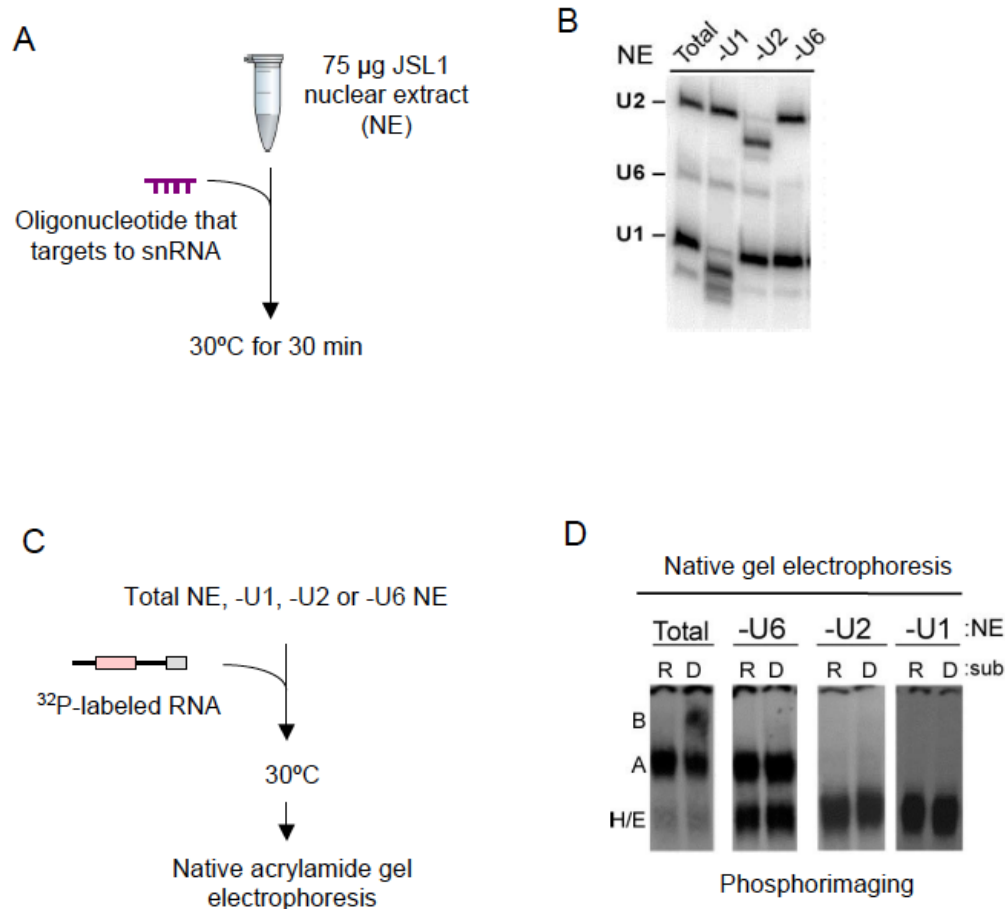
Figure 1.10 ESS1 represses the progression from the spliceosomal A to B complex. (A) Schematic of the oligonucleotide-directed cleavage of snRNAs in nuclear extract (NE). NE was incubated oligonucleotides that are complementary to U snRNAs to induce their cleavage by RNase H in NE. (B) Analysis of the efficiency of the cleavage of U snRNAs. RNAs extracted from H_2O-treated NE (Total) or oligo-treated NE (-U1, -U2, and -U6) were analyzed by primer extension to detect the full-length and cleaved U snRNAs. (C) Schematic of the *in vitro* spliceosome assembly assay. The ^{32}P-labeled RNA substrates were incubated with the indicated nuclear extracts followed by native acrylamide gel electrophoresis. (D) Representative phosphorimaging of the spliceosome assembly assay. The ^{32}P-labeled R and D substrate, as in Figure 1.9B, were incubated in total splicing-competent NE (Total), or NE depleted of U1, U2 or U6 snRNP. Comigrating H and E complexes (H/E), A and B complexes are labeled.

Combined the results from the *in vitro* splicing and spliceosome assembly assays,

we provide the model in which hnRNP L represses the progression from the A to B

complex to repress the splicing of CD45 exon 4. By contrast, mutating ESS1 to disrupt its

association with hnRNP L allows the recruitment of the tri-snRNP into the A complex to

form the B complex, which is then converted to C complex for the catalysis of splicing

(Figure 1.11) (House and Lynch, 2006).
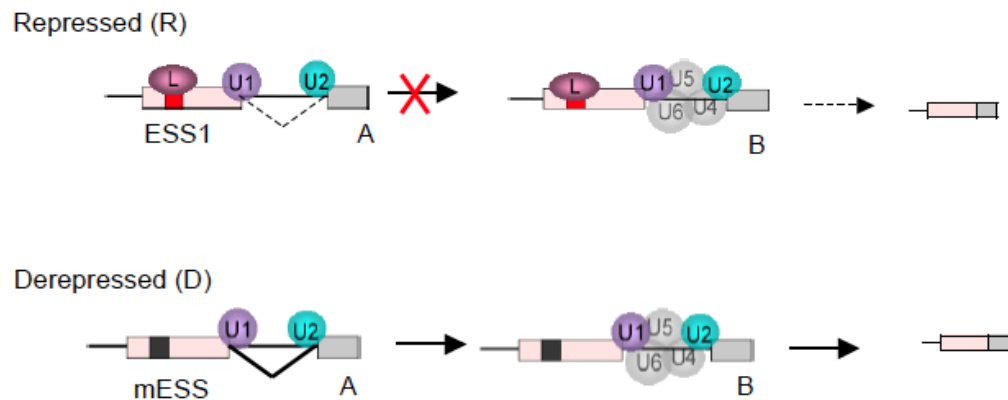
Figure 1.11 Model for hnRNP L function in blocking the later spliceosome assembly steps to repress the splicing of CD45 exon 4. Binding of hnRNP L to ESS1 blocks the progression from the A to B complex, which results in repressing the splicing of the intron downstream of CD45 exon 4.

Based on the 2-exon substrate, a model for alternative splicing of the 3-exon

substrate was provided, in which hnRNP L interferes the B complex assembly on the

downstream intron to promote the splicing of the intron between upstream and

downstream constitutive exon. (Figure 1.12A) (House and Lynch, 2008). This is a novel

mechanism in that typical hnRNP proteins bind to ESS to block the E complex formation

by sterically interfering with U1 snRNP binding at the 5' splice site such that lower

affinities for U1 snRNP binding reduces the use of the 5' ss (Figure 1.12B) (Eperon et al.,

2000). The fact that hnRNP L does not affect the A complex formation indicates that

hnRNP L does not affect the initial recognition of the 5' ss by U1 snRNP. Instead,

hnRNP L blocks the steps after U1 binding to repress the use of the 5' ss of the ESS1-

containing exon. Together, the *in vitro* splicing and spliceosome assembly assays

demonstrate that the later spliceosome assembly steps are the novel regulation points for

hnRNP L in inducing the skipping of CD45 exon 4.
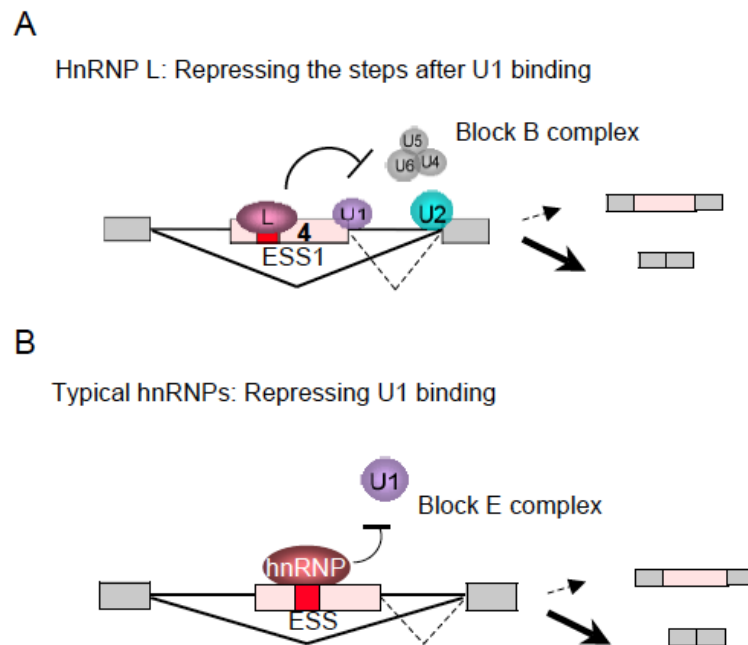
Figure 1.12 The assembly steps after U1 binding are novel points for regulating alternative splicing. (A) The 3-exon pre-mRNA model of hnRNP L-regulated alternative splicing in which U1 snRNP binding is not blocked. (B) The mechanism of other hnRNPs, such as hnRNP A1, in mediating the exclusion of exon by interfering U1 snRNP binding.

Chapter 2

ESS1 induces novel interactions of both U1 snRNA and hnRNP A1 with the 3' end

of CD45 exon 4

To regulate alternative splicing, most of the splicing regulators have been shown to sterically block the initial association of U1 snRNP, U2AF or U2 snRNP with splice sites (see chapter 1.4). HnRNP L, the splicing regulator of CD45 exon 4, does not block association of U1 snRNP with the 5'splice site, but instead, it represses the steps after U1 binding at the 5'ss to block the B complex formation (see chapter 1.5 and 1.6). However, it was unknown how hnRNP L perturbs the molecular interactions of the U1-5'ss complex to interfere the subsequent spliceosome assembly steps. Therefore, my initial goal was to elucidate how the binding of hnRNP L to ESS1 within CD45 exon 4 induces the aberrant molecular interactions between U1 snRNP and the pre-mRNA.

2.1 Introduction: Motivation for characterizing U1 snRNP interactions within the hnRNP L-repressed spliceosome

Recently studies have shown that hnRNP L, PTB and RBM5 all function in repressing the B complex formation to induce the skipping of CD45 exon 4, Fas exon 6 and N-src exon, respectively (Bonnal et al., 2008; House and Lynch, 2006; Sharma et al., 2008). Although both of RBM5 and PTB have been shown to block the conversion from the cross-exon to cross-intron complex to repress the B complex formation, it is unknown exactly which spliceosome interactions are altered to repress the spliceosome assembly and induce the skipping of exons.

Tim Nilsen's group identified the other splicing silencer elements that can reduce the rate of splicing at the proximal strong 5' splice site to promote the use of the distal weak 5' ss for splicing (Figure 2.1A; compare black with blue line) (Yu et al., 2008). The splicing silencers do not alter the affinity of U1 binding at the 5' ss, but instead, the splicing silencers perturb the molecular interactions of the U1 snRNP-5'ss complex (Figure 2.1A; compare the hexagon with the circle U1). Thus, the molecular interactions between U1 snRNP and the 5'ss are potential regulation points for alternative splicing. Here, I hypothesize that on the repressed RNA, the binding of hnRNP L to ESS1 also alters the U1-5'ss complex, which blocks the subsequent transition from the A to B complex and represses the splicing of CD45 exon. By contrast, on the derepressed RNA, U1 snRNP presumably binds in a canonical way that allows the assembly of the B complex and the subsequent catalysis (Figure 2.1B; compare repressed with derepressed).
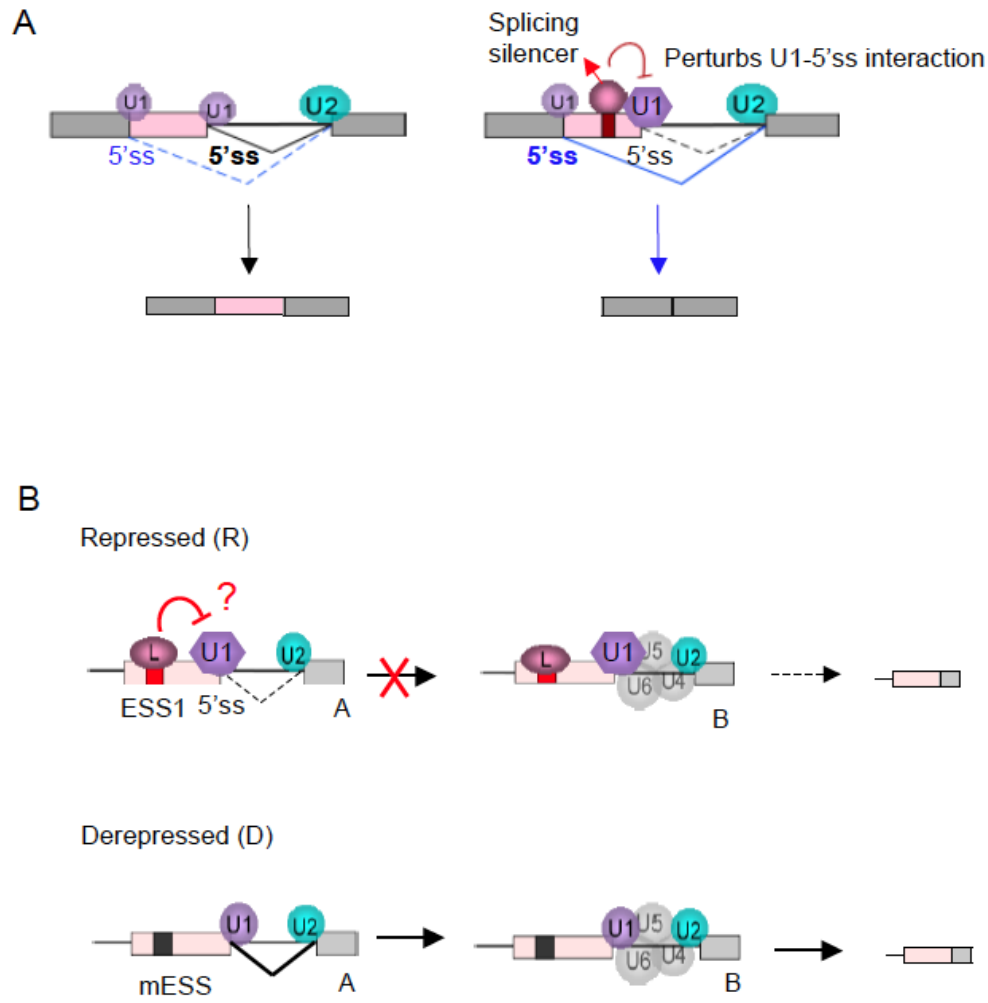
Figure 2.1 Splicing silencers that shift the use of the 5' splice site perturb the molecular interactions of the U1 snRNP-5'ss complex. (A) On the hypothetical RNA, the proximal strong 5' splice site (5' ss in blue text) is located downstream of a weakened 5' splice site (5' ss in black text). The splicing silencing elements (red box) that reduce the rate of splicing at the proximal 5' ss promotes the use of the distal 5' ss for splicing. The splicing silencers were shown to perturb the molecular interactions of U1 snRNP/5'ss complex. Blue and black lines indicate the proximal and distal 5' splice sites, respectively, that are paired with the 3' splice site for splicing. The circle U1 and hexagon U1 indicate the canonical and altered U1 binding, respectively. Adapted in part from (Yu et al., 2008). (B) Hypothesis of hnRNP L function in altering the U1 snRNP interaction within the A complex on the repressed substrate to block its transition into B complex and repress the splicing catalysis of the downstream intron.

2.2 Enrichment of the hnRNP L-repressed and -derepressed A complex

In the spliceosome assembly assays as described in chapter 1.6, the A complex is stalled on the ESS1-repressed substrate whereas the A complex is progressed into B complex on the derepressed substrate. The differences of U1 snRNP binding within the repressed versus derepressed A complex would indicate the U1-5'ss interactions that are altered by hnRNP L. Because U6 snRNP also interacts with the 5'ss in the B complex (see Figure 1.4), I set to separate the B from A complex and then compare U1 snRNP binding at the 5' ss within the repressed and derepressed A complex.

To isolate and enrich the A complex, spliceosome assembly reactions were fractionated by glycerol-gradient centrifugation (Hartmuth et al., 2004). Based primarily on the size, spliceosome complexes sediment into different glycerol gradients under high-speed centrifugation (Figure 2.2A). The complexes across the top to bottom gradient fractions were analyzed by native gel electrophoresis. This showed that the A complex is enriched in the middle (M) fractions whereas the B complex is fractionated into the later (L) fractions (Figure 2.2B; compare the M with L fractions). Thus, for the derepressed complexes, the A complex is separated from the B complex and enriched in the middle fractions. It seems that higher levels of the E complexes co-sediment with the repressed- than with the derepressed-A complex in the M fractions. The levels of the E complex are variable among different sets of experiments so that I do not conclude that the progression from the E to A complex is blocked on the repressed substrate. Moreover, the variable levels of E complexes do not interfere the subsequent analysis as shown in the following chapters. Since the A complex is the most dominant complex in M fractions, the M fractions were collected for further analysis of U1 snRNP binding at the 5'ss.
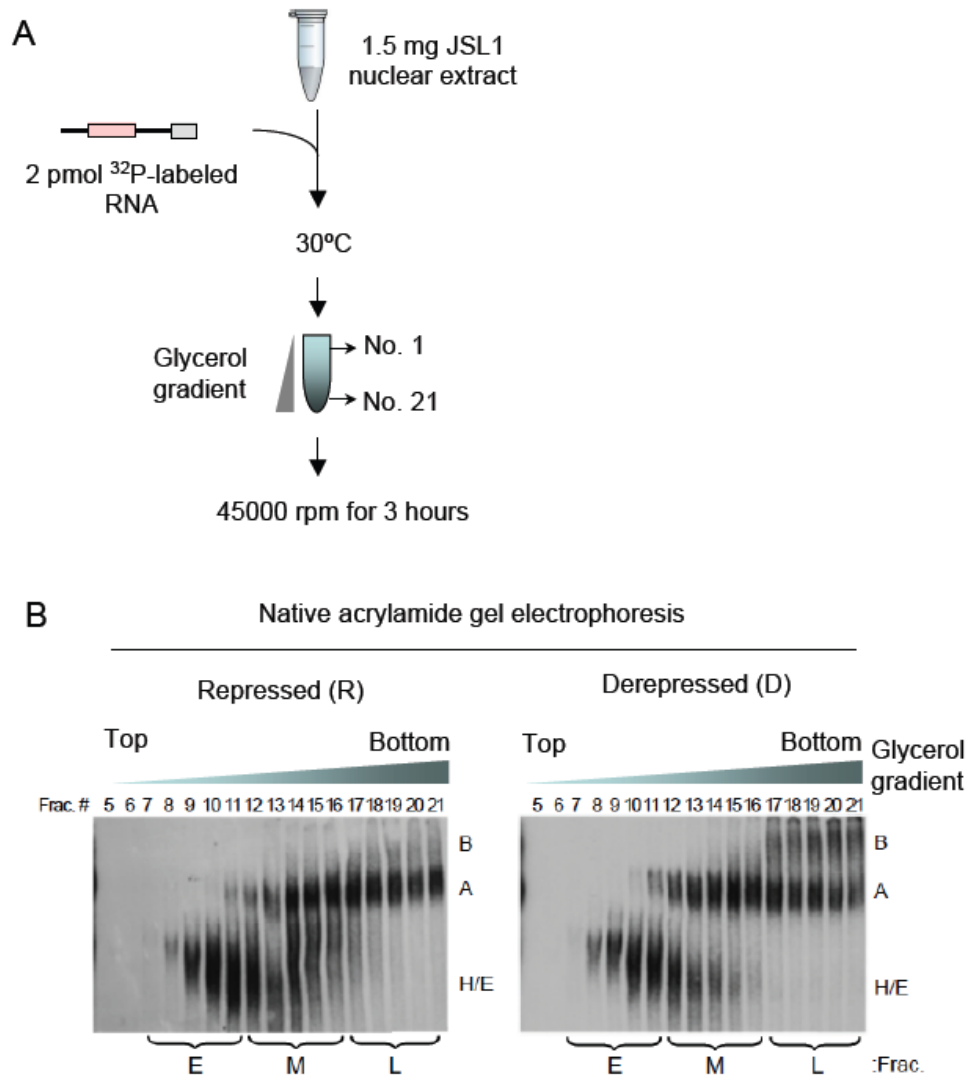
Figure 2.2 Sedimentation of the A complex into the middle fraction. (A) Schematic of glycerol gradient centrifugation of the spliceosome assembly reactions. The spliceosome assembly reactions containing 2 pmol RNA substrates were layered on the glycerol gradient and then centrifuged at 45000 rpm for 3 hours. The gradient fractions were collected from top to bottom into 21 fractions. (B) Native gel electrophoresis of the gradient fractions. The complexes in gradient fractions were resolved in a native gel and analyzed by phosphorimager. The early (E), middle (M) and later (L) fractions were enriched for the H/E, A and B complex, respectively, for the derepressed substrate. Identifies of the complexes were primarily based on their migration in the native gel.

2.3 HnRNP L induces a novel pairing interaction between the U1 snRNA and the 3'

end of CD45 exon 4

Along the splicesome assembly pathway, U1 snRNP binding at the 5' splice site in the A complex proceeds progression into the B complex (Figure 1.4). The binding of U1 snRNP at the 5' splice site involves both of RNA-RNA and protein-RNA interactions. U1 snRNP consists of U1 snRNA, seven Sm proteins, U1C, U1A, U1-70K and other minor protein components (Figure 2.3A). The canonical base-paring interactions between the 5' end of U1 snRNA and the 5' splice site involve 3 to 8 base-pairs that are typically not fully complementary (Figure 2.3A; pairing of the yellow box in U1 with the 5' ss). The base-pairing interactions have critical roles in the recognition of the 5' splice site (Guthrie and Patterson, 1988; Ruby and Abelson, 1988; Zhuang and Weiner, 1986). Recent crystal structural analysis of U1 snRNP showed that the zinc-finger domain of U1C binds across the RNA duplex at the 5'ss, which has been implicated in stabilizing the base-pairing interactions at the 5' ss (Pomeranz Krummel et al., 2009).

To analyze the base-pairing interactions in the A complex, I incubated the pooled middle fractions with AMT-psoralen to induce the crosslinks of the base-paired regions upon UV-light irradiation. Site of crosslinks around the 5' splice sites were then visualized as psoralen/UV-dependent stops in a primer extension reaction using primer that is complementary to the downstream region of the 5' ss (Figure 2.3B).
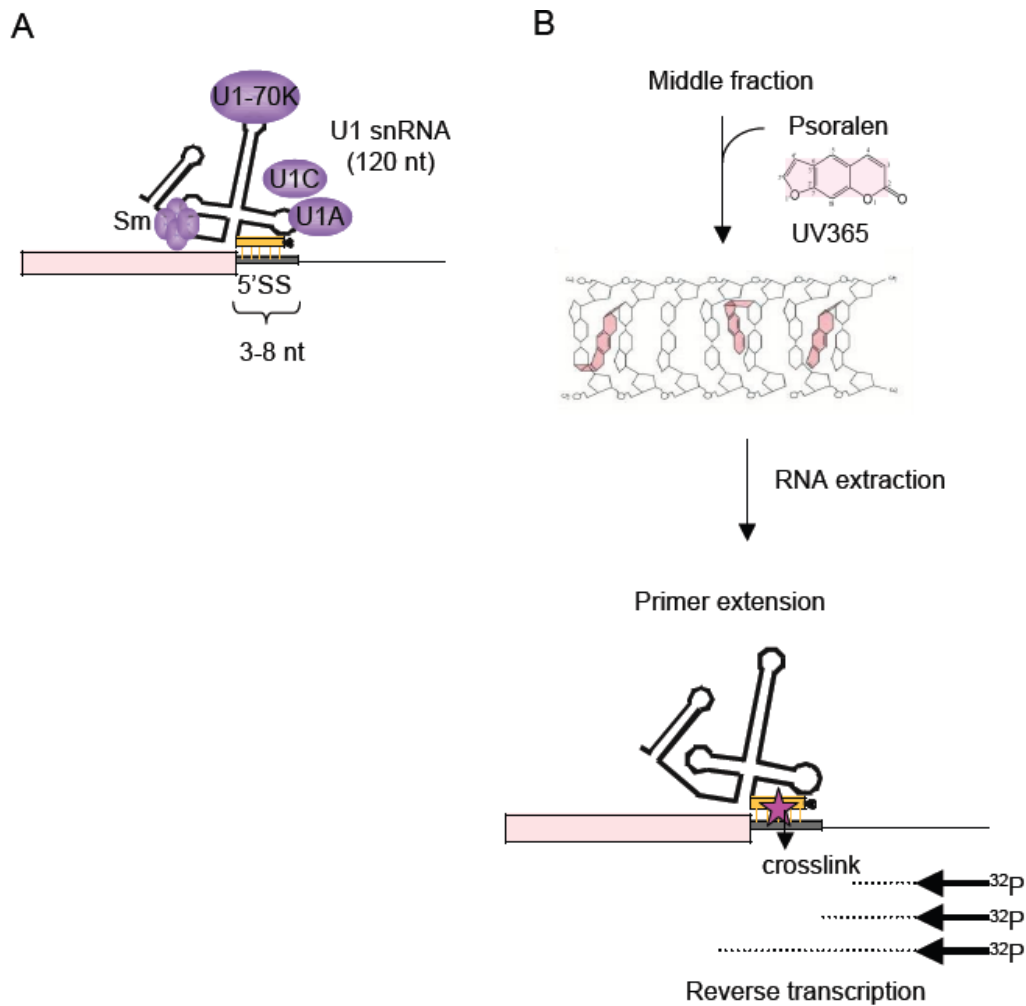
Figure 2.3 Interrogation of base-pairing interactions on the pre-mRNA substrate by psoralen crosslinking assays. (A) Schematic of RNA-RNA and RNA-protein interactions of U1 snRNP binding at the 5' splice site. (B) Schematic of primer extension analysis of the psoralen-crosslinked RNAs. AMT-psoralen was added into the colleted middle fractions from glycerol gradient centrifugation of spliceosome assembly reactions as in Figure 2.2. AMT-psoralen can intercalate between base-paired regions of RNAs. Upon UV-light irradiation, it forms the covalent bonds with the nearby RNA regions. To detect the crosslinked sites, the RNAs were extracted followed by primer extension, in which the reverse transcription stops at the crosslinked sites.

Besides analyzing the 5' ss by R2 primer, the psoralen-induced crosslinks around the branch point sites (BPSs) of exon 4 and AdML exon were also interrogated using the R1 and R3 primer (Figure 2.4A). Primer extension analysis of the psoralen-crosslinked RNAs did not detect any differences of the croslinking patterns around BPSs on repressed versus derepressed substrate (Figure 2.4B; R1 and R3). Moreover, the patterns of the crosslinking around the 5'ss are similar between the repressed and derepressed RNA (Figure 2.4C; 5'ss). Surprisingly, there is a crosslink upstream of the 5' ss in the repressed but not derepressed substrate (Figure 2.4C; red arrow). By running the sequencing reactions with primer R2 in parallel with the crosslinking analysis around the 5' ss, the repression-dependent crosslink is mapped to a cytosine residue 15 nucleotides upstream of the 5'ss (Figure 2.4D; C-15). Therefore, the psoralen-crosslinking assays identified a repression-dependent C-15 crosslink at the 3' end of exon 4.
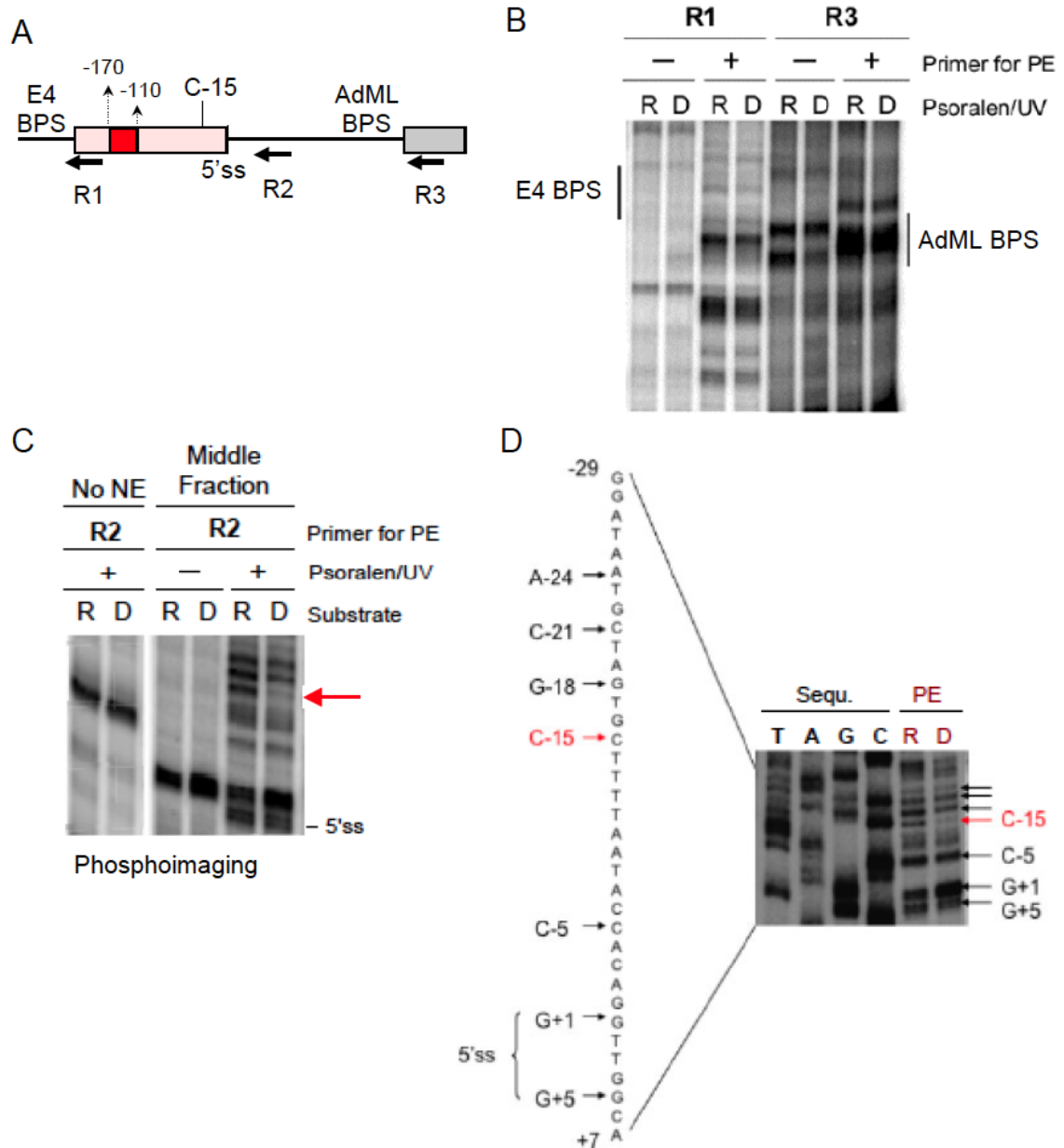
Figure 2.4 An ESS1-dependent crosslink is mapped to the cytosine residue, which is 15-nucleotide upstream of the 5' splice site. (A) Schematic of the repressed substrate showing relative location of primers (R1-3) used for mapping psoralen-crosslinked sites on branch point sites from exon 4 and AdML exon (E4-BPS and AdML-BPS), and the 5' ss from exon 4. (B) Primer extension analysis of psoralen-induced crosslinked sites of the complexes in the middle fraction using primer R1 and R3 as described in Figure 2.3B. (C) Primer extension analysis using primer R2 as in panel B. The red arrow points at the repression-specific crosslink. (D) Primer extension analysis of psoralen-crosslinked reactions (PE) or a sequencing reaction with ddNTPs (Sequ.) using primer R2. Locations of several crosslinks are shown, including the 5' ss and the primary differential crosslink (C-15).

To determine whether U1 snRNP is involved in the crosslink at C-15, I performed the psoralen-crosslinking with the complexes assembled in nuclear extract depleted of U1 snRNP. The fact that the crosslinks at the 5' ss are reduced after depleting U1 snRNP indicates U1 snRNP is vacated from the 5'ss. Moreover, in the absence of U1 but not U2 snRNP, the C-15 crosslink on the repressed substrate is significantly disrupted (Figure 2.5A). To more rigorously analyze the RNA crosslinked to the C-15 region, the complexes assembled on the ^{32}P-labeled 5'ss RNA fragments are psoralen-crosslinked followed by denaturing gel electrophoresis (Figure 2.5B; panel C). While most of the 5' ss RNA fragments were not crosslinked, a small portion of the 5' ss RNA is crosslinked to form a supershifted band (Figure 2.5C; black arrow). Additionally, in the absence of U1 snRNP, the supershifted band is reduced. To further demonstrate that the psoralen-induced supershifted band contains the U1 snRNA, I performed the oligo-directed cleavage of the psoralen-crosslinked RNAs (Figure 2.5B; panel D). Using the oligos to cleave the internal region of the U1 snRNA, the intensity of the supershifted band is reduced with the concurrent generation of two new bands, which are supposed to be the cleaved RNAs (Figure 2.5D; U1$_{internal}$). When the 5' end of the U1 snRNA is cleaved, the supershifted band is not changed (Figure 2.5D; U1$_{5'end}$). This indicates that the internal region but not the 5' end of the U1 snRNA is involved in the psoralen-induced supershift of the 5' ss RNA fragment.
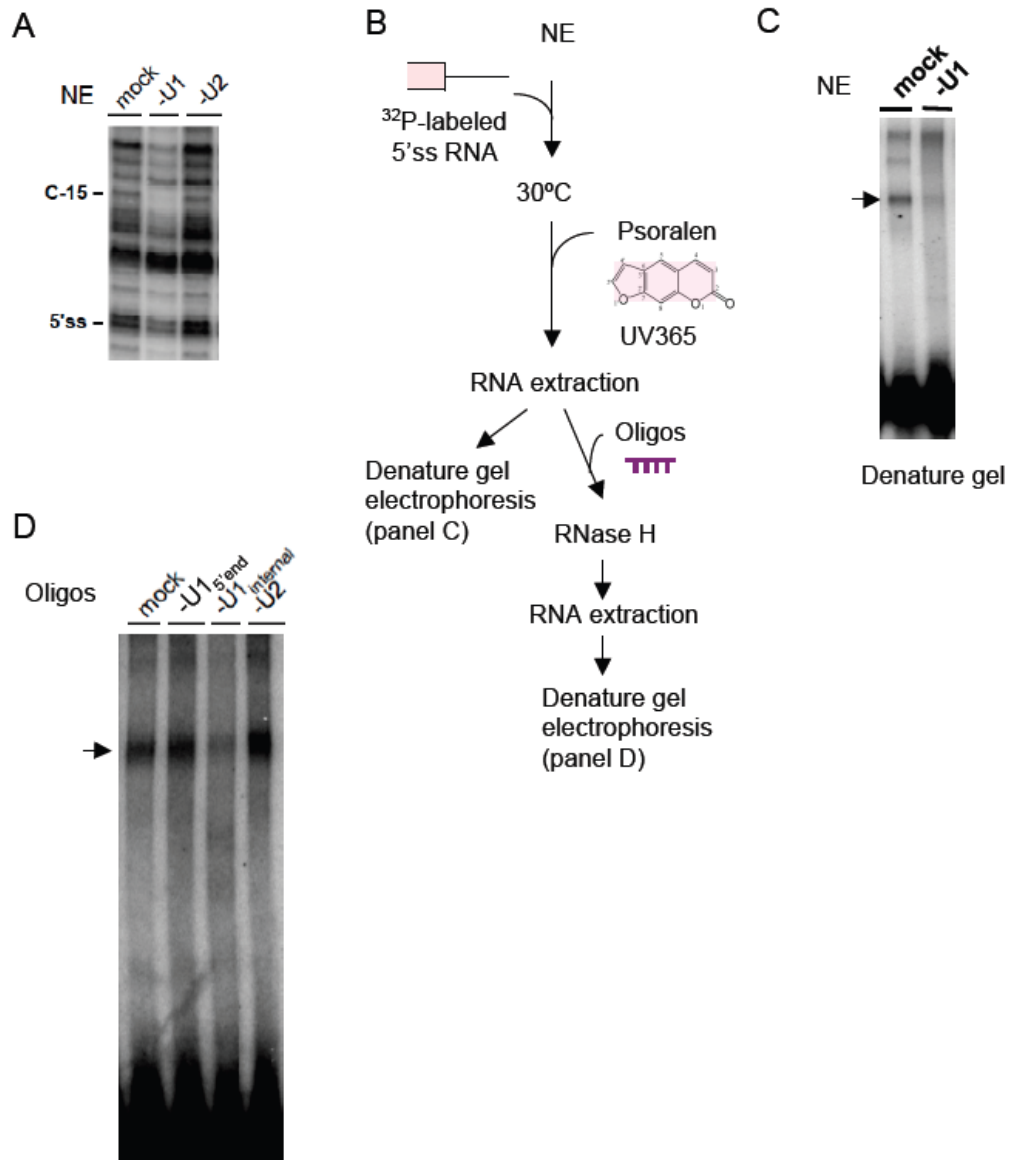
Figure 2.5 The internal region of the U1 snRNA is crosslinked to the 3' end of exon 4. (A) Primer extension analysis of psoralen-crosslinked reactions containing the 5' ss RNA fragment (see panel B) incubated with the splicing-competent nuclear extract (mock), or extract depleted of U1 or U2 (-U1 or -U2). (B) The schematic of supershift assays. The 5' ss RNA fragment encompasses the sequence spanning -45 to +76 relative to the 5' ss was incubated with NE followed by psoralen crosslinking. The RNA extracted from the psoralen crosslinked reactions was directly analyzed by denature gel as in panel C or treated with oligos to induce its cleavage by RNase H followed by denature gel analysis as in panel D. (C) Supershift analysis of the poralen-crosslinked 5' ss RNA fragment incubated with the indicated NE. The arrow points at the supershifted band that is dependent on U1. (D) Supershift analysis of the psoralen crosslinked RNAs that were cleaved by oligo-directed RNase H cleavage. The sequences of the oligonucleotides are listed in Chapter 6.

2.4 The extended U1 interaction involves the 3' portion of helix H in U1

To investigate the region of the U1 snRNA that is involved in the novel pairing interaction with CD45 exon 4, I examined the sequence and secondary structure of the U1 snRNA. The internal region of U1 snRNA includes four stem loops and one helix H located between the stem loop I and III (Figure 2.6A; U1 snRNA). Several studies have shown that interactions of the 5' end of U1 snRNA with the 5' ss can extend into the 5' stem of helix H in U1 (Abad et al., 2008; Kaida et al., 2010). This indicates that the two stems of helix H do not always keep paired, but instead, it could unwind to allow the extended U1 interactions with the substrate (Figure 2.6A; unwinding of U1 snRNA). Thus, while the 5'end of U1 snRNA interacts with the 5' ss, the 3' stem of helix H of U1 snRNA could potentially make the extended contacts with the C-15 region of exon 4. Sequence analysis of helix H region of U1 snRNA revealed that the GCAU sequence in the 3' stem of helix H could potentially base-pair with the GUGC sequence with the C-15 region within exon 4 (Figure 2.6B; purple sequence of U1). Moreover, the extended U1 base-pairing interaction at the C-15 region could co-exist with the canonical U1 interaction at the 5' ss (Figure 2.6B; yellow box of U1).
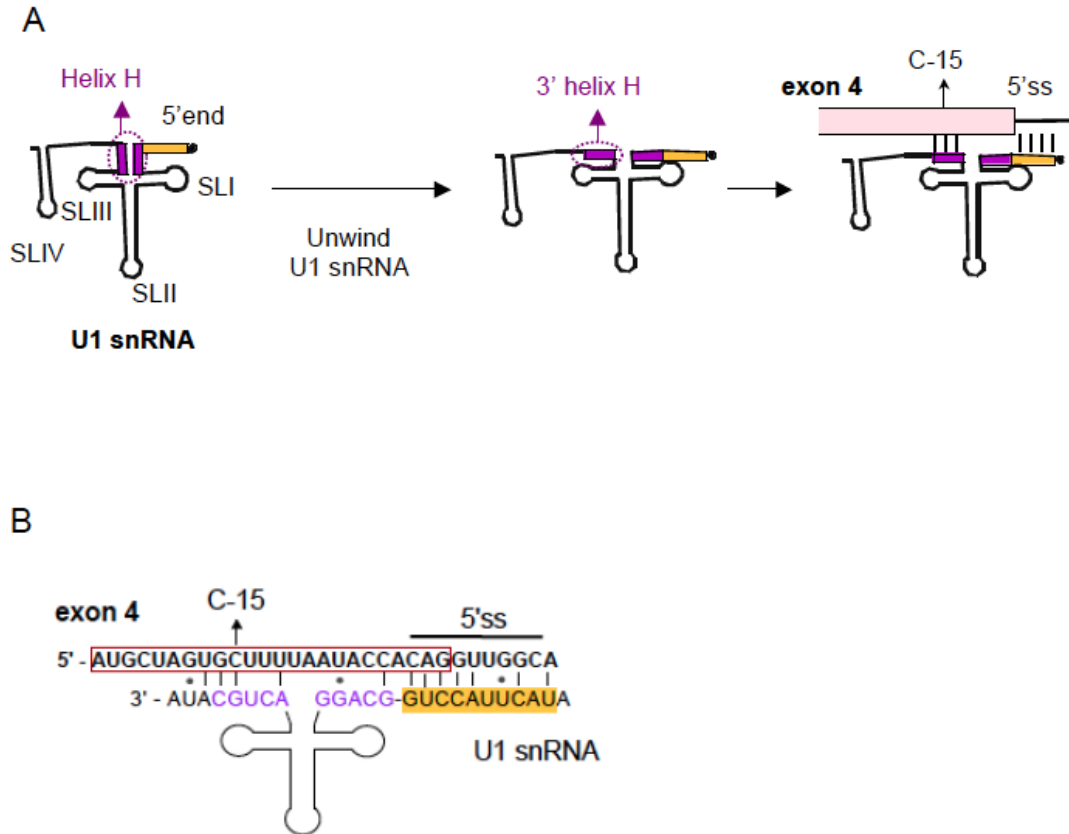
Figure 2.6 Model of base-pairing interactions between the 3' portion of helix H in U1 with the 3' end of exon 4. (A) Schematic of model of unwinding helix H in U1 for making the extended U1 interactions. (B) The putative U1 sequences for making the extended interaction with the 3' end of exon and the canonical interaction with the 5' ss. The helix H region in U1 is shown in purple sequence. The sequence of the 5' end of U1 is shaded with the yellow color. The sequence of the C-15 region within exon 4 is inside the red box.

To support this model, I created several mutations within the C-15 region to potentially disrupt or enhance the putative extended U1 interaction. Previously, we have shown that mutating residues -24 to -13 reduces the skipping of exon 4 in cells although it has less effect than mutating ESS1 (Lynch and Weiss, 2001). Importantly, this functionally-defective mutation in the -24 to -13 region could reduce the extended U1 interaction (Figure 2.7A; QC9). I also mutated four nucleotides downstream of C-15 to allow the putative region that is involved in the extended U1 interaction to become fully complementary (Figure 2.7A; U1up). Consistent with the predicted interaction model, the QC9 mutation greatly reduces the C-15 crosslink, whereas the U1up mutation enhances it (Figure 2.7B). Additionally, the QC9 mutation within the C-15 region also reduces the supershifted band that is dependent on U1 (Figure 2.7C). Notably, neither of these mutations significantly impacts the crosslinks at the 5'ss, which indicates that hnRNP L-induced association of the internal region in U1 with the exonic region does not interfere base-pairing of the 5' end of U1 with the 5' ss.
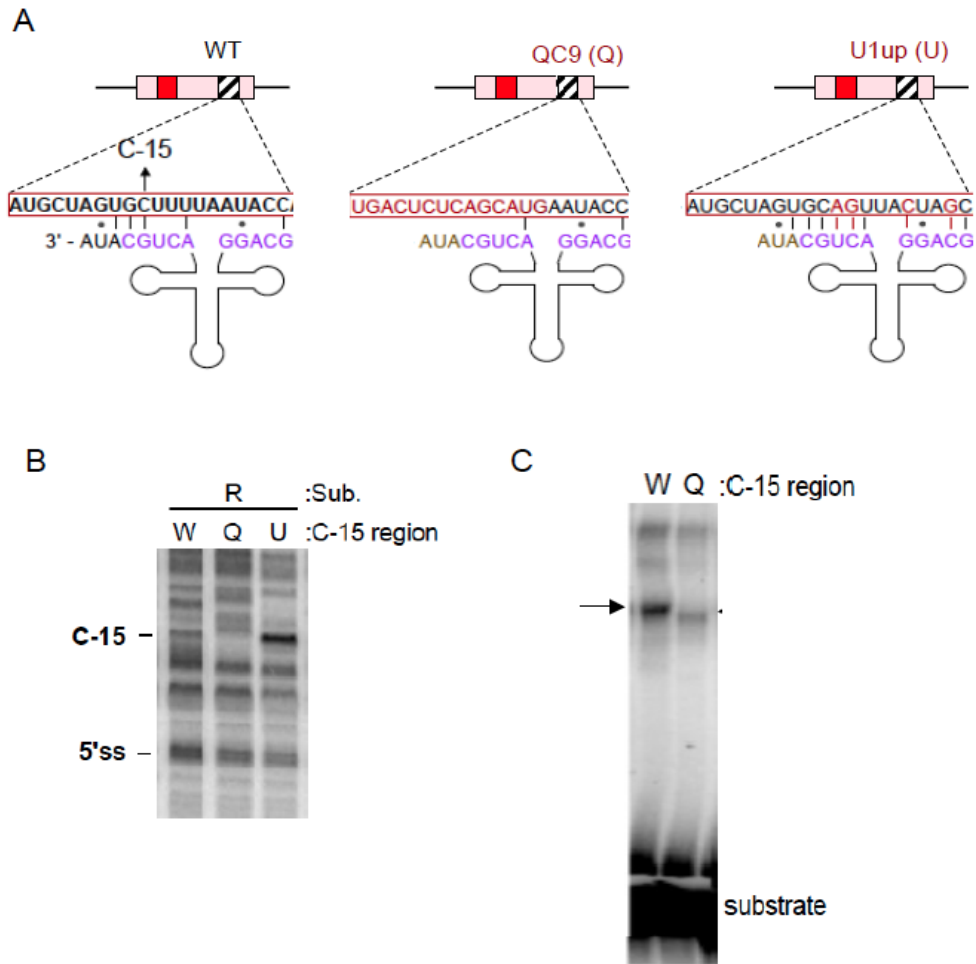
Figure 2.7 Mutant sequences at the 3' end of exon 4 that potentially alter the putative extended U1 base-pairing interaction. (A) Schematic of the potential changes of the U1 base-pairing interaction by creating QC9 and U1up mutation into the C-15 region. The nucleotides that differ from wildtype exon 4 are shown in red color. (B) Primer extension analysis of the psoralen-crosslinked reactions containing the repressed substrates with the wildtype or mutant sequences (Q and U) in the C-15 region. (C) Supershift analysis of the poralen-crosslinked 5' ss RNA fragment containing wildtype or mutant QC9 sequence in the C-15 region.

As a complementary approach, I attempted to map the psoralen-induced crosslinks within the U1 snRNA that are dependent on the association of U1 with the 3' end of exon 4. To eliminate the background crosslink patterns from the free U1 snRNP, I set to

analyze the purified U1-5' ss complexes. To permit purification, the hairpin sequence binding site for the MS2 viral coat protein was inserted into the 3' end of the 5' ss RNA (Jurica et al., 2002; Zhou et al., 2002). The MS2MBP-tagged 5' ss RNA is incubated with nuclear extract followed by affinity-purification using amylose resin (Figure 2.8A). The primer that targets to the SLII in U1 was used for interrogating the psoralen-induced crosslinks within the U1 snRNA in the purified U1-5' ss complex (Figure 2.8B). This revealed that the crosslink at the 5' helix H is reduced when the C-15 region contains the wild-type sequence (Figure 2.8C). This suggests that the interaction of 5' stem with 3' stem of helix H is reduced when the substrate contains the wildtype sequence for its interaction with the 3' stem of helix H (Figure 2.8B; wildtype). By contrast, the helix H in U1 keeps in the helical form on the substrates when the extended U1 interaction with the C-15 region is disrupted (Figure 2.8B; Q mutation).

I also attempted to map the crosslinks within the 3' stem of helix H in U1. However, the 3' helix H in U1 is predicted to not only pair with the 3' end of exon 4 but also with the 5' helix H in U1 (Figure 2.8B). Thus, although I observed a strong the crosslink at 3' helix H in U1 snRNA even in the absence of the 5'ss RNA substrate (data not shown), I cannot distinguish intra- versus inter-molecular interactions.

To further determine whether the unwinding of helix H of the U1 snRNA alters association of the U1 snRNP proteins with the U1 snRNA, I performed western blotting analysis of the purified U1-5' ss complex. This showed that the levels of U1 snRNP proteins are not significantly changed by creating the QC9 mutation into the C-15 region of the 5' ss RNA fragment (Figure 2.8D).
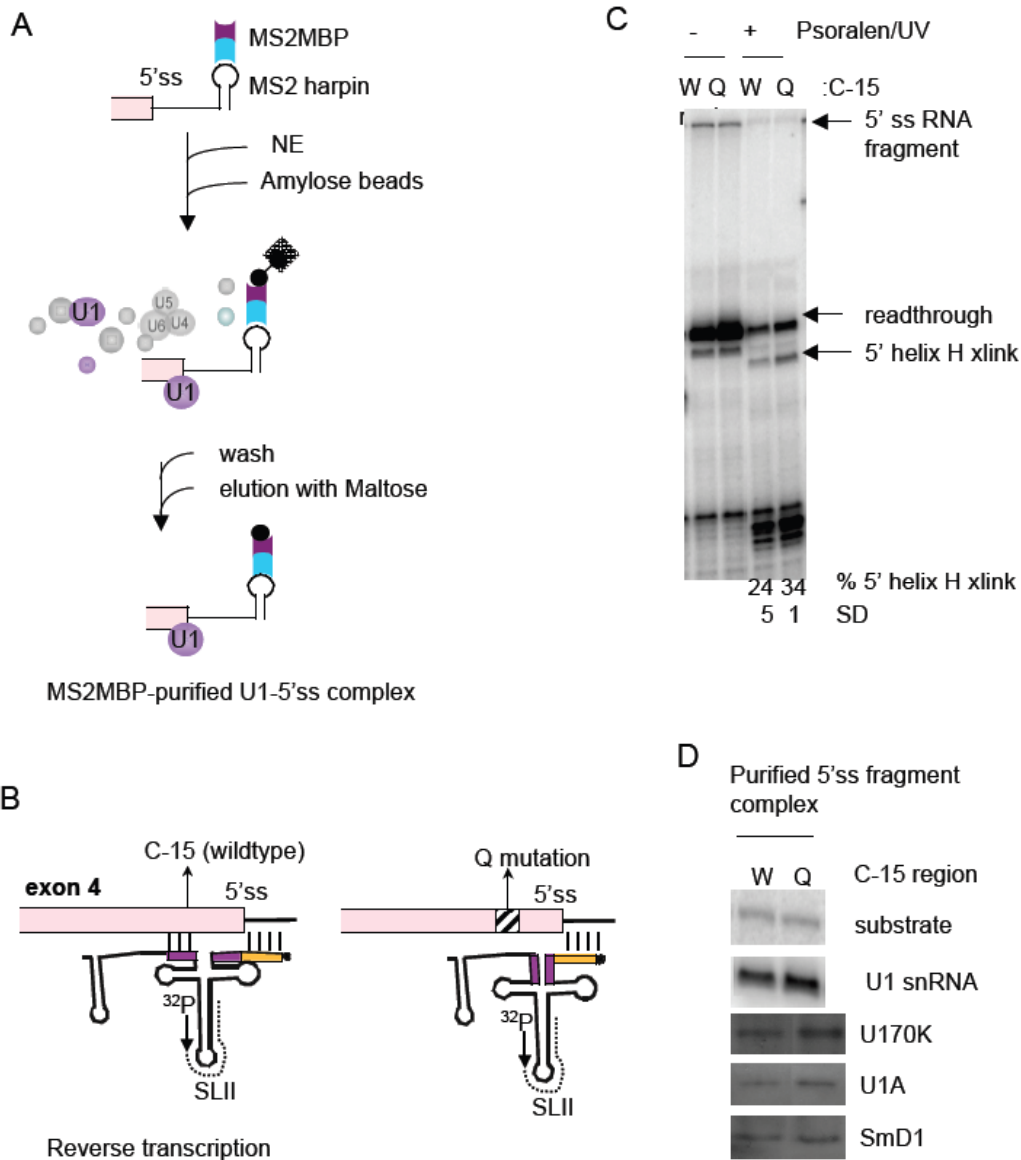
Figure 2.8 Disrupting association of the U1 snRNA with the 3' end of exon 4 increases the helical form of helix H in U1. (A) Schematic of MS2MBP purification of the U1-5'ss complexes. After incubating the MS2MBP-tagged 5'ss RNA with NE, the entire splicing reaction is immobilized onto the amylose beads followed by the steps of washing and elution. The 5'ss RNA fragment is the same as in Figure 2.5A. (B) Schematic of potential differences of the U1 helix H structure upon disrupting the extended U1 interaction by the QC9 mutation. Primer that targets to SLII in U1 was used for interrogating the psoralen-crosslinked sites of the U1 snRNA in the purified U1-5' ss complex. (C) Analysis of psoralen-crosslinked U1 snRNA. "Readthrough" and "5' helix H" are the products from the reverse-transcription of the non-crosslinked U1 snRNA or U1 RNA crosslined at helix H, respectively. % crosslinking is calculated from the ratio of 5' helix H xlink to readthrough. (D) Western blot analysis of the purified complexes assembled on the 5' ss RNA containing either wild-type (W) or mutant (Q) C-15 region.

2.5 The extended U1 interaction alters the structural flexibility of the U1 snRNA

The effects of the extended U1 interactions on the conformational changes of U1 snRNP in the purified U1-5' ss complex were further investigated. I used the strategy of RNA selective 2'-hydroxyl acylation analyzed by primer extension (SHAPE) to map the regions of the U1 RNA that displays differential flexibility upon disrupting the extended U1 interaction (Mortimer and Weeks, 2009).

After MS2-MBP affinity selection of the assembled complexes from the spliceosome assembly reactions (see the procedure in Figure 2.8A), the purified complexes were treated with benzoyl cyanide (BzCN) followed by the RNA extraction and primer extension (Figure 2.9A). The hydroxyl-selective electrophile of BzCN reacts with the flexible nucleotides to form the 2'O-adduct nucleotide (Figure 2.9B). By contrast, base-paired or otherwise conformationally constrained nucleotides are unreactive. Primer extension analysis of the 2'O-adduct formation in the U1 snRNA showed that the 5' helix H and stem loop I regions are more accessible on the wildtype than QC9 mutant substrate (Figure 2.9C). The fact that the 5' helix H is more flexible on wildtype substrate is consistent with the model in which the pairing interaction within the 5' helix H in U1 is disrupted to allow the formation of the extended U1 interactions in the C-15 region on the wildtype substrate (Figure 2.8B).
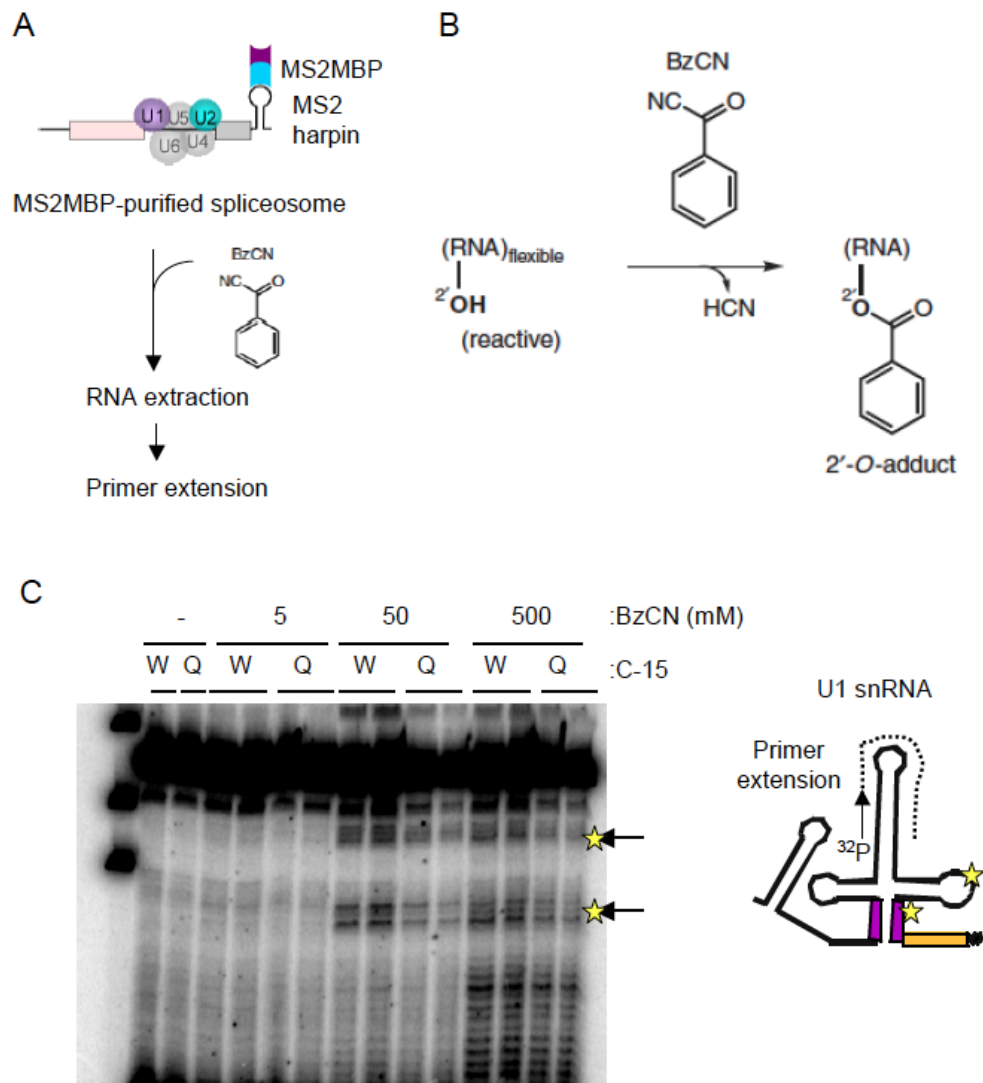
Figure 2.9 SHAPE analysis of the U1 snRNA in the absence or presence of the extended U1 interaction. (A) The schematic of SHAPE analysis of the MS2MBP-purified spliceosome. (B)The mechanism of RNA SHAPE chemistry with BzCN. BzCN reacts with 2'-hydroxyl groups at conformationally flexible positions to form a 2'-O-adduct. (C) SHAPE analysis of the purified U1-5' ss RNA complexes. Primer extension analysis of BzCN-treated purified U1-5'ss complexes. Arrows indicate the regions of U1 snRNA that show differential accessibility for reacting with BzCN in the wildtype versus QC9 mutant complexes.

**2.6 HnRNP L recruits hnRNP A1 to induce association of the U1 snRNA with the 3'
end of exon 4**

In the CD45 exon 4, the location of the ESS1 is 110 nt upstream of the 5' splice
site (Figure 2.1A). Other proteins that associate with the region nearby the C-15 region
could mediate the ESS1/hnRNP L-induced extended U1 interaction. To investigate the
presence of proteins in the vicinity of the U1-exon interaction, I synthesized a site-
specific-labeled repressed or derepressed substrate in which the G-16 nucleotide is
radiolabeled. Spliceosome complexes assembled on these substrates were crosslinked
with shortwave UV light followed by RNase digestion (Figure 2.10A). I observed two
proteins, a ~65 and ~35 kDa protein, that are crosslinked to the radiolabled G-16 in the
repressed but not derepressed substrate (Figure 2.10B). Using antibodies that are against
hnRNP L and A1 specifically immunoprecipitated the radiolabeled 65 and 35 kD protein,
respectively, from the UV-crosslinked complexes (Figure 2.10C). As hnRNP A1 is
specifically associated with the C-15 region on the repressed but not derepressed
substrate, hnRNP A1 could possibly mediate the ESS1/hnRNP L-induced extended U1
interactions.
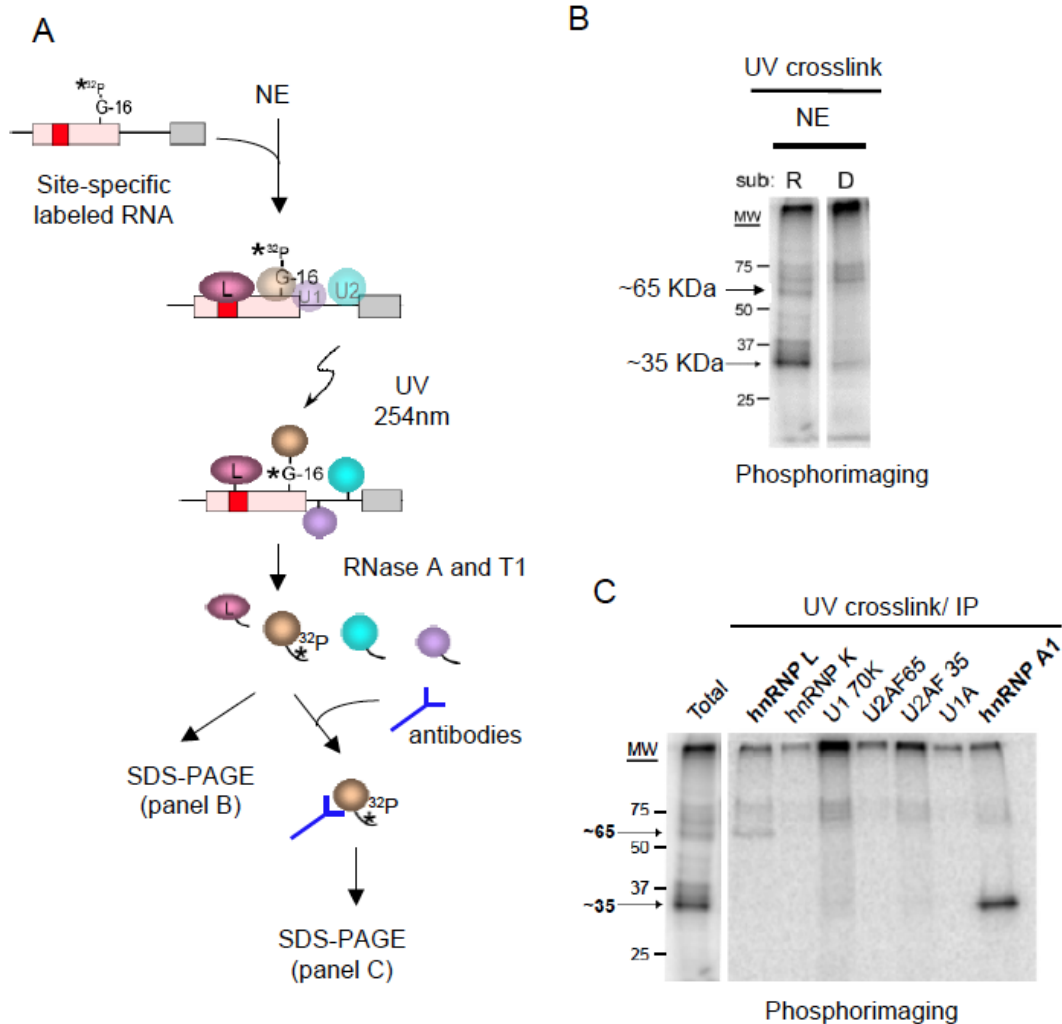
Figure 2.10 HnRNP A1 and L are crosslinked to the G-16 nucleotide in an ESS1-dependent manner. (A) Schematic of UV crosslinking assay. The site-specific labeled RNA containing a radiolabeled phosphate at G-16 is incubated with NE followed by UV254-irradiation, RNase digestion and SDS-page electrophoresis as in panel B. The crosslinked and RNase-digested reactions were also incubated with antibodies to immunoprecipiate the crosslinked proteins as in panel C. (B) Analysis of proteins crosslinked to G-16 nucleotide of the R or D substrates in a SDS-PAGE by phosphorimaging. (C) Analysis of the immunoprecipitated proteins in a SDS-PAGE by phosphorimaging.

Besides hnRNP A1 and L, there is a variable ~75 kDa band that is also crosslinked to G-16 (Figure 2.11A). Additionally, the binding of this 75 kDa protein is enhanced when U1 snRNP is depleted from nuclear extract (Figure 2.11A; -U1). This suggests that when U1 snRNP is vacated from the 5' splice site, it allows the binding of the 75 kDa protein into the C-15 region. Immunoprecipitation of UV crosslinked reactions using hnRNP M antibody showed that the 75 kDa protein is hnRNP M, a RNA-binding protein that prefers the poly-G or poly-U sequences (Figure 2.11B) (Huelga et al., 2012). Sequence analysis of the C-15 region showed that there is a stretch of poly U sequence downstream of C-15 (Figure 2.6B). However, further studies showed that the levels of hnRNP M in the C-15 region are not changed when the extended U1 interaction is disrupted (Figure 2.12B and C) or during the splicing repression or activation (Figure 3.3C and D). Thus, hnRNP M is considered to associate with the C-15 region when U1 snRNP is vacated from the C-15 region but not to be involved in inducing the extended U1 interactions or hnRNP L-mediated splicing repression.
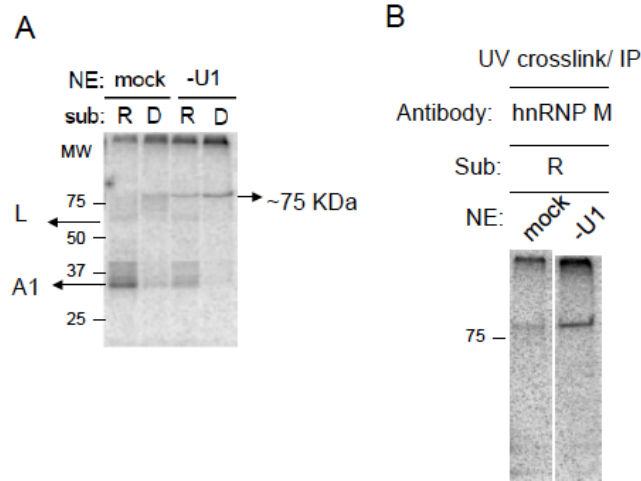
Figure 2.11 HnRNP M is crosslinked to the G-16 nucleotide when U1 snRNP is vacated from the 3' end of exon 4. (A) Analysis of proteins crosslinked to G-16 nucleotide of the R or D substrate in mock or U1-depleted NE. (B) Immunoprecipitation of the protein that was crosslinked to G-16 on the R substrate using hnRNP M antibody.

It has been shown that hnRNP L prefers the CA-rich RNA sequence for binding (Hui et al., 2005) whereas the consensus of hnRNP A1 binding site is UAGGGA/U (Burd and Dreyfuss, 1994). Analysis of the sequence around the G-16 nucleotide reveals that a UAGUG sequence element spanning from nucleotides -20 to -16 could be a weak hnRNP A1 binding site. (Figure 2.12A; UAGUG in blue box). To investigate whether hnRNP A1 mediates the extended U1 interactions at the C-15 region, I mutated the UAGUG sequence by replacing A by C nucleotide, which is predicted to disrupt the hnRNP A1 binding, but not alter the putative basepairing with the U1 snRNA (Figure 2.12A). Strikingly, this mutation not only abolishes crosslinking of hnRNP A1 to G-16 nucleotide (Figure 2.12B) but also reduces the C-15 crosslink and the U1-dependent supershifted-band (Figure 2.12C and D). Thus, binding of hnRNP A1 at the 3' end of exon 4 mediates the hnRNP L-induced extended pairing interactions of the U1 snRNA.
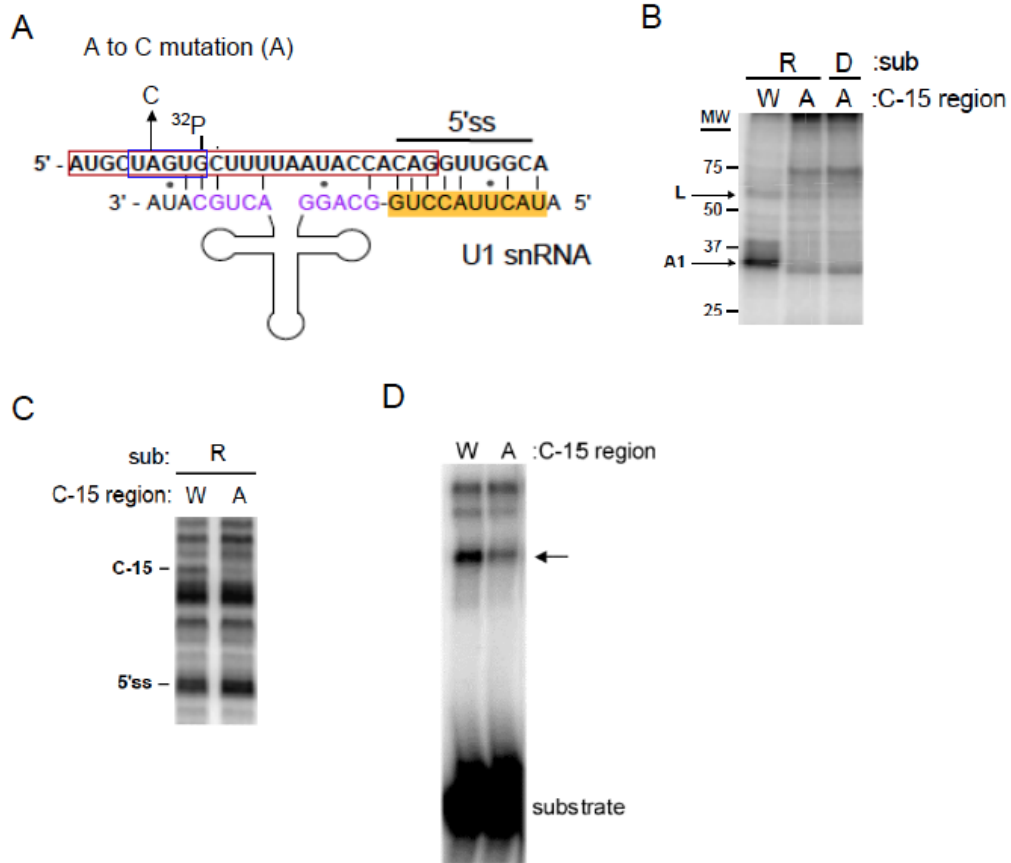
Figure 2.12 Binding of hnRNP A1 to G-16 is required for hnRNP L-induced extended U1 interaction in the C-15 region. (A) Schematic of the A-to-C mutation within the putative hnRNP A1 binding site (UAGUG in blue box) and the G-16 containing the radiolabeled phosphate. (B) UV crosslinking as in Figure 2.11A with the substrate containing wildtype (W) or A-to-C mutant (A) C-15 region. (C) Primer extension analysis of psoralen-crosslinked sites with primer R2 as in figure 2.4. (D) Supershift analysis of the psoralen-crosslinked RNAs as in figure 2.5.

2.7 HnRNP A1 and the U1 snRNA associate cooperatively with the 3' end of exon 4 in an ESS1-dependent manner

As mentioned in chaper 2.6, the UAGUG in the C-15 region is not a conserved binding sequence for hnRNP A1. As this binding site is nearby the 5' splice site, I set to investigate the correlation between the hnRNP A1 binding and the U1 snRNA association at the 3' end of exon 4. In chapter 2.3, the QC9 and U1up mutation have been shown to disrupt and enhance the extended U1 interactions, respectively, on the repressed substrate. The substrates containing these mutations were radiolabeled at G-16 followed by UV-crosslinking analysis. It showed that crosslinking of hnRNP A1 to G-16 is reduced by the QC9 mutation, whereas it is not interfered by the U1up mutation (Figure 2.13A). Additionally, in the absence of U1 but not U2 snRNP, hnRNP A1 binding at G-16 is abolished (Figure 2.14B). This demonstrates that U1 binding at the C-15 region enhances association of hnRNP A1 with the same region to mediate the extended U1 interaction. Therefore, hnRNP A1 and the U1 snRNP associate cooperatively with the 3' end of exon 4 in a manner that is dependent on the ESS1.
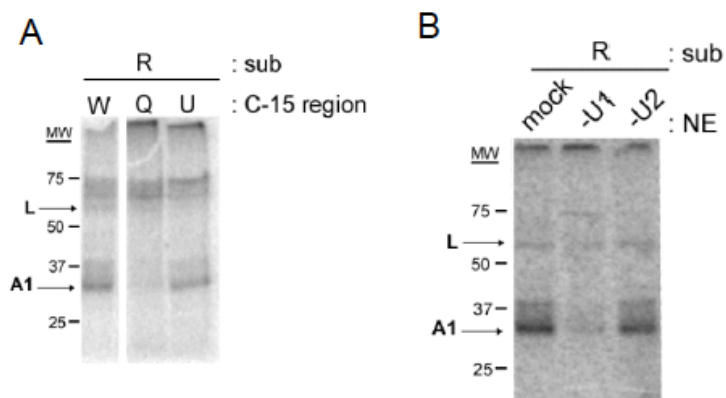
Figure 2.13 HnRNP A1 and U1 snRNA are cooperatively associated with the C-15 region. (A) UV crosslinking as in Figure 2.11A with the indicated substrate. (B) UV crosslinking as in Figure 2.11A with the repressed substrate incubated with the mock, U1 or U2-depleted NE.

2.8 The potential interactions between hnRNP L or A1 with the U1 snRNP

Although I have shown binding of hnRNP L and A1 in the ESS1 and C-15 region is correlated the extended U1 interaction (Figure 2.5 and 2.12), it is not known whether hnRNP L or A1 directly remodels the molecular interactions of U1 snRNP with the substrate. HnRNP A1 was shown to have both helix destabilizing and RNA annealing activities, such that hnRNP A1 promotes interconversion of RNA basepairing interactions (Grohman et al., 2013; Kumar and Wilson, 1990; Pontius and Berg, 1990). However, no specific substrate of hnRNP A1 RNA chaperon activity has yet been identified in the spliceosome. The direct interactions between hnRNP A1 and U1 snRNA might aid in inducing the extended U1 interaction with the substrate. Previously, PTB has been shown to bind directly to U1 snRNA to potentially alter the interaction of U1 snRNP with other spliceosome components (Sharma et al., 2011). To investigate the interactions between hnRNP proteins and the U1 snRNA, I analyzed the RNA components in the UV-crosslinked nuclear extracts that were immunoprecipitated by hnRNP L or LL-antibody (Figure 2.14A). It showed that there is no significant increased binding of L or LL protein with the U1 snRNA in a UV-dependent manner (Figure 2.14B). Therefore, future work would be to investigate whether hnRNP L or A1 interacts with the protein components of U1 snRNP to remodel its binding at the region around the 5' ss.
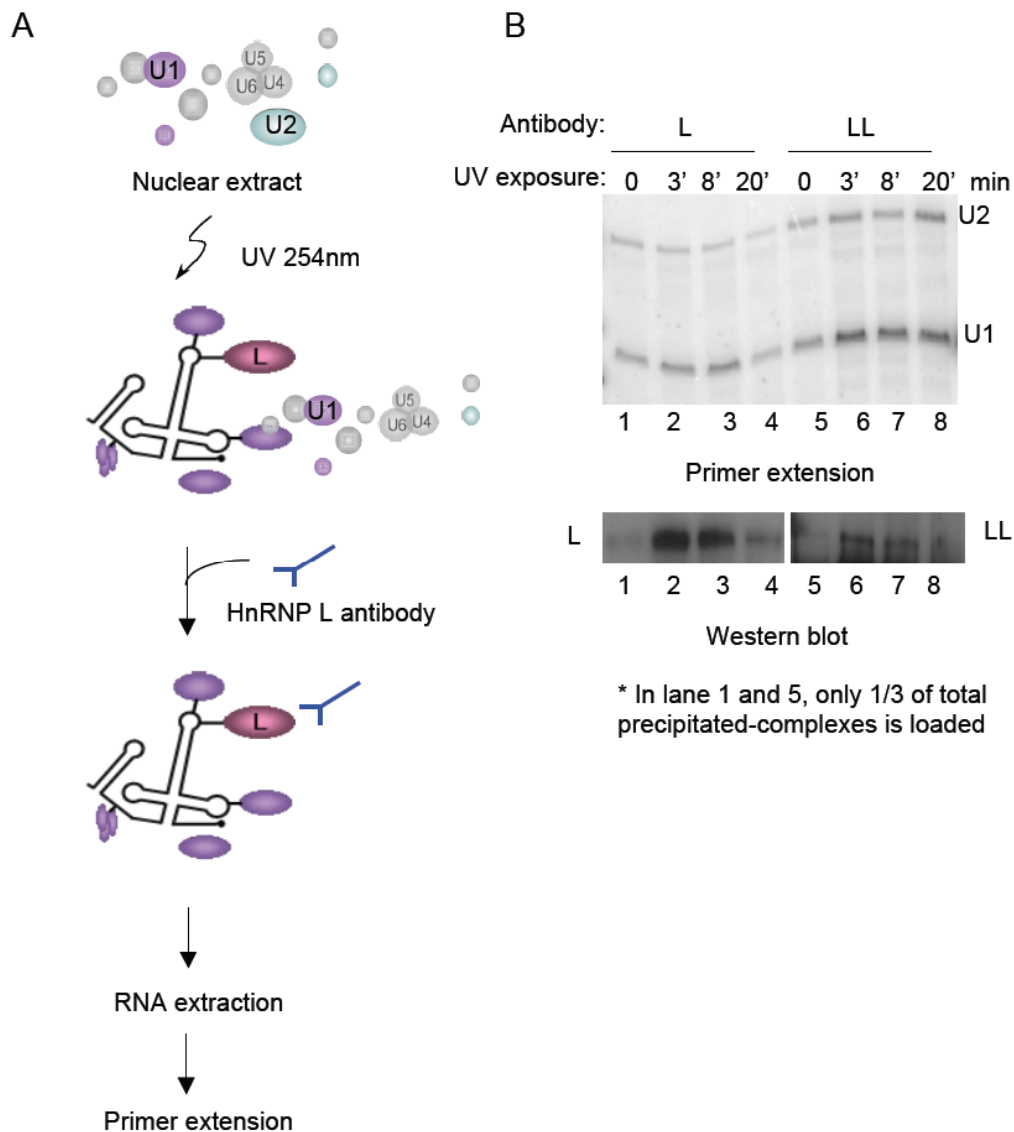
Figure 2.14 HnRNP L and L-like may not directly interact with the U1 snRNA. (A) Immunoprecipitation of hnRNP L from UV-crosslinked nuclear extract. The UV crosslinked NE was incubated with antibodies to immunoprecipitate the crosslinked RNA-protein complexes. The RNA components in the immunopreciptated, crosslinked complexes were extracted and analyzed by primer extension. (B) Analysis of levels of U1 and U2 snRNA by primer extension in hnRNP L or LL-antibody-precipitated UV-crosslinked complexes. The levels of the precipitated hnRNP L or LL proteins were detected by western blot. Because the antibodies precipitated more hnRNP L or LL protein from the non-UV-treated reactions, only 1/3 of the precipitated complexes were used for both the primer extension and western blot analysis.

2.9 Discussion

Previously, binding of hnRNP L to ESS1 was shown to be required for repressing the progression from the A to B complex and splicing. In this chapter, ESS1/hnRNP L is demonstrated to induce the cooperative binding of hnRNP A1 and the U1 snRNA with the 3' end of exon 4 within the hnRNP L-repressed A complex (Figure 2.15), which could potentially function in repressing spliceosome assembly and splicing catalysis. The pairing interaction between the 3' portion of helix H in U1 with the C-15 region is demonstrated by a series of biochemical approaches including U1-oligo-directed cleavage of the psoralen-crosslinked 5' ss RNA fragment (see chapter 2.3), psoralen-crosslinking analysis of the C-15 region mutant substrate (see chapter 2.4), and SHAPE analysis of the U1-5'ss complex (see chapter 2.5). Moreover, western blot analysis of the U1-5'ss complex showed that unwinding helix H in U1 to form the extended interaction does not interfere with association of the U1 snRNP proteins (see chapter 2.4). UV crosslinking analysis of site-specific-labeled RNA revealed that hnRNP L recruits hnRNP A1 to induce the extended U1 pairing interaction (see chapter 2.6 and 2.7). Although it is possible that hnRNP L or A1 directly interact with the U1 snRNA to induce the extended pairing interaction, immuno-precipitating the UV-crosslinked U1 snRNP by hnRNP L antibody did not reveal the crosslinking of hnRNP L to the U1 snRNA (see chapter 2.8). Future work will be required to identify the protein-protein interactions that allow hnRNP L at the ESS1 or hnRNP A1 at the 3' end of exon 4 to induce the extended conformation of U1 snRNP at the 5' ss.
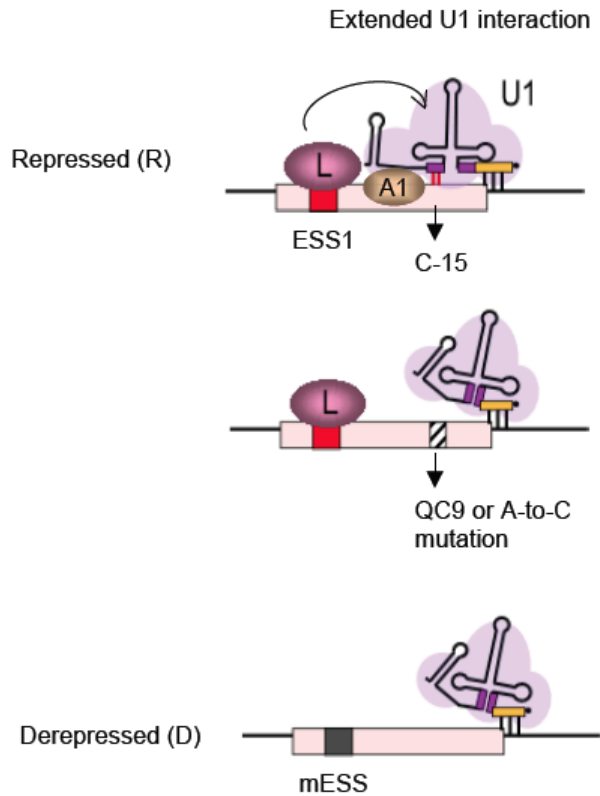
Figure 2.15 Model for recruitment of hnRNP A1 and the U1 snRNA to the 3' end of exon 4 by hnRNP L. HnRNP L recruits hnRNP A1 to the C-15 region, which induces the extended U1 interaction with the 3' end of exon 4 on the repressed substrate. By contrast, creating the QC9 and A-to-C mutations at the C-15 region or mutating ESS1 on the derepressed substrate disrupts association of hnRNP A1 and U1 snRNA with the 3' end of exon 4.

Chapter 3

HnRNP L recruits hnRNP A1 and the U1 snRNA to the 3' end of exon 4 to induce

the skipping of exon 4

In chapter 1, I showed that ESS1 represses the splicing of the downstream intron to induce the skipping of CD45 exon 4. In chapter 2, the exonic splicing silencer (ESS1) within CD45 exon 4 is shown to promote the extra interactions between U1 snRNP and the 3' end of exon 4. Forcing aberrant spliceosome interactions has been demonstrated to alter splicing efficiency in other systems. However, it is unknown whether the ESS1-induced U1 interaction at the 3' end of exon 4 is required for ESS1 to induce the skipping of exon 4. The goal of this chapter is to elucidate whether the naturally occurring additional U1 interactions at the exonic region contribute to hnRNP L/ESS1-dependent splicing repression.

3.1 Introduction: Forcing aberrant snRNP interactions with the pre-mRNA alters splicing efficiency

The spliceosome assembly processes involve a multitude of interactions between spliceosome components and the reactive regions of pre-mRNA, which ensure the fidelity of splice site selection (also see chapter 4.1). Growing evidence showed that the steps of the spliceosome assembly can proceed in both the forward and reverse directions (Tseng and Cheng, 2008). This reversibility suggests that modulating spliceosome interactions would alter the kinetic equilibrium between spliceosome assembly steps to affect splicing efficiency (Smith et al., 2008). Two well-characterized examples of kinetic

competition occur in the transition from U1 to U6 binding at the 5' splice site and the transition from the first to second catalytic step (Figure 3.1). The group of Jon Staley demonstrated that hyperstabilization of the pairing interactions between the U1 snRNA and the 5' ss represses the subsequent binding of U6 snRNP (Staley and Guthrie, 1999). Additionally, Charles Query's group showed that hyperstabilization or destabilization of the pairing interactions between U6 snRNA and the 5' ss modulates the equilibrium between the conformations of the first and second catalytic step (Konarska et al., 2006). Differential favoring of one assembly pathway over another can lead to changes of the ratio of spliced product to pre-mRNA. Therefore, the dynamic RNA-RNA interactions are potential points for modulating splicing efficiency and directing splice site choice.
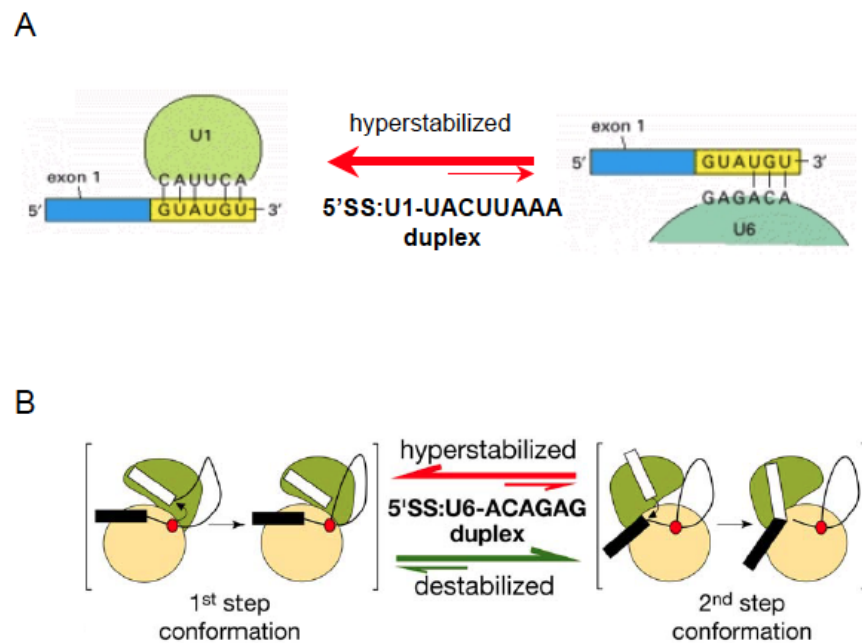
Figure 3.1 The spliceosome assembly steps proceed in both the forward and reverse directions. (A) Schematic of transition between U1 and U6 snRNP binding at the 5' ss. Mutating the sequence of the 5' splice site to extended the pairing interactions between U1 snRNA and the 5' ss hyperstabilizes U1 binding and represses the subsequent U6 binding. Adapted in part from Molecular Biology of the Cell, 4th edition. (B) Schematic of transition between the first and second catalytic step. Hyperstabilization and destabilization of the 5'ss-U6 duplex favors the conformation of the first and second step, respectively. Adapted in part from other figures (Konarska et al., 2006).

3.2 Association of hnRNP A1 and U1 with 3' end of exon 4 is required for ESS1/hnRNP L-mediated splicing repression *in vitro* and in cells

To investigate whether the extraneous U1 snRNP association with the exonic region also functions in altering splicing efficiency, the *in vitro* splicing assays were performed with the substrates containing mutations that disrupt binding of A1 and U1 at the C-15 region (Figure 3.2A and B). Remarkably, the splicing of the 2-exon-pre-mRNA and the inclusion of CD45 exon 4 on the 3-exon pre-mRNA are increased by ~2 fold when the C-15 region contains the Q or A mutation.
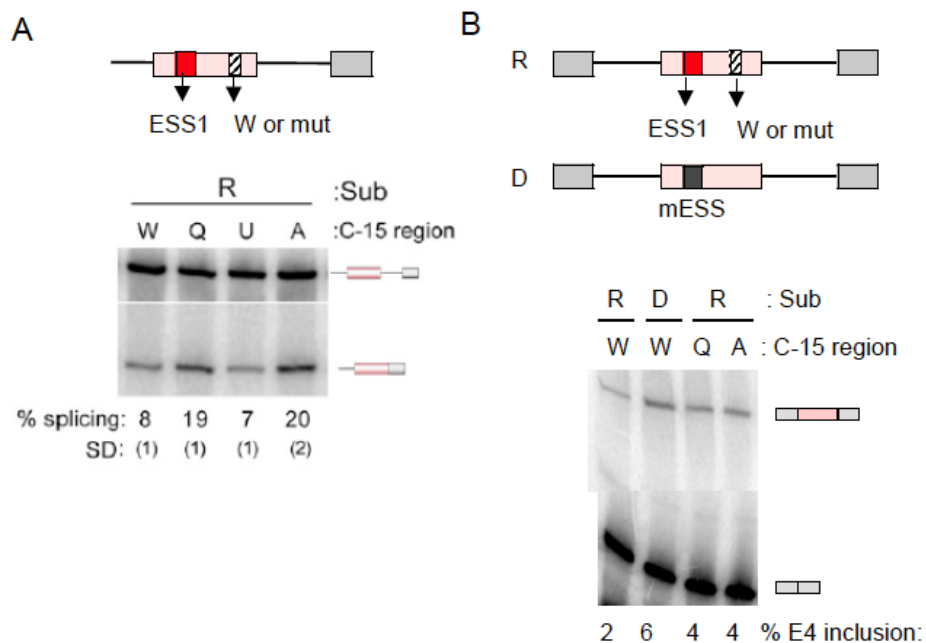
Figure 3.2 HnRNP A1 and U1 interactions at the C-15 region are required for ESS1-mediated splicing repression in vitro. (A) Top, schematic of the 2-exon repressed substrate containing wildtype or mutated C-15 region (Q, A, U as defined in Figure 2.7A). Bottom, RT-PCR analysis of the *in vitro* splicing assay using radiolabeled primers, as in Figure 1.9D. (B) Top, schematic of 3-exon repressed substrate containing wildtype or mutated C-15 region or derepressed substrate. Bottom, RT-PCR analysis of the *in vitro* splicing reactions using radio-labeled primers.

To further investigate the importance of the molecular interactions at the 3'end of exon 4 in splicing repression, I designed an anti-sense 2'O-methyl oligonucleotide that is complementary to the sequences spanning -24 to -13 of exon 4 to block the association of hnRNP A1 and the U1 snRNA with the C-15 region (Figure 3.3A; anti-E4). Pre-incubating the anti-E4 oligo with the pre-mRNA substrate under splicing conditions abolishes the psoralen-induced C-15 crosslink and the UV-induced crosslinking of hnRNP A1 to G-16 nucleotide (Figure 3.3B and C). Importantly, in the presence of anti-E4 oligo, the increase in splicing is more for the repressesd versus derepressed substrate (Figure 3.3D). Therefore, binding of A1 and U1 at the C-15 region specifically mediates the splicing repression of the ESS1-repressed substrate but not depressed substrate.
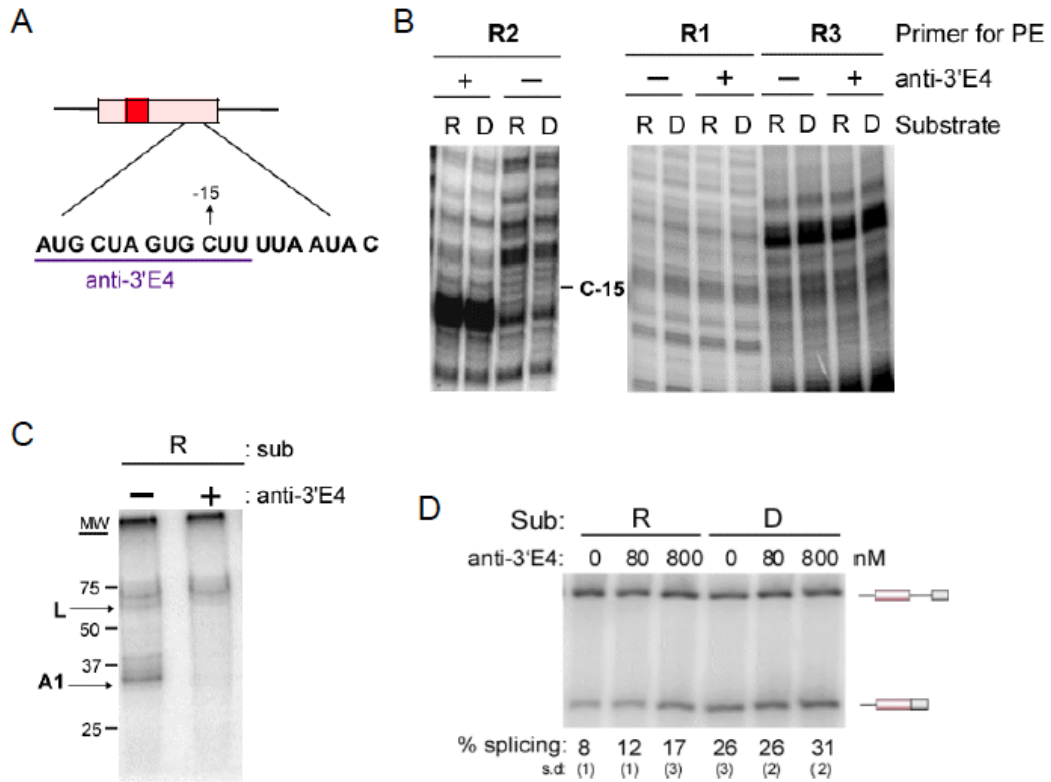
Figure 3.3 Blocking association of hnRNP A1 and U1 with the 3' end of exon 4 by an anti-sense oligo disrupts ESS1-medaited splicing repression. (A) Schematic of 2'O-methyl anti-3'E4 oligo pairing with exon 4. (B) Primer extension analysis of psoralen-crosslinked sites of complexes in the splicing reactions using indicated primers as in Figure 2.4. In the splicing reactions, the substrates were treated with (+) or without (-) the anti-3'E4 oligo followed by incubating in the NE. (C) UV crosslinking analysis as in Figure 2.11 in the presence (+) and absence (-) of the anti-3'E4 oligo. (D) *In vitro* splicing of the substrates that are pre-incubated with indicated concentration of the anti-3'E4 oligo.

Previously, binding of hnRNP L to ESS1 has been shown to repress the splicing of the upstream intron by blocking the progression from the A to B complex (Figure 3.4A and B). Notably, the anti-E4 oligo does not enhance the splicing of the upstream intron on the ESS1-repressed substrate (Figure 3.4C and D). This indicates that the mechanism by which ESS1 regulates spliceosome assembly and splicing repression of the upstream intron does not require the molecular interactions at the C-15 region.
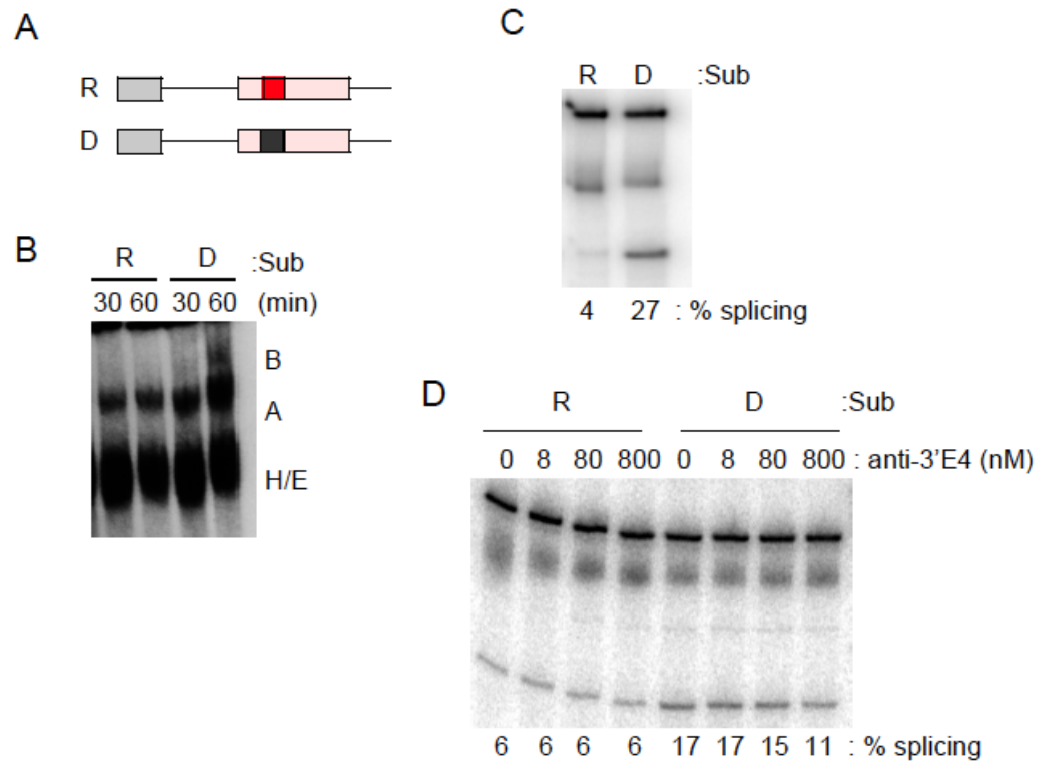
Figure 3.4 Blocking association of hnRNP A1 nd U1 with the 3' end of exon 4 does not overcome the ESS1-mediated splicing repression on the upstream intron. (A) Schematic of the 2-exon substrates in which exon 4 is flanked by the upstream exon. (B) Spliceosome assembly assays as in Figure 1.10. (C) *In vitro* spilcing assays as in Figure 3.2A. (D) *In vitro* splicing of the substrates that are pre-incubated with the indicated concentrations of the anti-3'E4 oligo.

To investigate the effect of the association of hnRNP A1 and the U1 snRNA with exon 4 in cells, the 3-exon CD45 minigenes containing wildtype or mutated C-15 region were delivered into JSL1 cells (Figure 3.5A; top). The 3-exon CD45 minigenes have been demonstrated to recapitulate the hnRNP L/ESS1-mediated skipping of exon 4 (Figure 1.8). The QC9 and A-to-C mutations in the C-15 region reduce the skipping of CD45 exon 4 in cells (Figure 3.5A; bottom). Moreover, knockdown of either hnRNP L or A1 results in a reduction in exon 4 skipping in the 3-exon pre-mRNA expressed from the minigene (Figure 3.5B and C). Notably, the U1up mutation that has been shown to increase the C-15 crosslink does not further repress the splicing of exon 4 either in vitro or in cells (Figure 3.2A and 3.5A). Our explanation is that the presence of ESS1 has already made the maximal splicing repression of exon 4. Moreover, other positive factors, such as SR protein, have been shown to function in enhancing exon 4 splicing. Further strengthening the aberrant U1 interaction by U mutation may not overcome the positive effects induced by these SR proteins such that U mutation cannot induce further repression beyond the silencing activity of ESS1.
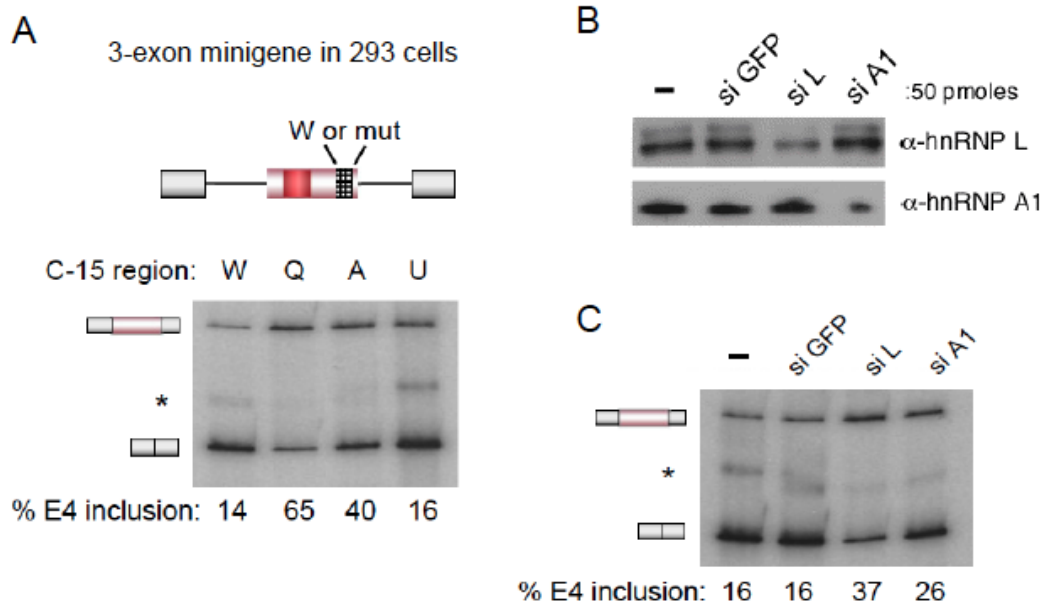
Figure 3.5 Association of hnRNP A1 and U1 with the 3'end of exon 4 is required for ESS1- and hnRNP L-induced skipping of exon 4 in cells. (A) Top, schematic of the CD45 exon 4 minigene containing wildtype or mutated C-15 region. Bottom, RT-PCR analysis of the splicing of the indicated minigenes expressed in 293 cells. (B) Knockdown efficiency of hnRNP L and A1 for experiments in panel C. (C) RT-PCR analysis of the splicing of the wildtype exon 4 minigene expressed in 293 cells transfected with nothing (-), siRNAs to hnRNP L (si L), hnRNP A1 (si A1) or GFP as a control.

3.3 MS2-tethering system for studying the silencer activity of hnRNP L

In chapter 3.2, I investigated the splicing silencing activity of hnRNP L through comparing the splicing efficiency of the substrate containing CD45 exon 4 ESS1 versus mESS. The three point mutations within the ESS1 element generate the mESS sequence and disrupt binding of hnRNP L. Although the most dominant protein that associates with the ESS1 element is hnRNP L, other RNA binding proteins, such as hnRNP L-like (hnRNP LL) and hnRNP E2, also associate with ESS1. Moreover, binding of these proteins also can be disrupted by the three point mutations within the ESS1 sequence (Rothrock et al., 2005; Topp et al., 2008).

To directly study the silencing activity of hnRNP L, Dr. Ganesh Shankarling in the Lynch lab set up the MS2-tethering system, an ESS1-independent splicing assay, to recapitulate hnRNP L-induced exon skipping. In the MS2-tethering system, the MS2-exon 4 minigene is created by replacing the ESS1 element on CD45 exon 4 with an MS2-hairpin sequence and hnRNP L is expressed as an MS2 fusion protein (Figure 3.6A). Expression of MS2-hnRNP L fusion protein specifically repressed the inclusion of the exon containing the MS2-hairpin sequence but not the exon with the mutated MS2-hairpin (Figure 3.6B and C). Therefore, MS2-hnRNP L specifically represses the inclusion of MS2-exon 4 by binding to the MS2-hairpin sequence within the exon.
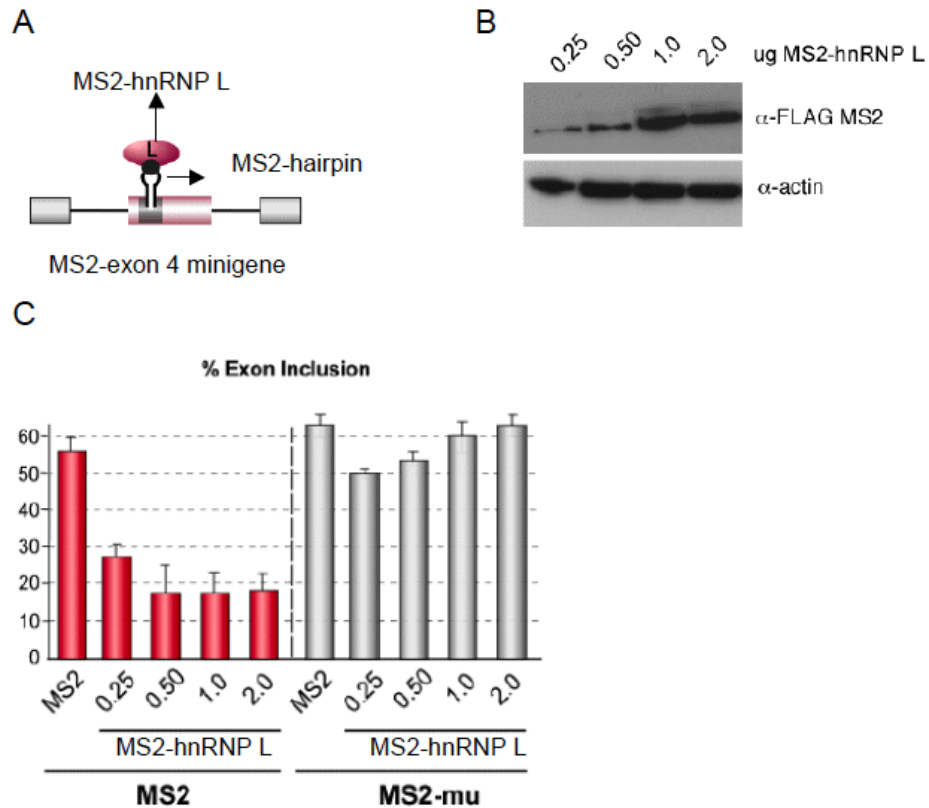
Figure 3.6 MS2-tethering system for studying hnRNP L-regulated alterantive splicing. (A) Schematic of MS2-tehtering system. MS2-hnRNP L fusion protein specifically associates with the MS2-hairpin-containing exon of the 3-exon pre-mRNA. (B) The expression levels of MS2-hnRNP L proteins in 293 cells transfected with the indicated amount of an MS2-hnRNP L expression construct. (C) Specific and robust repression of exon inclusion via the MS2-hnRNP L fusion protein. Quantification of RT-PCR analysis of the splicing in 293 cells expressing different levels of MS2-hnRNP L. Additionally, the 293 cells are also transfected with either wildtype-MS2-hairpin-containing minigene (MS2) or the minigene in which the MS2-hairpin sequence is mutated (MS2-mu) and thus does not bind MS2 fusion protein.

To directly link the molecular interactions within the C-15 region to the silencing activity of MS2-hnRNP L, the C-15 region within the MS2-exon 4 is further mutated to determine whether hnRNP A1 and the U1 snRNA binding at the C-15 region is required for MS2-hnRNP L-mediated splicing repression in the MS2-tethering system. Importantly, the skipping of MS2-exon 4 is reduced upon introducing QC9 or A-to-C mutation into the C-15 region or upon knockdown of hnRNP A1 (Figure 3.7A and B). Therefore, MS2-hnRNP L induces the skipping of MS2-exon 4 by the same mechanism, as does hnRNP L bound to the ESS1 within CD45 exon 4.
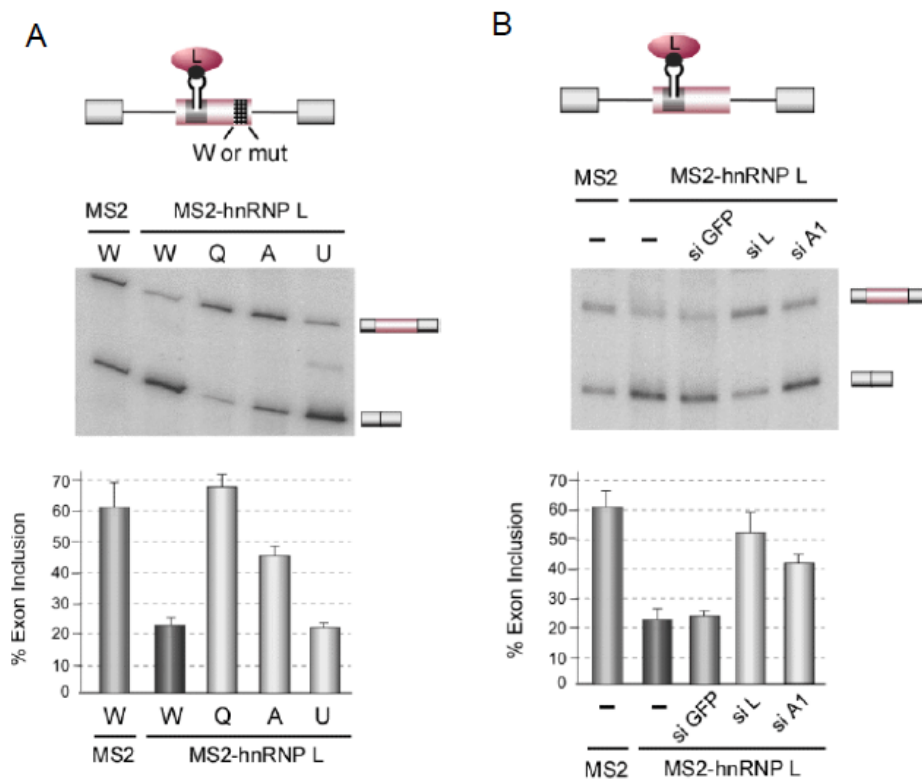
Figure 3.7 The sequence integrity of the C-15 region and hnRNP A1 are required for MS2-hnRNP L-mediated splicing repression in the MS2-tethering system. (A) Top, RT-PCR and bottom, quantification of the skipping of exons containing wildtype or mutated C-15 region in an MS2-tethering system. (B) Top, RT-PCR and bottom, quantification of the skipping of wildtype exons regulated via MS2-hnRNP L upon knockdown of hnRNP A1 or L.

3.4 The linker region of hnRNP L recruits hnRNP A1 and is required for exon repression

The MS2-tethering system described in chapter 3.3 is a robust tool for dissecting the protein domains of MS2-hnRNP L that are involved in regulating alternative splicing. As described in the chapter 2.9, I showed that the crosslinking of hnRNP A1 to G-16 nucleotide is dependent on the ESS1 element within CD45 exon 4. Moreover, addition of excess recombinant hnRNP L into the UV crosslinking assays promotes association of hnRNP A1 with G-16 (Figure 3.8A). This indicates that the domains of hnRNP L that are involved in recruiting hnRNP A1 to G-16 could be required for inducing exon skipping.

To determine the domains of hnRNP L that are involved in association with hnRNP A1, Dr. Ganesh Shankarling in the Lynch lab used epitope-tagged hnRNP L that is expressed in cells to precipitate hnRNP A1 from cell extract. Interesting, the ability of hnRNP L to co-precipitate hnRNP A1 depends on a proline-rich linker sequence within hnRNP L (Figure 3.8B and C). To further demonstrate that the interaction between hnRNP L and A1 is required for silencer activity of hnRNP L, different domain deletion was created within MS2-hnRNP L in the MS2-tethering system. Specifically, deletion of the proline-rich linker sequence disrupts MS2-hnRNP L-mediated repression of exon inclusion whereas deletion of other sequences that are not required for binding to hnRNP A1 has no effect on the repression activity of hnRNP L (Figure 3.8D). Therefore, it suggests that hnRNP L recruits hnRNP A1 to the C-15 region via its proline-rich linker domain to induce the skipping of exon 4.
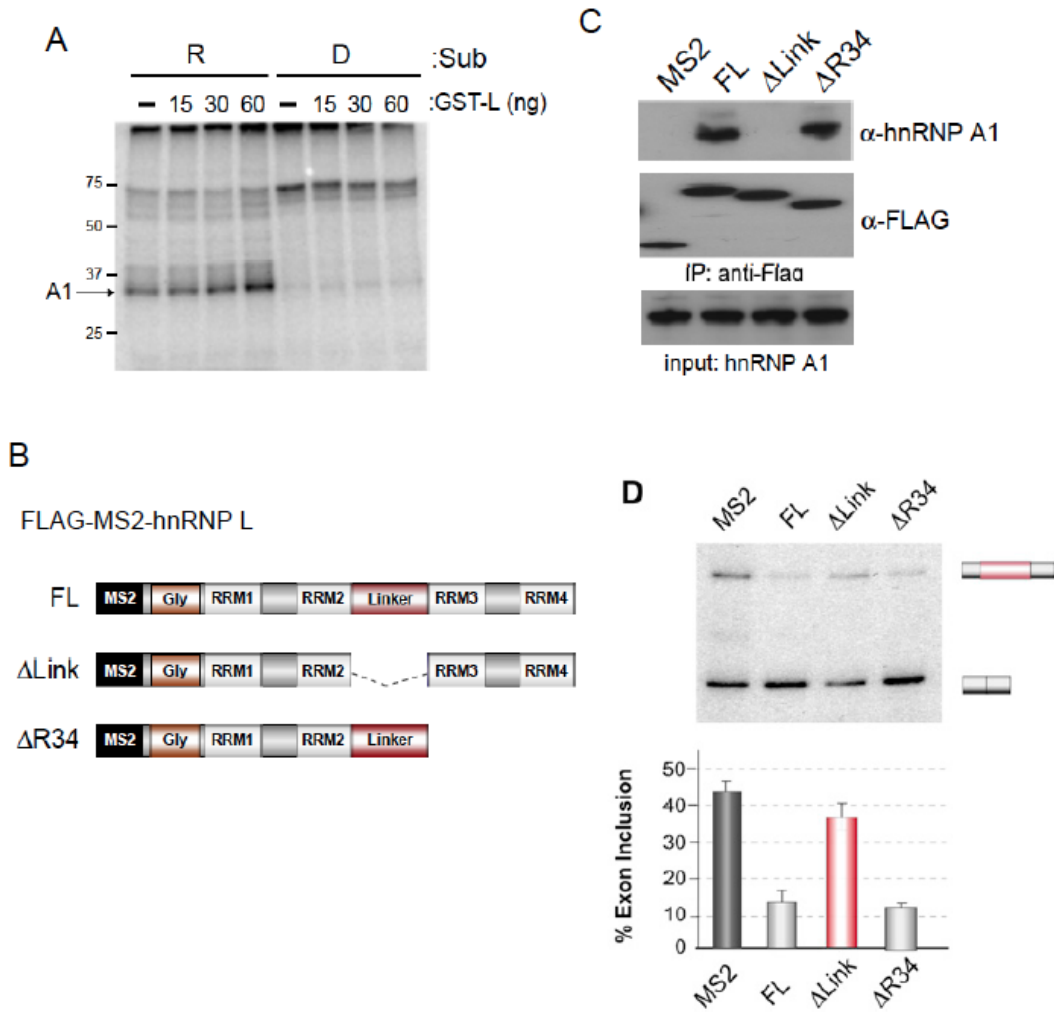
Figure 3.8 The linker domain of hnRNP L interacts and recruits hnRNP A1 to exon 4 to achieve splicing repression. (A) UV crosslinking analysis as in Figure 2.10 in the presence of indicated amount of purified, recombinant GST-L. (B) Schematic of hnRNP L domains included in MS2 fusion proteins. FL contains the completed hnRNP L protein sequence fused downstream of the MS2 protein as used in Figure 3.6. ΔLink lacks the hnRNP L sequence between RRM2 and 3. ΔR34 lacks all RRM 3 and 4. (C) Co-precipitation of hnRNP A1 with hnRNP L. Flag-MS2 control or Flag-MS2-hnRNP L containing various domain deletion shown in panel B was expressed in 293 cells followed by immunoprecipitation using anti-FLAG-antibody. The co-precipitated hnRNP L and hnRNP A1 proteins were analyzed with anti-hnRNP A1 or anti-FLAG antibodies. (D) RT-PCR (Topp et al.) and quantification (bottom) of the skipping of wildtype MS2-exon 4 as in Figure 3.6, comparing the activity of the indicated MS2-hnRNP L deletion mutants relative to full-length.

3.5 Induction of extended U1 interaction may play a general role in regulating alternative splicing

An important question from these data is whether the hnRNP L and A1-induced extended pairing of U1 snRNA is unique to exon 4 or may play a more general role in splicing regulation. It has been shown that PSI regulates the splicing of P-element by directly interacting with U1 snRNP 70K protein and hrp48, a protein similar to the mammalian spicing factor hnRNP A1 (Labourier et al., 2001; Siebel et al., 1992; Siebel et al., 1994). The hnRNP A1-mediated induction of the extended U1 pairing with the substrate may be responsible for the splicing regulation of P-element. Moreover, recently, the group of Gene Yeo performed a genome-wide analysis of hnRNP A1 binding sites and hnRNP A1-regulated alternative splicing events by Clip-seq and micrrarrary-detection of variable exons (Huelga et al., 2012). These studies revealed that hnRNP A1 dominantly binds within the 3' terminal 50 nucleotides of exons. Additionally, binding of hnRNP A1 to this region correlates with the its activity to induce the skipping of the exon (Figure 3.9). Such biased localization of hnRNP A1 suggests that fostering extended interactions of the 5' splice site bound U1 snRNA with neighboring exonic sequences may be a widespread mode of hnRNP A1 action.

Genome-wide analysis of hnRNP A1 binding sites
within the exons it regulates
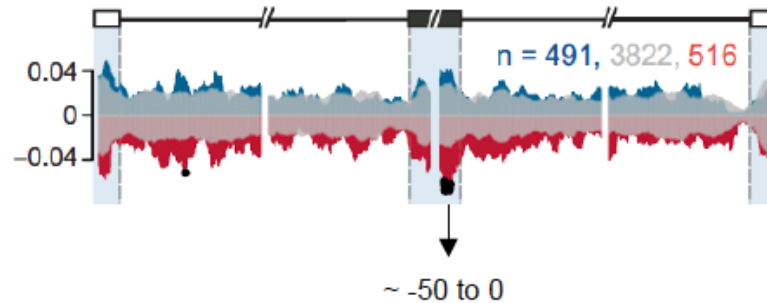
Figure 3.9 HnRNP A1 binds significantly at the 3'end of the exons it represses. RNA splicing maps showing the fraction of microarray-detected cassette exons with CLIP-seq reads located proximal to activated (positive y axis, blue), represses (negative y axis, red), and unaffected cassette exons (reflected on positive and negative y axis, transparent gray). Light blue shading sequences in the cassette exon (middle left, 0 to 50; middle right, -50 to 0). Black dots represent nucleotide positions where significantly more hnRNP-A1-repressed cassette exons showed binding. Adapted in part from (Huelga et al., 2012).

To investigate the generality of the inducible U1 interaction in regulating alternative splicing, I further analyze the sequences within the 3' end of the variable exons from Chemokine receptor 6 (CCR6) and Globin gene that are regulated by hnRNP A1 and L, respectively (Huelga et al., 2012; Rothrock et al., 2005). Surprisingly, both of the variable exons from these two genes contain the sequences that are potentially involved in pairing with the 3' helix H region of U1, which could result in inducing the extended pairing interactions from the 5' splice site bound U1 snRNP (Figure 3.10). Comparison of the sequences of other exons regulated by hnRNP L and A1 will be required for identifying more exons that are potentially regulated by inducting extended U1 interactions.
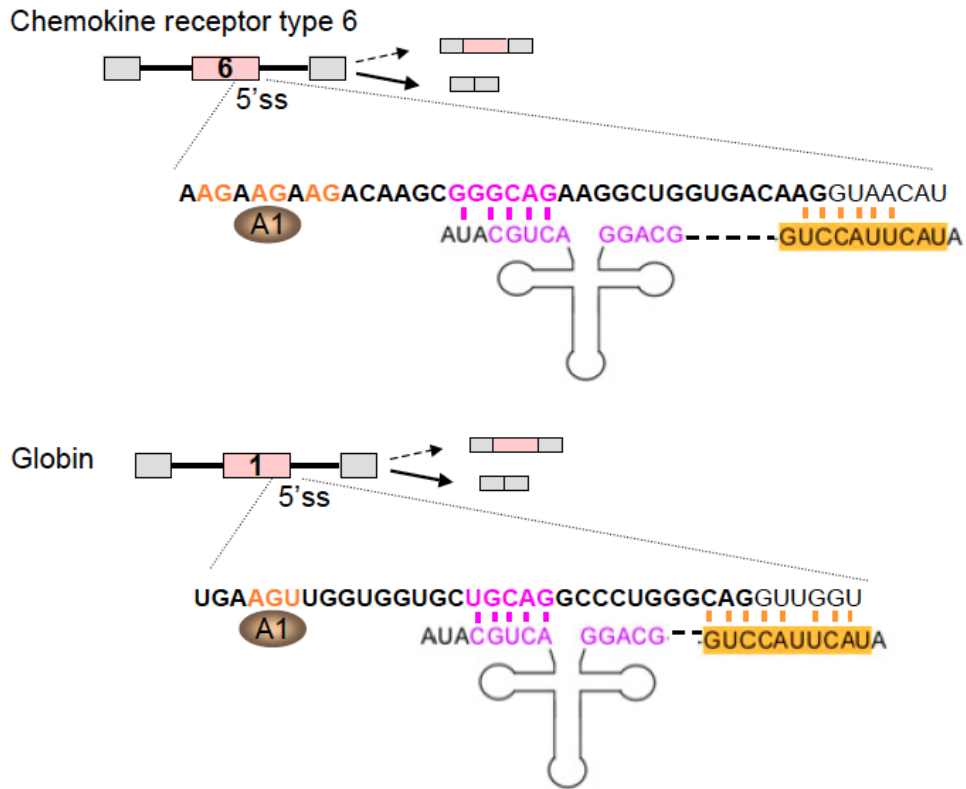
Figure 3.10 Induction of the extended U1 interaction with substrate may be the mechanism for hnRNP L and A1 in inducing the skipping of other variable exons. Sequence analysis of the 3' end of the variable exons in Chemokine receptor type 6 and Globin gene. The sequences within the exon that could be potentially associated with hnRNP A1 and 3' helix H of the U1 snRNA are in orange and pink color, respectively. The sequences in bold text are in the exonic region. The sequences of the 5' splice site are paired with the 5'end of the U1 snRNA (yellow box in U1).

As the splicing of Globin exon 1 can be regulated by hnRNP L and the 3' exon of Globin exon 1 also contains the UGCU motif that could potentially base-pair with the U1 snRNA (Figure 3.11A; pink region of globin E1 5' ss), I performed the psoralen crosslinking assays with the 5'ss RNA fragment from the Globin exon 1. Unfortunately, although there is an U1-dependent U+2 crosslink at the 5'ss, there are no crosslinks upstream of the Globin 5'ss that are dependent on the U1 snRNP in nuclear extract (Figure 3.11B). Supershift assays also revealed that the psoralen-crosslinked 5' ss RNA fragment from Globin exon 1 lacks the supershifted band that contain the U1 snRNA crosslinked to the 3' end of exon (Figure 3.11C). It is very likely that the sequences flanking the UGCU motif influence the psoralen-crosslinking efficiency at the 3' end of Globin exon 1. However, it is still possible there are contacts between the U1 snRNA and the Globin exon which are required for hnRNP L-dependent splicing repression. Therefore, future work will be to determine whether the splicing of Globin exon 1 or CCR6 exon 6 is dependent on the integrity of the sequences within the 3' end of these exons.

A

CD45 E4 5'ss   UGGAUAAUGCUAGUGCUUUUAAUACCACAGGUUGGCACA

Globin E1 5'ss   UGAAGUUGGUGGUGCUGCAGGCCCUGGGCAGGUUGGUAUC

B

Sub: CD45 E4 5'ss   Globin E1 5'ss

NE: mock -U1   mock -U1

C-15 —

G+5 —   —U+2

C

Sub: CD45 E4 5'ss   Globin E1 5'ss

NE: mock -U1   mock -U1

U1-5'ss interaction

U1-C-15 interaction
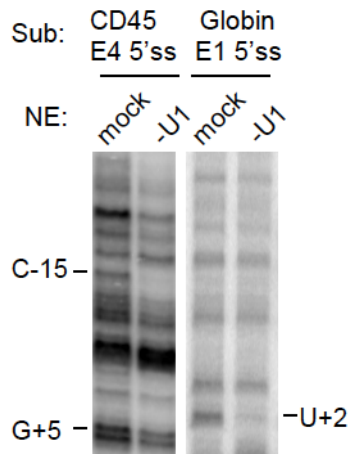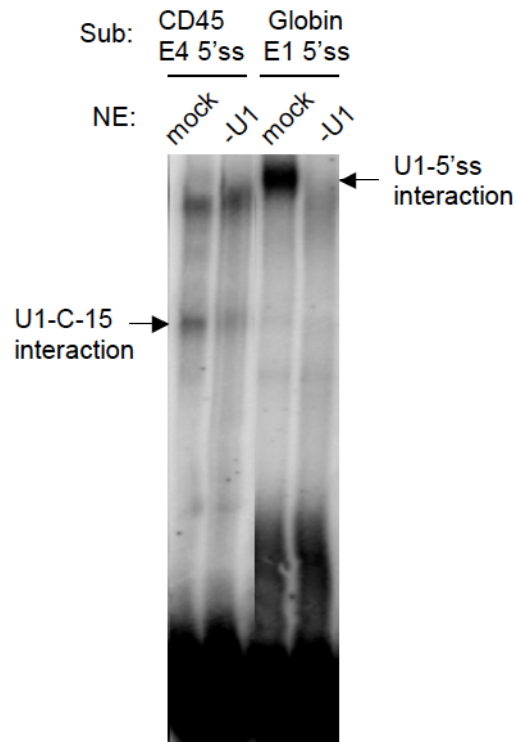
Figure 3.11 Interrogation of the U1-dependent crosslinks at the 3' end of Globin exon 1 by psoralen crosslinking assays. (A) Comparison of the sequences around the 5' ss between CD45 exon 4 and globin exon. (B) Primer extension analysis of psoralen-crosslinked sites with primer R2 as in Figure 2.4. Here, the 5'ss RNA fragments of CD45 exon 4 and globin exon 1 were used for the psoralen crosslinking assays. The 5' ss RNA fragment of exon 4 and globin exon are spanning from -45 to +76 and from -47 to +74, respectively. (C) Supershift analysis of the psoralen-crosslinked 5' ss RNA fragment as in Figure 2.5C.

3.6 Discussion

In chapter 2, hnRNP L and hnRNP A1 are shown to together induce the extraneous U1 interaction with the exonic region. In this chapter, the hnRNP L/A1-induced U1-exon interaction is further demonstrated in repressing the splicing of the downstream intron of CD45 exon 4, which results in enhancing the splicing of the intron between the upstream and downstream exon (Figure 3.12).
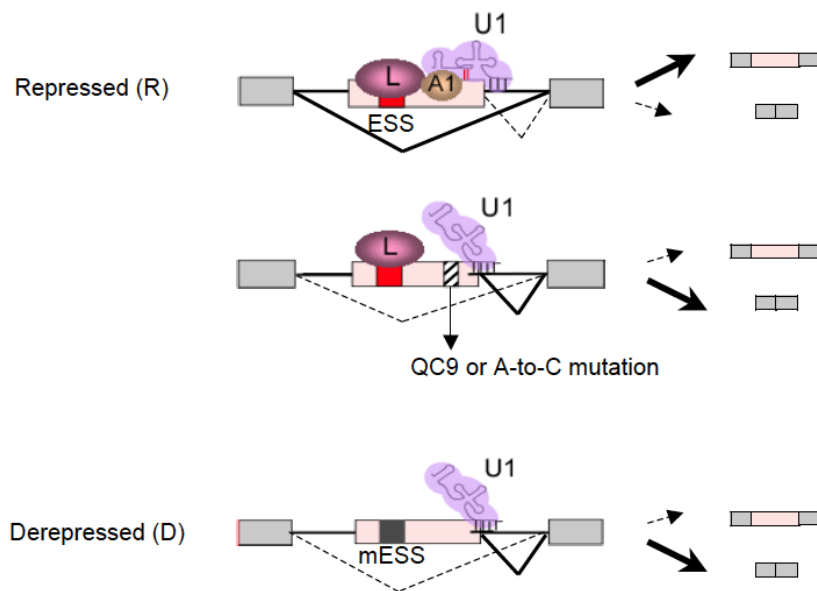
Figure 3.12 Model for association of hnRNP A1 and the U1 snRNA with the 3'end of exon 4 in repressing the splicing of exon 4. Association of hnRNP A1 and the U1 snRNA with the 3' en of exon 4 is required for hnRNP L in inducing the skipping of exon 4. Creating QC9 and A-to-C mutations at the C-15 region or mutating ESS1 disrupts hnRNP L-induced exon skipping.

To provide this model, the splicing of 2-exon and 3-exon pre-mRNA containing different mutant sequences at the C-15 region was analyzed *in vitro* and in cells (see chapter 3.2). Moreover, MS2-tethering system was established to demonstrate that the linker region of hnRNP L recruits hnRNP A1 to repress the inclusion of exon 4 (see

70

chapter 3.3 and 3.4). Finally, sequence analysis of the 3' end of the other two exons that are regulated by hnRNP L or A1 showed that the extraneous U1 pairing interactions could occur on these exons (see chapter 3.5).

All of the evidence described above comes from mutating the pre-mRNA substrate to block the U1 snRNA binding at the C-15 region. As a complementary approach, creating mutations into the U1 snRNA will be required to fully prove the model as described in Figure 3.12. To demonstrate pairing interactions within the 3' portion of helix H in U1 is involved in splicing repression, the U1 snRNA carrying mutations at the 3' portion of helix H while keeping helical form of helix H will be expressed in cells. This type of informational suppression analysis is known as suppressor U1 experiments (Roca and Krainer, 2009; Zhuang and Weiner, 1986). Besides creating mutations into the 3' portion of helix H, the compensatory mutations in the 5' portion of helix H should also be made to keep helical form of helix H. The simplest way to mutate U1 snRNA is to flip the 5' portion and 3' portion of helix H in U1. Expression of the suppressor U1 snRNA in cells will compete with the endogenous U1 snRNA to bind to the 5' ss. If expression of the suppressor U1 snRNA enhances the inclusion of wild type CD45 exon 4 but not the exon containing mutant sequence at the C-15 region, it will further support that the 3' portion of helix H in U1 is required for repressing the inclusion of exon 4 by pairing with the C-15 region.

Chapter 4

HnRNP L and A1-induced extended U1 interaction blocks the catalytic complex

formation by repressing the U1/U6 exchange at the 5'splice site

In the chapter 2 and 3, hnRNP L is shown to repress splicing by inducing an extended U1 interaction at the 3' end of CD45 exon 4. Along the spliceosome assembly pathway, the RNA-RNA and RNA-protein interactions are extensively rearranged to allow splicing to occur. It is unknown how hnRNP L-induced extended U1 interaction blocks the spliceosome assembly to repress splicing. Therefore, as described in this chapter, I next set out to identify the spliceosome complexes, components or interactions that are altered by the hnRNP L-induced extended U1 interaction. These aberrant spliceosome interactions are further investigated to understand how they are regulated by hnRNP L to block the formation of the catalytically active spliceosome.

4.1 Introduction

4.1.1 Protein components of the spliceosome A, B and C complex

The human spliceosomal complexes contain ~45 distinct snRNP associated proteins and ~170 spliceosome associated factor (Jurica and Moore, 2003). During the splicing processes, snRNPs enter and leave the spliceosomes from one stage to the next (Figure 1.3). Thus, the number of the total spliceosomal proteins varies among different pre-spliceosomal intermediates. In general, each of the spliceosomal A, B and C complexes contains ~ 125 proteins (or less in the case of the A complex) (Wahl et al., 2009). Table 4.1 lists some of these proteins that have the well-known functions.

U snRNP/ NTC/ spliceosomal factors	Representative proteins	Present in the complex			functions/ interactions/ modifications
		A	B	C	
A complex factors (~10)	RBM5	+			Block the conversion from a cross-exon to a cross-intron complex
U1 snRNP (~14)	Sm (7)	+	+		Bind to the sm site of U1 snRNA
	U170K	+	+		Bind to the SLIII of U1 snRNA
	U1A	+	+		Bind to the SLII of U1 snRNA
	U1C	+	+		Mediate the base pairing interactions between U1 snRNA and 5'SS
U2 (~17)	Sm (7)	+	+	+	Bind to the sm site of U2 snRNA
	SF3a (3)	+	+	+	
	SF3b (7)	+	+	+	Mediate the base-pairing interactions between U2 and BPS
U2-related (~10)	U2AF35	+	+		Bind to AG nucleotide at 3'SS
	U2AF65	+	+		Bind to PPT
	SPF30	+	+		Bridges an interactions between U2AF35 and Prp3
	Prp5/DDX46	+	+		Bridges a U1 and U2 snRNP interaciton network
U5 (~14)	Sm (7)		+	+	Bind to sm site of U5 snRNA
	hSnu114		+	+	GTPase; Promote Brr2 helicase activity
	hBrr2		+	+	RNA helicase; Unwinding U4/U6 hairpin
	hPrp8		+	+	Bind to both of 5' and 3' exon during the catalytic step II
	hPrp6		+	+	Phosphorylated during B complex formation
	hPrp28		+	+	RNA helicase; Exchange of U1 for U6 snRNP at 5'SS
U5-related (~11)	hPrp38		+	+	Promote U4/U6 snRNA dissociation
U4 (~12)	Sm (7)		+		Bind to sm site of U4 snRNA
	hPrp31		+		Phosphorylated during B complex formation
	hPrp4		+		phosphorylate Prp31 and Prp6
	hPrp3		+		Ubiquitinated by NTC
	hPrp24		+		Facilitates the association of U4 and U6 snRNPs
U6 (7)	Lsm2-8 (7)		+		Bind to the Lsm site of U6 snRNA
NTC (7)	Prp19		+	+	Stablize the association of U5 and U6 with the spliceosome after U4 is dissociated
	CDC5L		+	+	
	SPF27		+	+	
	PRLG1		+	+	
NTC-related (~12)	RBM22		+	+	Promote the catalytic conformation
B complex factors (~8)	UBL5		+		Unknown
C complex factors (~37)	Prp22			+	Required for the second catalytic step
	Prp16			+	Required for both catalytic steps
	Slu7			+	Mediates 3' splice site choice

Table 4.1 Protein components of the spliceosome A, B and C complex. The total number of protein components (in parenthesis) in each of the complexes and functions of some of these proteins are listed in the table.

The spliceosomal A complex mainly consists of U1 and U2 snRNPs. During the progression from the A to B complex, ~35 U6/U4.U5 tri-snRNP proteins and ~25 non-snRNP proteins are recruited (see Table 4.1). The major part of these non-snRNP proteins is the nineteen complex (NTC). The human Prp19 complex is comprised of 7 distinct subunits with four copies of Prp19 protein (Grote et al., 2010). This complex is thus similar to the size of the snRNPs, but unlike the snRNPs, the NTC contains no RNAs.

The transition from the B to B^{act} complex involves the release of both of RNA and protein components of U1 and U4 snRNP (Figure 4.1). Although U6 snRNA is not released, most of its protein components also fall off before the formation of the B^{act} complex (Figure 4.1; U6 Lsm2-8). Moreover, although NTC interacts with the spliceosome at the stage of the B complex formation, its association is stabilized during the progression to the B^{act} complex (Behzadnia et al., 2007; Deckert et al., 2006; Makarova et al., 2004). It is possible that the NTC forms new interactions with U2, U5 or U6 snRNA such that its association in the B^{act} complex is stabilized. Association of the NTC with the spliceosome also promotes interaction of U6 snRNA with the splice sties of pre-mRNA in creating the active splice sites of the spliceosome (Chan and Cheng, 2005). Among the protein components of the tri-snRNP, only U5 snRNP proteins remain associated with the spliceosome during the transition from the B to B^{act} complex (Table 4.1; U5).

During the transition from the B^{act} to C complex, ~30 non-snRNP proteins are recruited (Table 4.1; C complex factors). Among these proteins, the RNA-dependent ATPases/helicases, Prp2, is shown to promote the catalytic step I to generate the 5' exon

and the lariat intermediates in the C complex. Besides the splicing intermediates are generated, SF3b155 is dephosphorylated whereas CDC5L is phosphorylated during the progression from the B^{act} to C complex (Figure 4.1; compare B^{act} with C complex).
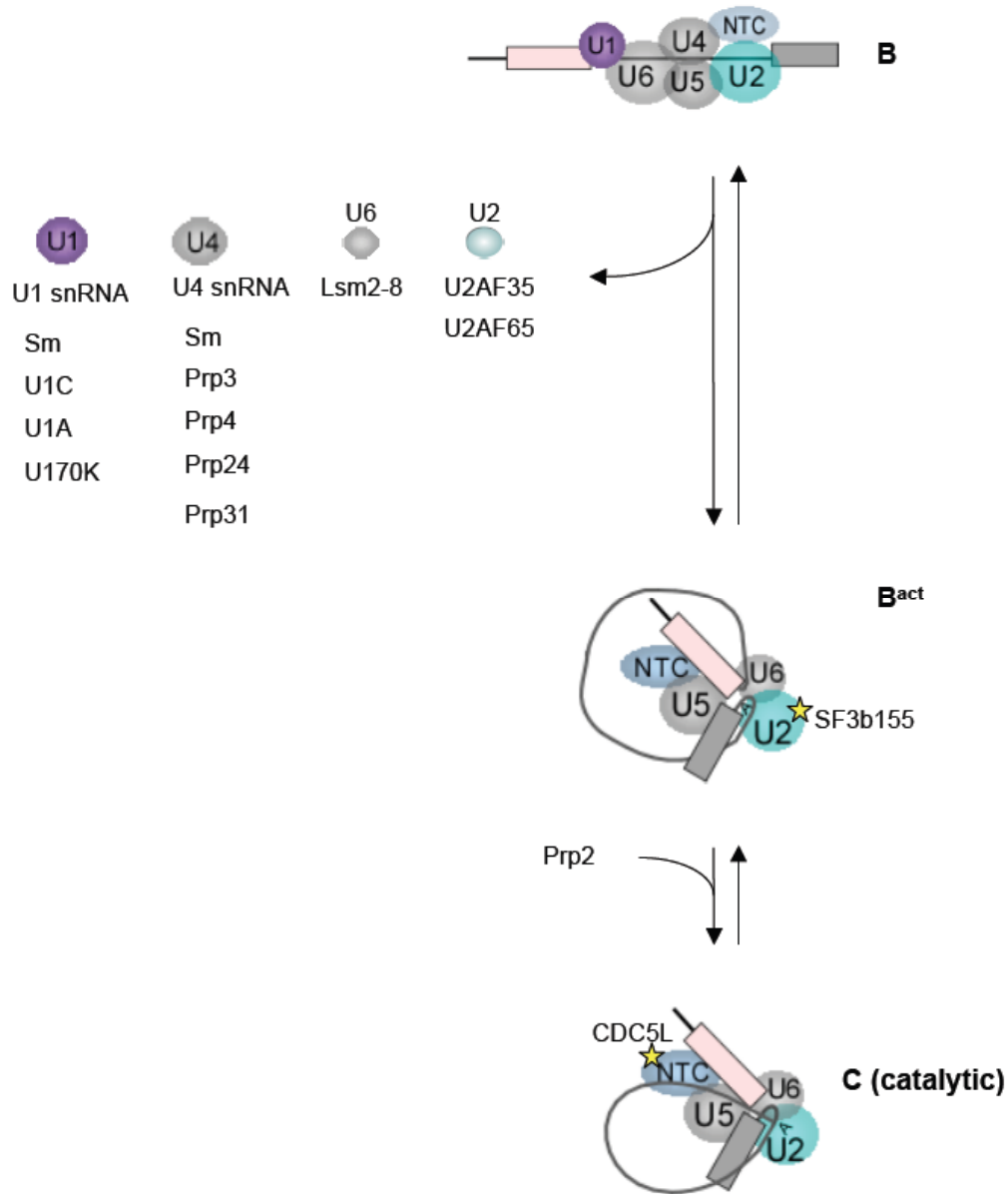
Figure 4.1 Compositional dynamics during the catalytic activation of the spliceosome. The components that are released or changed during the transition from the B to B^{act} complex or from the B^{act} to the C complex. The B complex contains all five snRNPs and NTC. To establish the catalytic site of spliceosome, The RNA and protein components of U1, U4 snRNP and the protein components of U6 snRNP dissociate while more NTC components are integrated at the time of activation. The yellow stars indicate

the protein components that are specifically phosphorylated in the B^{act} versus the C complex. Protein components of the B and C complex are listed in Table 4.1.

4.1.2. Structural rearrangements during catalytic activation of the spliceosome

Along the spliceosome assembly pathways, there is an enormously intricate network of RNA-RNA interactions. As mentioned in chapter 2.2, the 5' end of the U1 snRNA base-pairs with the 5' splice site. Additionally, a stretch of GUAGUA sequence within the U2 snRNA is engaged in the pairing interaction with the BPS (Figure 4.2; cyan box of U2). The U5.U4/U6 tri-snRNP is recruited by U1 and U2 snRNP to form the B complex, in which the base-paring interactions between snRNAs and pre-mRNA are extensively rearranged to generate the C complex (Figure 4.2) (Staley and Guthrie, 1998; Wahl et al., 2009). One of the rearrangement events involves the disrupting the binding between the U1 snRNA and the 5' ss to allow the highly conserved CAGAG motif of U6 to base-pair with the 5' end of the intron. Concomitant with, prior or posterior to this, U4 snRNP is released to allow the formation of new U2/U6 base-pairing interactions, which is though to comprise the heart of the catalytic center of the spliceosome (Figure 4.2) (Madhani and Guthrie, 1992; Villa et al., 2002).
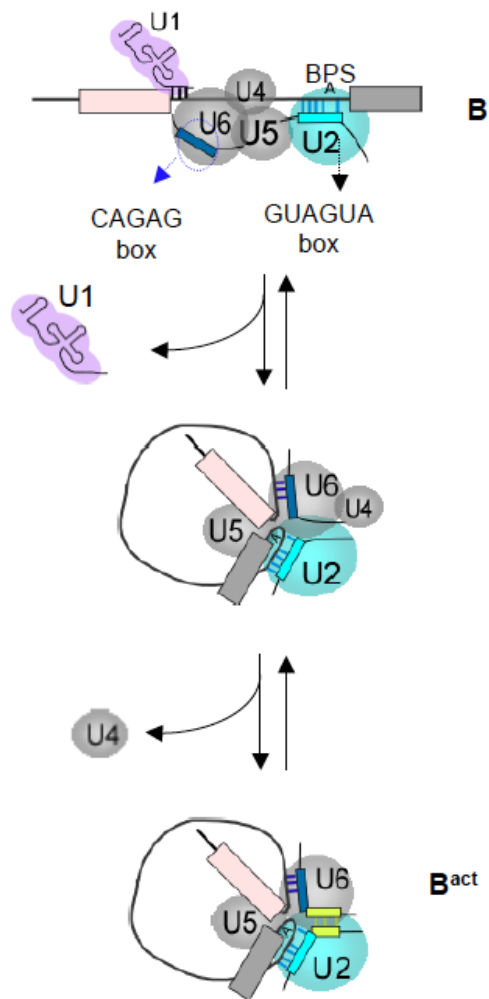
Figure 4.2 Dynamics of the network of RNA-RNA interactions during the catalytic activation of the spliceosome. Schematic of regions of U2 and U6 snRNA that undergo major rearrangements during the transition from the B to C complex. The GUAGUA sequence of U2 snRNA pairs with the BPS (cyan box of U2). The destabilization of U1 allows the CAGAG motif of the U6 snRNA base pairs to the 5' splice site (blue box of U6). The releasing of U4 allows the region next to CAGAG motif in U6 engages in the interaction with U2 (yellow box). Although here it shows that the release of U1 and U4 is two separated events, it is unknown which one occurs first or whether they occur concurrently.

In the B complex, which does not yet have an active center, U4 and U6 snRNA are held firmly by base-pairing interactions while the U5 snRNA associates with U4 snRNA through RNA-protein interactions (Figure 4.3A). The U4 and U6 base-pairing interactions inactivate the catalytically important regions of U6 to prevent from cleaving pre-mRNA prematurely. During the catalytic activation of the spliceosome, U4/U6 base-pairing interactions are taken apart, which frees U6 snRNA and allows the formation a catalytically important U6 internal stem loop (ISL) (Figure 4.3A; red box of U6). The U6 snRNA that is not paired with U4 engages in the new basepairing interactions with the 5'ss and the U2 snRNA. Interestingly, the U2/U6 basepairing interactions involve the region upstream of CAGAG motif of U6 and the region proximal to the GUAGUA sequence of U2 (Figure 4.3B), which allows the juxtaposition of two splice sites. Additionally, the stem loop region of U5 snRNA contacts the nucleotides of the 5' and 3'exon to bring the two exons into proximity (Figure 4.3B; U5). The network of RNA-RNA interactions also brings U5 snRNP proteins close to the splice sites to create the catalytic center. A wealth of evidence shows that the U5 snRNP protein, prp8, is located at the heart of the spliceosome and the RNase H domain of Prp8 is thought to promote two catalytic steps (Query and Konarska, 2013). Thus, the network of RNA-RNA and RNA-protein interactions creates the catalytic active site of the spliceosome.
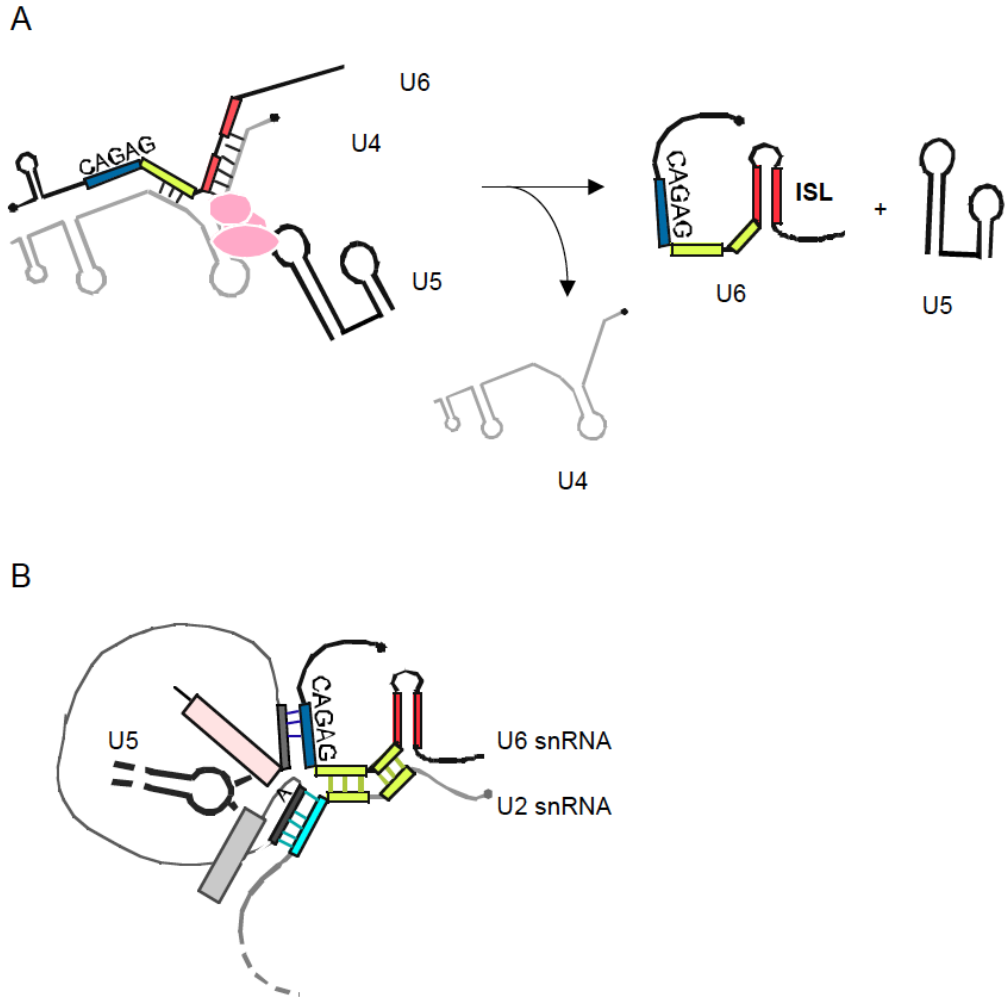
Figure 4.3 Remodeling of the U5.U6/U4 tri-snRNP. (A) Disruption of U4/U6 base-pairing interactions in the tri-snRNP. After releasing from U4 snRNA, the U6 internal stem loop (ISL) forms a hairpin and the regions upstream ISL engages in new pairing interactions, as in panel B. (B) Schematic of critical base-pairing interactions in the catalytic spliceosome. For U5 and U2 snRNA, only the stem loop I of U5 and the internal region of U2 are shown. For U6 snRNA, the whole structure is depicted. The U6 ISL stabilizes the RNA network in the catalytic spliceosome.

4.2 The transition from the B to B^{act}/C complex is blocked on the repressed substrate

As mentioned in chapter 1.6, hnRNP L was previously reported to repress the progression from the spliceosomal A to B complex. To more rigorously characterize the assembled spliceosome complexes, I set to purify the complexes assembled on the repressed- and derepressed-substrate. To perform the affinity-selection of the assembled spliceosome, I engineered the MS2-hairpin sequence into the 3'end of the pre-mRNA (Figure 4.4) (Jurica et al., 2002; Zhou et al., 2002). The MS-hairpin sequence can be tightly bound by MS2MBP protein without interfering splicing efficiency and spliceosome assembly. The MS2MBP-tagged spliceosome complexes in the spliceosome assembly reactions were immobilized onto the amylose beads. After rigorously washing away the non-specific protein and RNA components from the immobilized complexes, maltose solution was used to elute the complexes from the amylose resin.
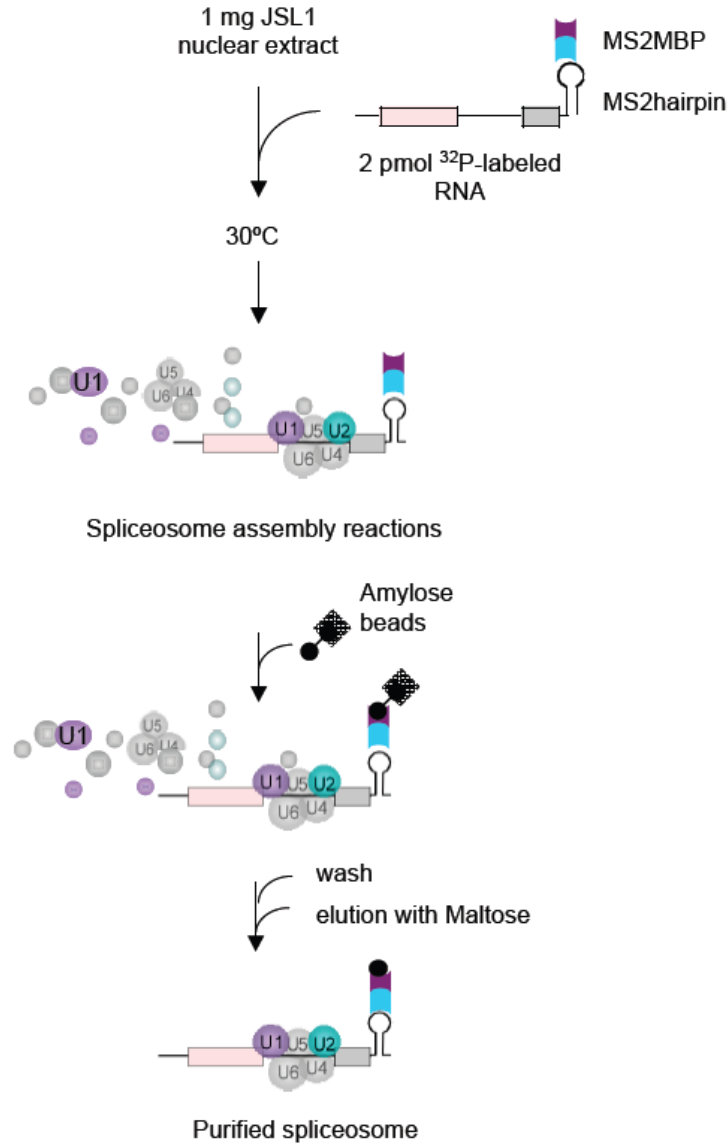
Figure 4.4 MS2MBP affinity purification strategy used to isolate the complexes from the splicesome assembly reactions. About 2 pmol RNA substrates pre-bound by MS2MBP were incubated with 1.5 mg JSL1 nuclear extract followed by amylose-resin purification. The volume of the purified spliceosome is ~200 μl and the purification efficiency is ~10% so that the concentration of the purified spliceosome is ~ 1 nM.

To identify the snRNP components in the purified spliceosome, the RNA components of the purified complexes were isolated and analyzed by silver-staining. The presence of the snRNAs is the indicative of the presence of the snRNPs. It showed that

the H/E complexes purified from the ATP-depleted nuclear extract have no tri-snRNP and much lower levels of U2 snRNP (Figure 4.5A and B; -ATP). This is consistent with the fact that the association of these components requires ATP. This also suggests that the purification conditions are stringent enough to wash away the ATP-dependent components from the complexes assembled in the ATP-depleted nuclear extract. Strikingly, the purified repressed and derepressed complexes assembled in the presence of ATP contain similar levels of the tri-snRNP (Figure 4.5A; +ATP). Thus, the middle band resolved from the repressed complexes may be the mixture of the A and the tri-snRNP-containing B complex (Figure 4.5D; A/B).

As mentioned in chapter 1.6, the tri-snRNP was not thought to associate with the repressed substrate because the B complex is not assembled on the repressed substrate in a native gel (Figure 4.5B). The label of the complexes in a native gel is based on the fact that the formation of the top band but not the middle band is reduced when the U6 snRNP is depleted from the nuclear extract (Figure 4.5B; +ATP, -U6). To more accurate determine the snRNP components, I purified complexes assembled in nuclear extract depleted of U6 activity by the cleavage of U6 snRNA. This showed that the purified complexes assembled in the U6-depleted nuclear extract contain the tri-snRNP in which the U6 snRNA is cleaved (Figure 4.5C; +ATP, -U6). This indicates that cleavage of U6 snRNA does not inhibit recruitment of tri-snRNP but may repress the subsequent tri-snRNP rearrangements required for the formation of the B^{act} or C complex, which migrates shower than the B complex as shown by other groups (Bessonov et al., 2010). Thus, the top band could be the mixture of B^{act} and C complex, which is supposed to be reduced when the U6 snRNA is cleaved (Figure 4.5D). Based on this conclusion, I re-

82

label the complexes in a native gel so that the new label of the middle band is A/B whereas the top band is renamed as B^{act}/C (Compare Figure 4.5D with B; labels in red color).
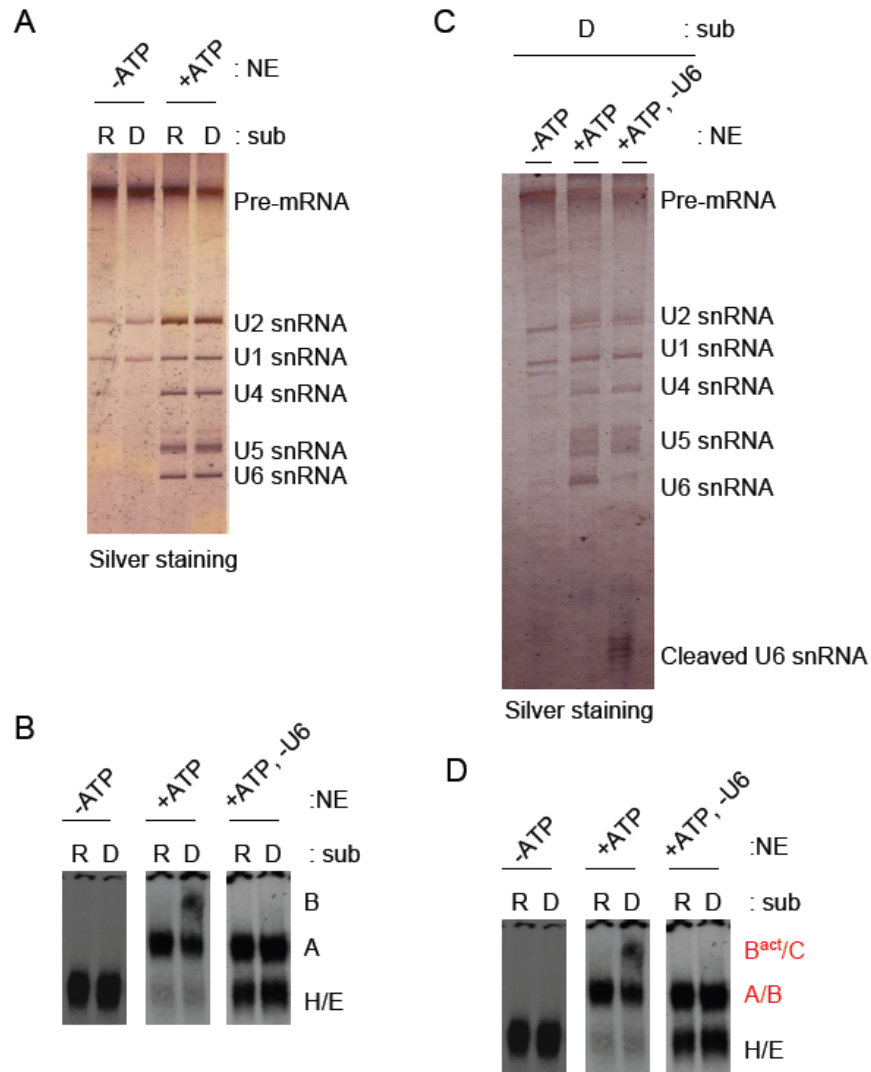
Figure 4.5 The tri-snRNP is associated with both of the repressed and derepressed complexes even when the B complex is not resolved in a native gel. (A) Silver-staining of the RNA components extracted from the purified complexes assembled in the absence (-ATP) or in the presence of ATP (Total). (B) Spliceosome assembly assays, as in Figure 1.10D. (C) Silver-staining of the RNA components extracted from the purified complexes assembled in the absence (-ATP), in the presence of ATP (Total) or in the U6-depleted nuclear extract (-U6). (D) Spliceosome assembly assays, as in panel B, with new labels.

In general, spliceosome assembly reactions are treated with heparin, a highly sulfated glycosaminoglycan, to allow the resolution of the assembled complexes in a native gel (Figure 4.6A). Without adding heparin into the spliceosome assembly reactions, it showed that most of the reactions are stuck in the well and no obvious assembled complexes are resolved in a gel (Figure 4.6B).
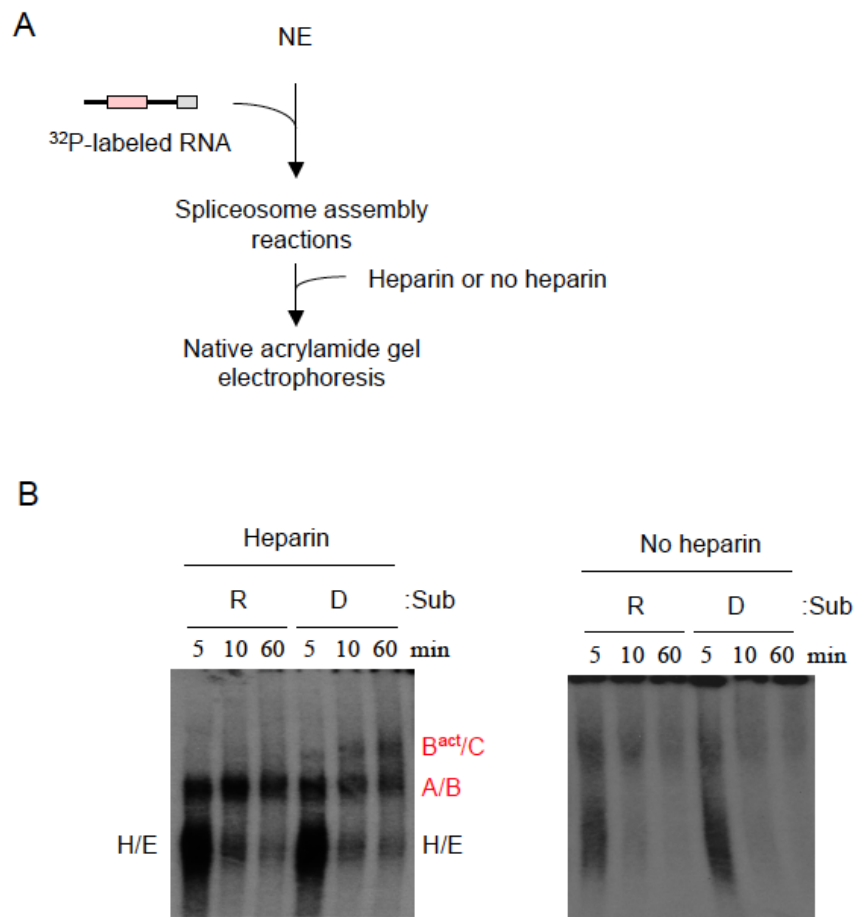
Figure 4.6 Heparin is required for resolution of complexes in a native gel in the splicesome assembly assays. (A) Schematic of the addition of heparin into spliceoosme assembly assays before native gel eletrophresis. (B) Native gel electrophoresis of the gradient fractions. When heparin was not added into the spliceosome assembly reactions, no obvious complexes are resolved in a native gel.

After gradient fractionation of the spliceosome assembly reactions, heparin is also added into fractions before native gel electrophoresis (Figure 4.7A). Unexpectedly, in the absence of heparin, the complexes in glycerol-gradient fractions can be resolved in a native gel (Figure 4.7; no heparin). It is likely that during the glycerol-gradient centrifugation, the non-specific proteins or RNAs are removed from the assembled complexes to allow their migration in a native gel. Strikingly, in the conditions without heparin, both of the A and B complex are resolved from the middle fractions containing the repressed substrate. Moreover, the B^{act}/C complex is resolved from the later fractions containing the derepressed substrate (Figure 4.7B; no heparin). It is possible that heparin reorganizes the complexes in the middle fractions so that the A and B complex comigrate into a single band in the conditions with heparin. Additionally, the B^{act}/C complex is reorganized by heparin as well so that it migrates faster in the conditions with heparin than without heparin (Figure 4.7B; compare heparin with no heparin). Thus, the native-gel analysis of the spliceosome in gradient fractions further supports that binding of hnRNP L to ESS1 on the repressed substrate does not sterically inhibit the tri-snRNP association, but instead, it interferes the subsequent transition into the B^{act}/C complex.

Other groups also observed that the complex, which is called as the A complex in a native gel in the presence of heparin, contain the tri-snRNP after purification (Roybal and Jurica, 2010; Schneider et al., 2010a; Schneider et al., 2010b). Therefore, MS2MBP-affinity purification of the spliceosome provides more accurate analysis of the snRNP composition of the complexes assembled on the pre-mRNA substrates.
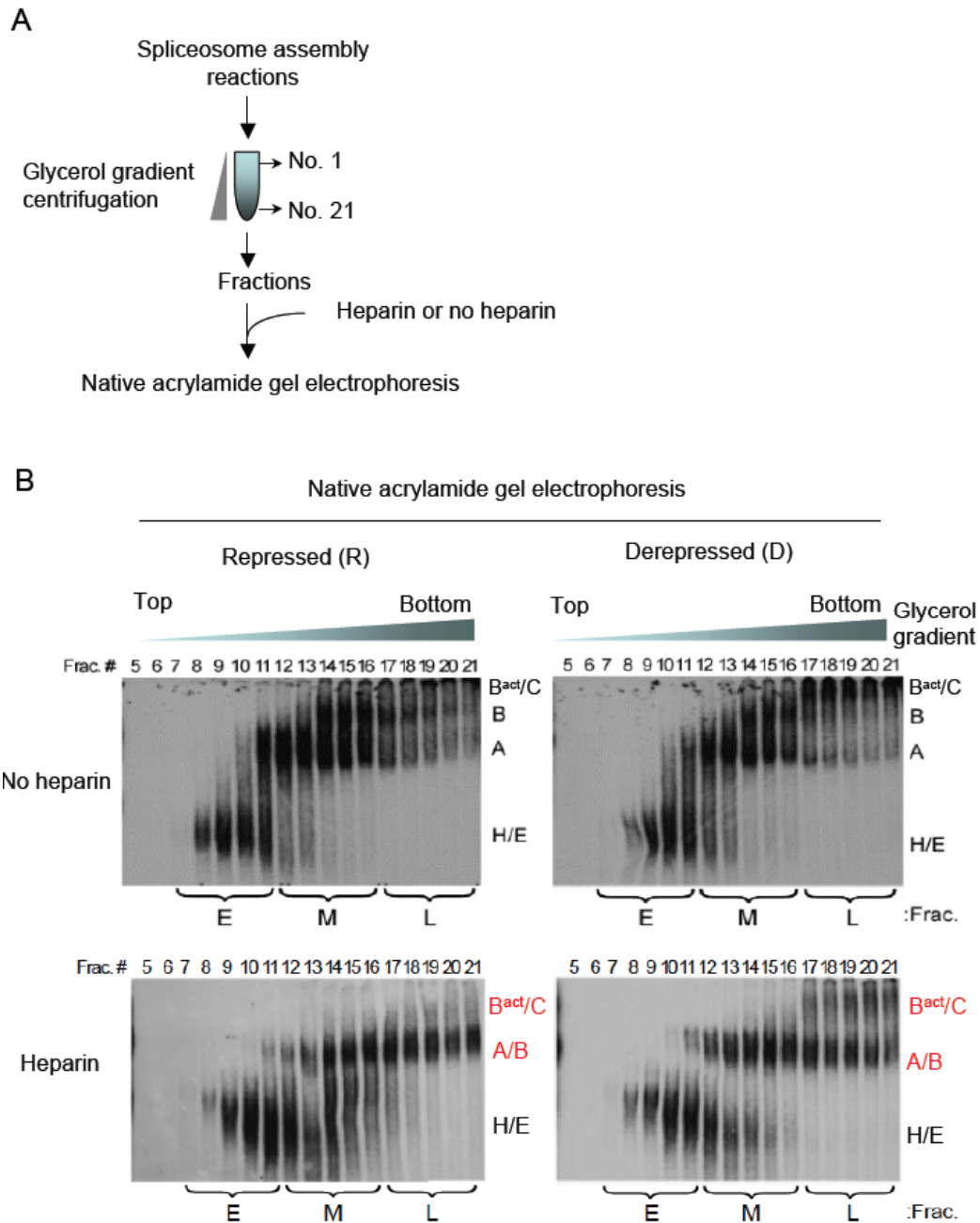
Figure 4.7 Analysis of the ESS1-repressed complexes in gradient fractions demonstrated that the B complex is assembled but its transition to the B^{act}/C complex is blocked. (A) Schematic of addition of heparin into the gradient fractions before native gel electrophoresis. (B) Native gel electrophoresis of the gradient fractions in the absence and in the presence of heparin. Here, fractions no. 7-11 are E fractions; no.12-16 are M fractions; and no. 17-21 are L fractions. Identifies of the complexes were primarily based on their migration in the native gel. Base on the results in the presence of heparin, there are new labels for the spliceosome complexes in the absence of heparin. Middle band is labeled as comigration of the A and B complexes (A/B). Top band is labeled as the mixture of the B^{act} and C complex (B^{act}/C).

4.3 Derepressed complexes display higher levels of the hallmarks of the B^{act}/C complex

As described in chapter 1.3 and 4.1, the formation of the catalytic complex results in the release of U1 and U4 snRNP and generation of splicing intermediates and products. To investigate whether these components are different in repressed versus depressed complexes, I set to analyze the complexes purified from the gradient fractions. To have a negative control to show that the purification conditions are stringent enough to wash away the non-specific protein and RNA components, the spliceosome are assembled in the ATP-depleted nuclear extract to accumulated E complex followed by glycerol gradient centrifugation (Figure 4.8).
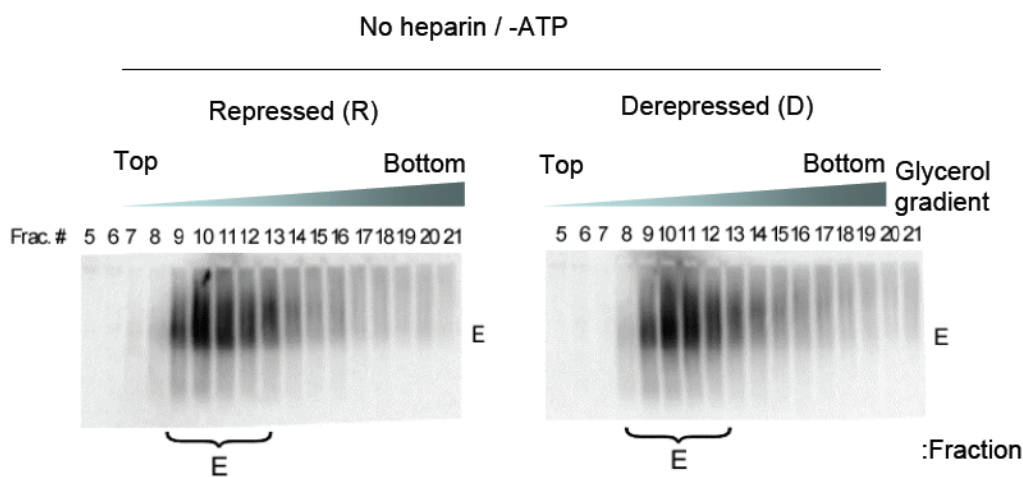
Figure 4.8 Gradient fractionation of the complexes assembled in nuclear extract depleted of ATP. Native gel electrophoresis of gradient fractions as in Figure 4.4 in the absence of heparin. In comparison to Figure 4.4, the complexes are assembled in the ATP-depleted nuclear extract before gradient centrifugation.

To further analyze the RNA and protein components that are associated with the repressed and derepressed complexes, MS2MBP-tagged spliceosome complexes

assembled in the absence ATP (Figure 4.8) or in the presence of ATP (Figure 4.7) were fractionated by glycerol gradient centrifugation followed by the amylose column purification.

The complexes purified from ATP-depleted nuclear extract are not associated with the tri-snRNP, which demonstrates that the washing conditions are stringent enough to eliminate the nonspecific association of snRNPs (Figure 4.9A; -ATP). Additionally, both of the repressed and derepressed complexes purified from M fractions contain similar levels of tri-snRNP, which is consistent with the fact that the B complex is assembled in M fractions (Figure 4.9A; M fractions). Surprisingly, the repressed and derepressed complexes purified from the L fractions contain similar levels of all five snRNAs although I expected to see the reduced levels of U1 and U4 snRNA in the purified B^{act}/C complex assembled on the derepressed substrate (Figure 4.9A; L fractions). It is likely that on the derepressed substrate, the released U1 and U4 snRNP still weakly associate with the C complex so that the purification strategy or silver-staining is not sensitive enough to detect the decreased levels of U1 and U4 in the C complex. Western blot analysis of the purified complexes revealed that the levels of NTC protein components, including Prp19, CDC5L, PLRG1 and SPF27, are higher in the derepressed than repressed complexes purified from L fractions (Figure 4.9B). As mentioned in chapter 4.1, during the transition into the B^{act} complex, the levels of NTC association is stabilized. Phosphorimaging analysis of the purified repressed and derepressed complexes showed that that the amount of lariat intermediates is higher in the derepressed than repressed complexes purified from the L fractions (Figure 4.9C). This suggests that the B^{act} complex is progressed into the C complex on the derepressed

substrate. Therefore, in comparison to the repressed substrate, the derepressed substrate display the higher levels of hallmarks of the B^{act}/C complex, including the enhanced NTC association and increased levels of splicing intermediates.
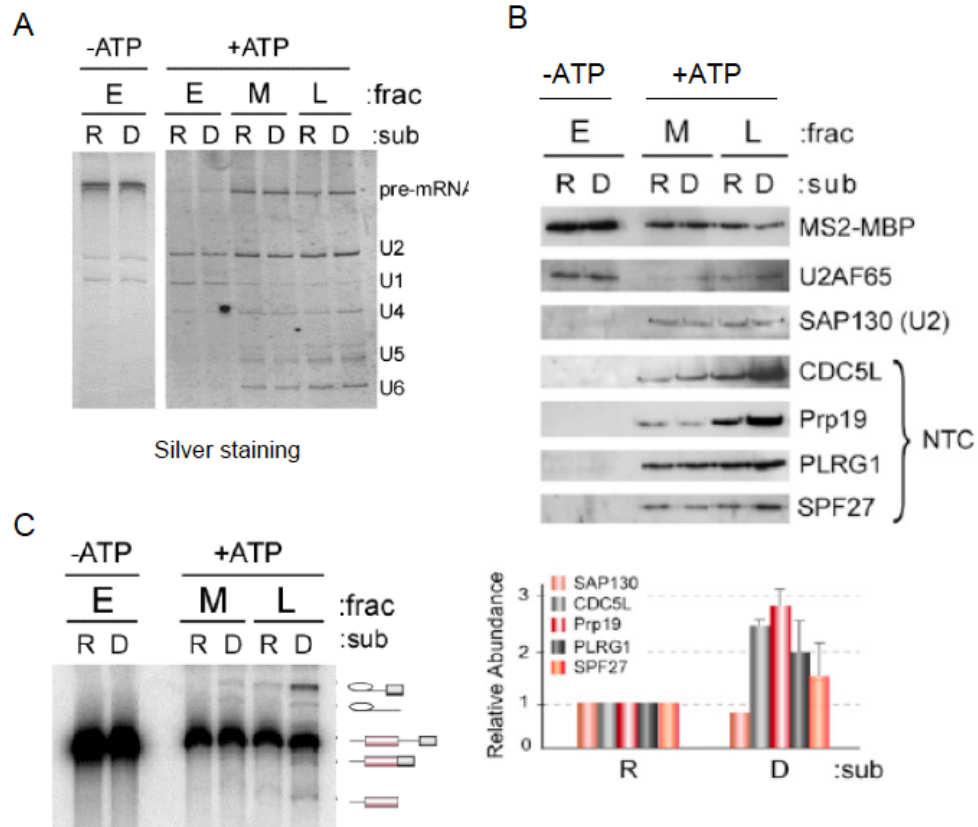
Figure 4.9 The levels of splicing intermediates and NTC association are higher in the purified derepressed than repressed complex in L fractions. (A) Silver-staining of the RNA components extracted from the purified complexes which were assembled in the ATP-depleted NE and then sediment into E fractions (Figure 4.8; -ATP) or assembled in the presence of ATP and then sediment into E, M or L gradient fractions (Figure 4.7B; +ATP). (B) Top, western blots and bottom, quantification of proteins in the purified complexes as in panel B. (C) Phosphorimaging analysis of the pre-mRNA, spliced products and splicing intermediates, including the lariat intermediate and 5' exon in the purified complexes, as in panel A.

4.4 Association of hnRNP A1 and the U1 snRNA with the 3' end of exon 4 is required for ESS1-dependent repression of the B^{act}/C complex formation

To confirm the requirement of the U1 snRNA and hnRNP A1 binding for the repression of the B^{act}/C complex formation, the spliceosome assembly assays were reconstituted with the substrates containing mutations at the C-15 region. Indeed, these mutations enhance the formation of the top band, which is supposed to be the B^{act}/C complex (Figure 4.10A).

To further support that the recruitment of the U1 snRNA and hnRNP A1 at the 3'end of exon 4 is required for ESS1-mediated repression of the B^{act}/C complex formation, complexes assembled on the substrates containing mutations at the C-15 region were further purified. It revealed that the levels of Prp19 and CDC5L are increased when association of hnRNP A1 and the U1 snRNA is disrupted by mutations at the C-15 region (Figure 4.10B) or in the presence of anti-E4 oligo (Figure 4.10C). As enhanced NTC association is a hallmark of the B^{act}/C complex formation, I conclude that ESS1/hnRNP L represses the B^{act}/C complex formation by recruiting hnRNP A1 and the U1 snRNA to the 3' end of CD45 exon 4.
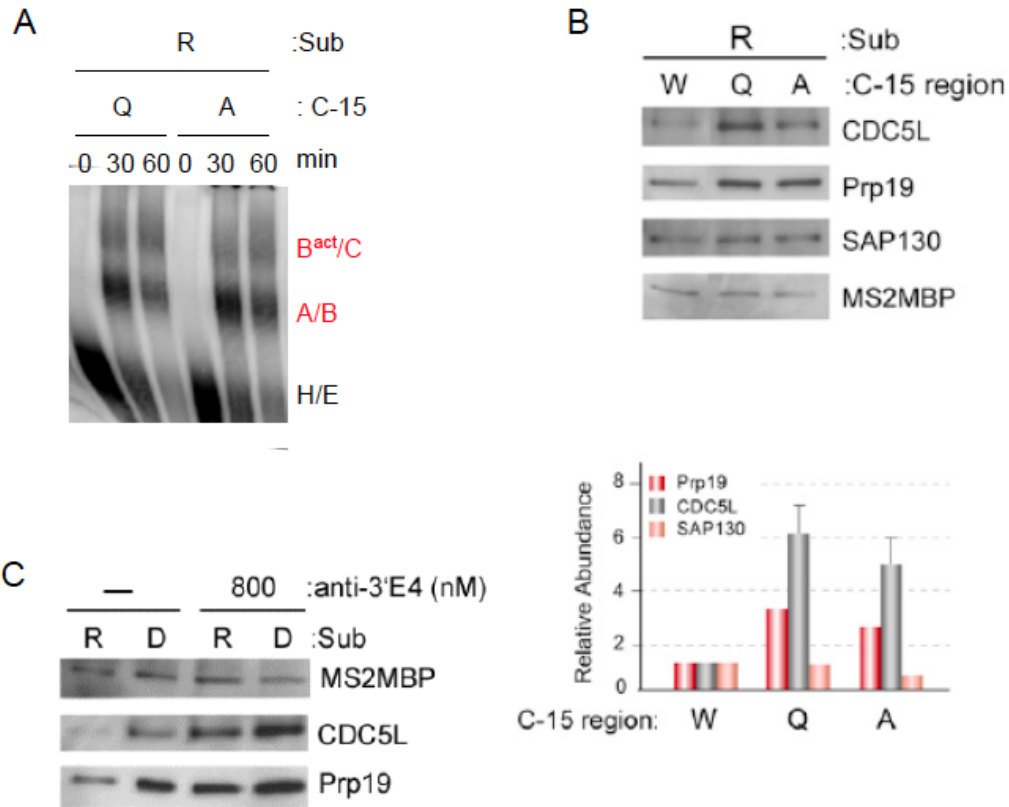
Figure 4.10 The sequence integrity of the C-15 region is required for ESS1-dependent repression of the B^{act}/C complex formation and NTC recruitment. (A) Spliceosome assembly assays, as in Figure 4.6B, with the indicated substrates. (B) Top, western blots and bottom, quantification of proteins in the purified complexes which were assembled on the indicated substrates in the presence of ATP and then sediment into L fractions. (C) Western blots of proteins in the purified complexes which were assembled in the presence or absence of anti-E4 oligo and then sediment into L fractions.

4.5 The transition from U1 to U6 binding at 5' splice site is repressed by the hnRNP L-induced extended U1 interaction

As described in chapter 4.1.2, several paring interactions are rearranged during the transition into the C complex. Since the extended U1 interaction could function in hyper-stabilizing binding of U1 snRNP to the 5'ss, the most likely rearrangement event that is altered by hnRNP L is the transition from U1 to U6 snRNP binding at the 5' ss (Figure 3.1A).

To access the state of U6 snRNP binding at the 5' ss, I performed the oligo-induced RNase H cleavage to interrogate the accessibility of the ACAGAG box of U6. In this assay, splicing complexes purified by MS2MBP-affinity selection were treated with varying concentrations of an oligo complementary to the ACAGAG box of U6 to induce RNase H cleavage (Figure 4.11A). The ACAGAG box of the U6 snRNA is unpaired when U6 is paired to U4 as part of the tri-snRNP, and thus should be highly accessible to RNase H cleavage (Figure 4.2; B complex). By contrast, when the U6 snRNA replaces U1 at the 5' splice site, the CAGAG box region of U6 become paired with the 5'ss, which should protect it from RNase H cleavage (Figure 4.2; C complex). If ESS1 blocks the replacement of U1 by U6, there would be less association of U6 snRNA with the 5' ss. Indeed, I observed less U6 protection in the repressed versus derepressed complexes at all concentrations of oligo tested (Figure 4.11B). Importantly, the extended U1 interaction with the 3'end of exon 4 is required for reducing U6 accessibility for cleavage, as the QC9 mutation increases the relative protection of U6, indicative of increased association of U6 with the 5' splices site.
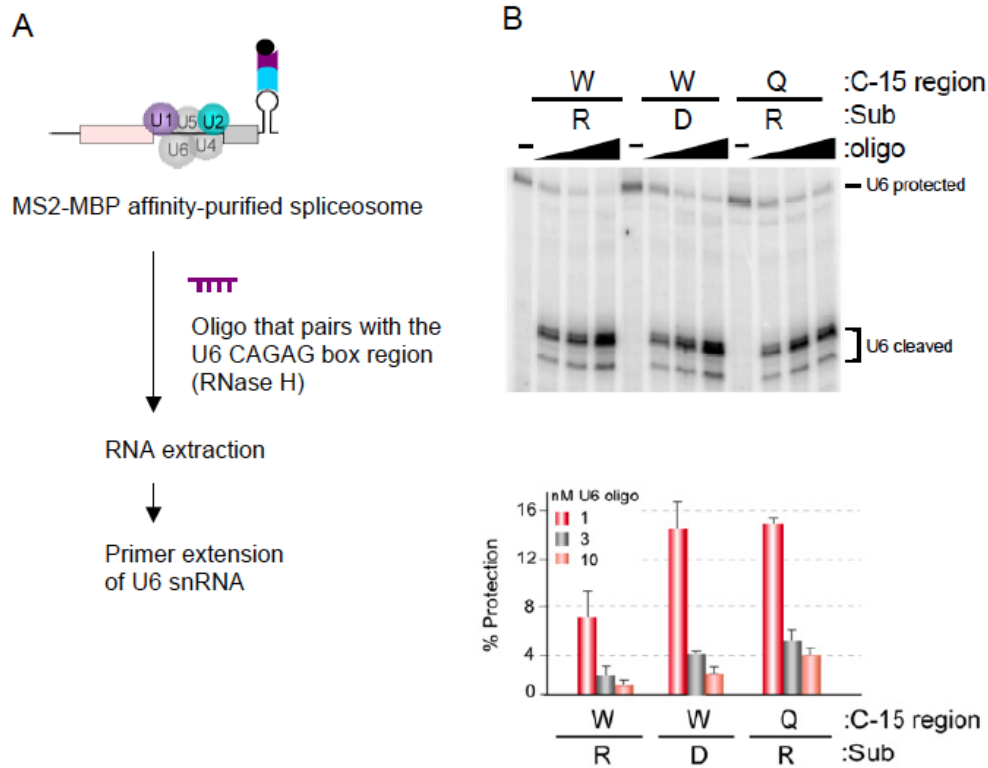
Figure 4.11 HnRNP L-induced extended U1 interaction represses association of U6 snRNP with the 5' splice site. (A) Schematic of RNase H-protection assays for accessing the pairing interactions in the CAGAG motif of U6 with the 5'ss. (B) Top, primer extension analysis; bottom, quantification of the cleaved and protected U6 snRNA.

If hnRNP L blocks association of U6 with the 5'ss to repress splicing, enhancing interaction of U6 snRNA with the 5' splice site would disrupt hnRNP L-mediated splicing repression (Figure 4.12A). Thus, I mutated the sequence downstream of the 5' ss to artificially extend the pairing interactions between U6 snRNA and the 5' ss (Figure 4.12B). Indeed, I observed increased splicing of the repressed substrate when the U6-5'ss pairing interaction is extended whereas the splicing of the derepressed substrate has only minor increase with this enhanced U6 binding (Figure 4.12C). Moreover, the control

mutations have no effect on exon 4 splicing. Since enhancing association of U6 snRNP with the 5' ss overcome the effect of the hnRNP L-induced extended U1 interaction, I conclude that hnRNP L represses splicing through inhibiting the U1/U6 switch at the 5'ss.
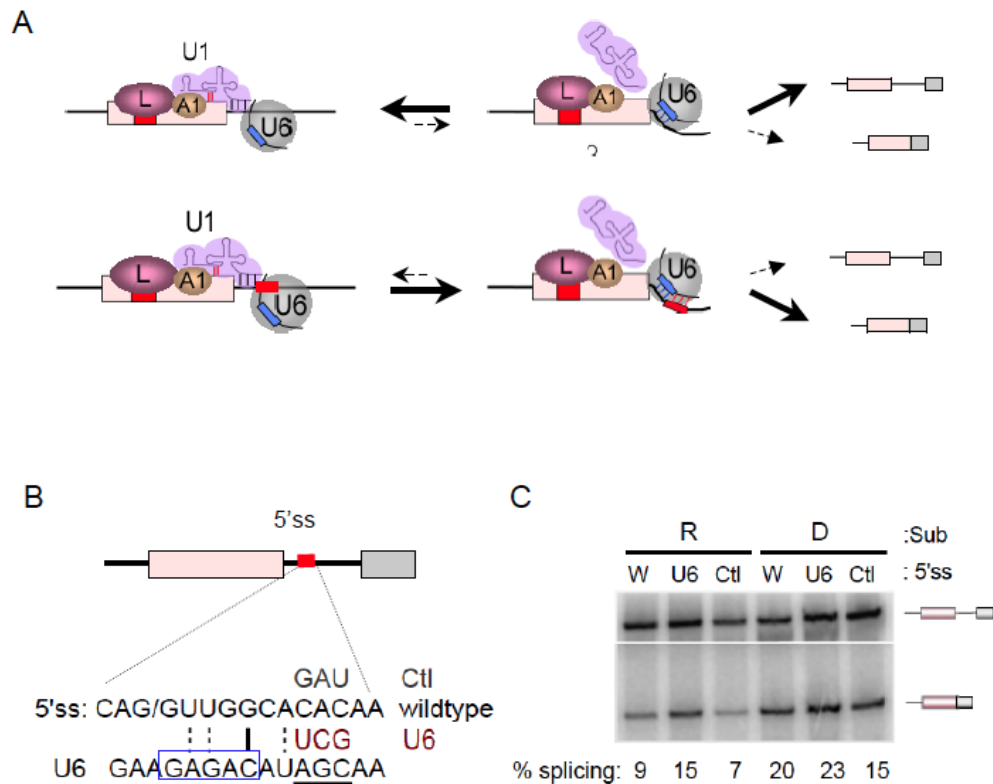
Figure 4.12 HnRNP L represses the exchange of U1 by U6 at the 5' splice site. (A) Schematic of the potential effect of enhancing the interactions of U6 with the 5' splice site. (B) Schematic of sequences of U6 enhanced (U6) and control mutations made in the region downstream of the 5' splice site. (C) In viro splicing assays with the substrates indicated in panel B.

4.6 Binding of Prp8 may be interfered by hnRNP A1 and the U1 snRNA binding at the 3' end of exon 4

As mentioned from the chapter 4.1.2, concomitant with, prior or posterior to the U1/U6 switch, the contacts between U5 snRNP and splice sites are formed. It has been shown that the U5 snRNP component, Prp8, can be crosslinked to the 5' ss (Grainger and Beggs, 2005). To investigate whether the extended U1 interactions interferes the contacts of U5 snRNP with splice sites, the G residue which is 15 nucleotide downstream of the 5' ss (G+15) on the repressed substrate is radio-labeled (Figure 4.13A). UV crosslinking assays showed that there is a ~250 KDa protein that is crosslinked to the G+15 when hnRNP A1 and the U1 snRNA binding are blocked by the anti-3'E4 oligo (Figure 4.13B). This suggests that binding of hnRNP A1 and the U1 snRNP at the 3'end of exon 4 also disrupts the association of Prp8 with the 5' ss. Since repressing U1/U6 switch may interfere the subsequent interaction of Prp8 with the 5'ss, the reduced level of Prp8 crosslinked to the 5'ss may not be an direct effect caused by the A1 and U1 binding at the 3' end of exon 4. However, the timing of these structural rearrangement events is debatable. Therefore, it is possible that hnRNP A1 binding at the 3'end of exon 4 sterically blocks association of Prp8 with the 5' ss, thereby repressing the U1/U6 switch.
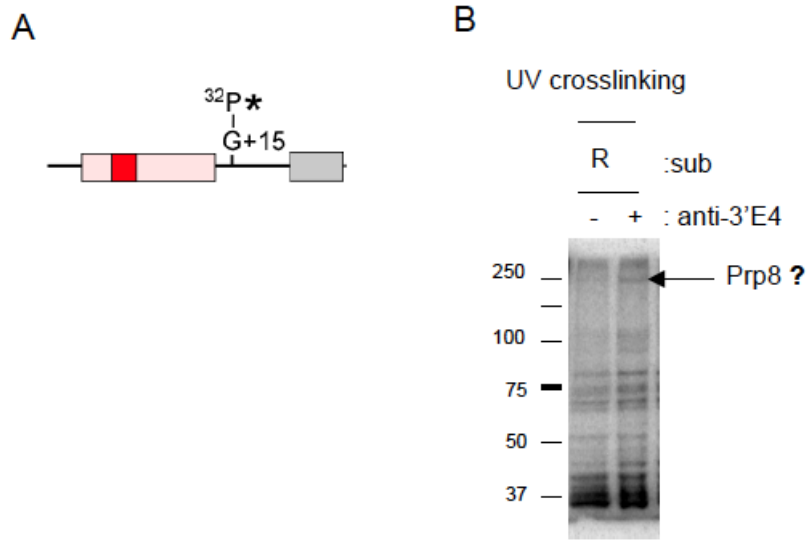
Figure 4.13 Blocking association of hnRNP A1 and the U1 snRNA with the 3' end of exon 4 enhances crosslinking of a ~250KDa protein to the G+15 nucleotide. (A) Schematic of the site-specific labeled RNA containing a radiolabeled phosphate at G+15. (B) Analysis of proteins crosslinked to G+15 nucleotide of the repressed substrate in the absence (-) or presence (+) of anti-3'E4 oligo in a SDS-PAGE.

4.7 Discussion

Spliceosome assembly has been described to be the stepwise assembly of snRNPs on the pre-mRNA. The studies in this chapter showed that hnRNP L represses exon 4 splicing by trapping the 5'ss-bound U1 snRNP in a stabilized conformation that inhibits the subsequent replacement of U1 by U6 at the 5'ss, thereby blocking the structural rearrangements required for the catalytic complex formation (Figure 4.14).
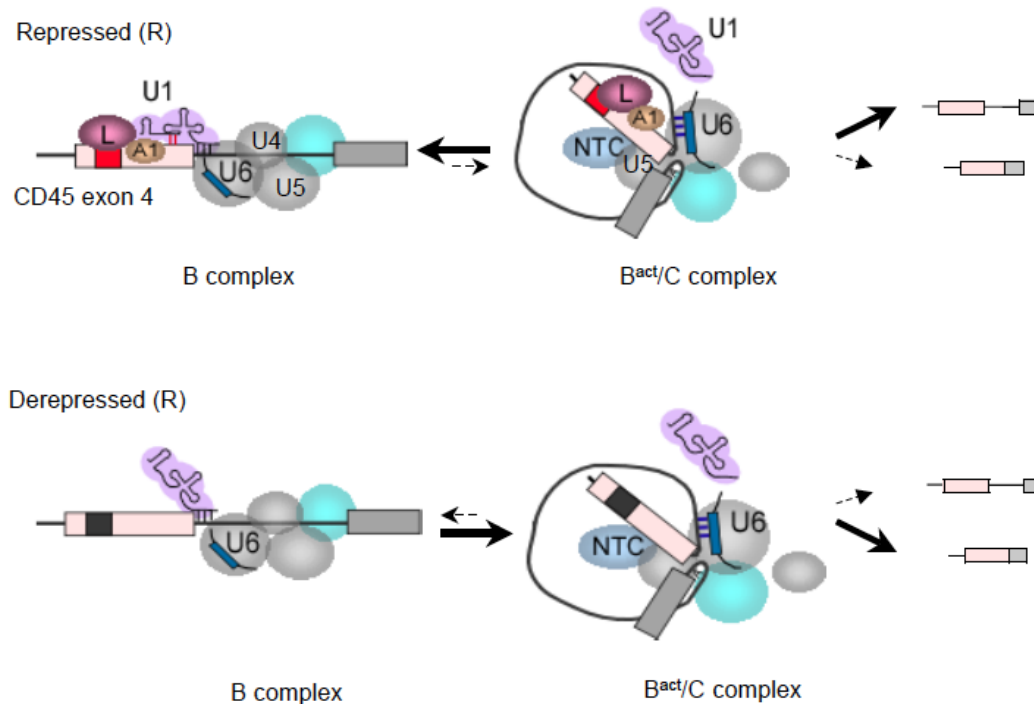
Figure 4.14 Model for hnRNP L function in repressing the U1/U6 switch at the 5' splice site to repress the formation of the B^{act}/C complex. The hnRNP L-induced extended U1 interaction within the B complex represses association of U6 with the 5'ss, which represses structural rearrangements required for the B^{act}/C complex formation. As a result, the splicing of the downstream is repressed. By contrast, the canonical binding of U1 at the 5' ss in the derepressed B complex allows the progression to the B^{act}/C complex and the subsequent splicing catalysis.

It has been shown that the transfer of the 5' ss from the 5' end of U1 snRNA to the ACAGAG motif of U6 snRNA is facilitated by the RNA helicase, Prp28 (Staley and Guthrie, 1999). Moreover, it has been demonstrated that artificially lengthening the U1-5'splice site duplex represses the replacement of U1 by U6 at the 5' ss (Staley and Guthrie, 1999). In this study, I showed that the extended interactions between U1 3' helix H and the 3' end of the exon could function similarly as the lengthened U1-5' ss duplex in stabilizing U1 snRNP binding to repress the Prp28-mediated U1/U6 switch at the 5'ss.

Besides lengthening basepairing interactions, U1C has been reported in stabilizing the U1-5'ss duplex. Moreover, mutation within U1C that disrupts its stabilization activity allows yeast to bypass the function of Prp28 (Chen et al., 2001). This further support that the stability of U1 snRNP binding at the 5'ss could influence the ability of Prp28 to mediate the subsequence rearrangement of spliceosome interactions.

To repress the catalytic activation of the spliceosome, besides the U1/U6 switch, the U5 snRNP component, Prp8, is possibly repressed by hnRNP A1 and the U1 snRNA in the hnRNP L-repressed complex (see chapter 4.5 and 4.6). During the catalytic activation, U4 is released from U6 to allow the formation of the U6/U2 duplex, which is mediated by the RNA helicase, Brr2 (Staley and Guthrie, 1998). Moreover, Prp8 has been shown to mediate the helicase activity of Brr2 (Mozaffari-Jovin et al., 2012). Thus, it is possible that the reduced binding of Prp8 on the repressed complex could interfere the activity of Brr2 for unwinding U4/U6 duplex. If Prp28, Prp8 or Brr2 all are located nearby the 5' splice site on the repressed substrate, it is also possible that the hnRNP L and A1 in the C-15 region directly influence the activities of these proteins. It would provide significant insight if I can detect the interactions between hnRNP L or A1 with spliceosome components bound at the 5'ss, including U1 snRNP, Prp28, Prp8 and Brr2. These molecular interactions could provide a light about other targets of hnRNP L or A1. Therefore, although I showed that the U1/U6 switch could be repressed directly by the extended U1 interactions at the 3' end of exon 4, other spliceosome components that interact with the 5'ss could be sterically blocked by hnRNP L or A1 to repress other structural rearrangement events during the catalytic activation.

Chapter 5

Conclusions and future directions

Although the 5' splice site on the pre-mRNA is defined by the sequence in the -3 to +6 region of the 5' ss, a multitude of factors have been demonstrated to contribute to 5' selection (Roca et al., 2013). In chapter 2, 3 and 4, I demonstrated a novel mechanism showing that ESS1/hnRNP L-induced binding of hnRNP A1 upstream of the 5' splice site causes an extended form of U1 snRNP, which represses the switch of U1/U6 at the 5' ss. In addition to the ESS1 element within CD45 exon 4, the exon-definition interactions formed across exon 4 also have been shown to mediate splicing repression (House and Lynch, 2006). Importantly, fully understanding the mechanisms of splicing choices has implications for predicting splicing patterns and genetic diseases. Based on the conclusion from chapter 2, 3, and 4, in this chapter, I discuss the future directions for understanding how exon-definition interactions, splicing regulators and spliceosome components could be combined to regulate 5' ss choices.

5.1 Forming exon-definition interactions is involved in ESS1-mediated splicing repression

As mentioned in chapter 1.3, in vertebrate cells, the average length of exons is about 10-fold longer than the intron, so that the exon-definition interactions are believed to occur before intron-definition interactions. The exon-definition interactions could occur in any spliceosome intermediate complexes and the transitions from exon- to intron-

defined complex could function as regulation points for alternative splicing (House and Lynch, 2008).

Within the hnRNP L-repressed B complex, U2 snRNP that associates with the upstream intron could form cross-exon interactions with spliceosome components in the downstream intron (Figure 5.1A). To disrupt the exon-definition interactions that are mediated by binding of U2 snRNP at the upstream intron, we removed the upstream intron to generate the R Δ3'ss or D Δ3'ss substrate (Figure 5.1B) (House and Lynch, 2006). The *in vitro* splicing assays showed that after removing the upstream intron, the splicing of the downstream intron is increased and is no longer regulated by the ESS1 element (Figure 5.1C). Moreover, spliceosome assembly assays demonstrated that the progression from the B to B^{act}/C complex is enhanced on the Δ3'ss substrates (Figure 5.1D). Thus, the exon-definition interactions within the B complex assembled are required for ESS1-mediated repression of the B^{act}/C complex formation.
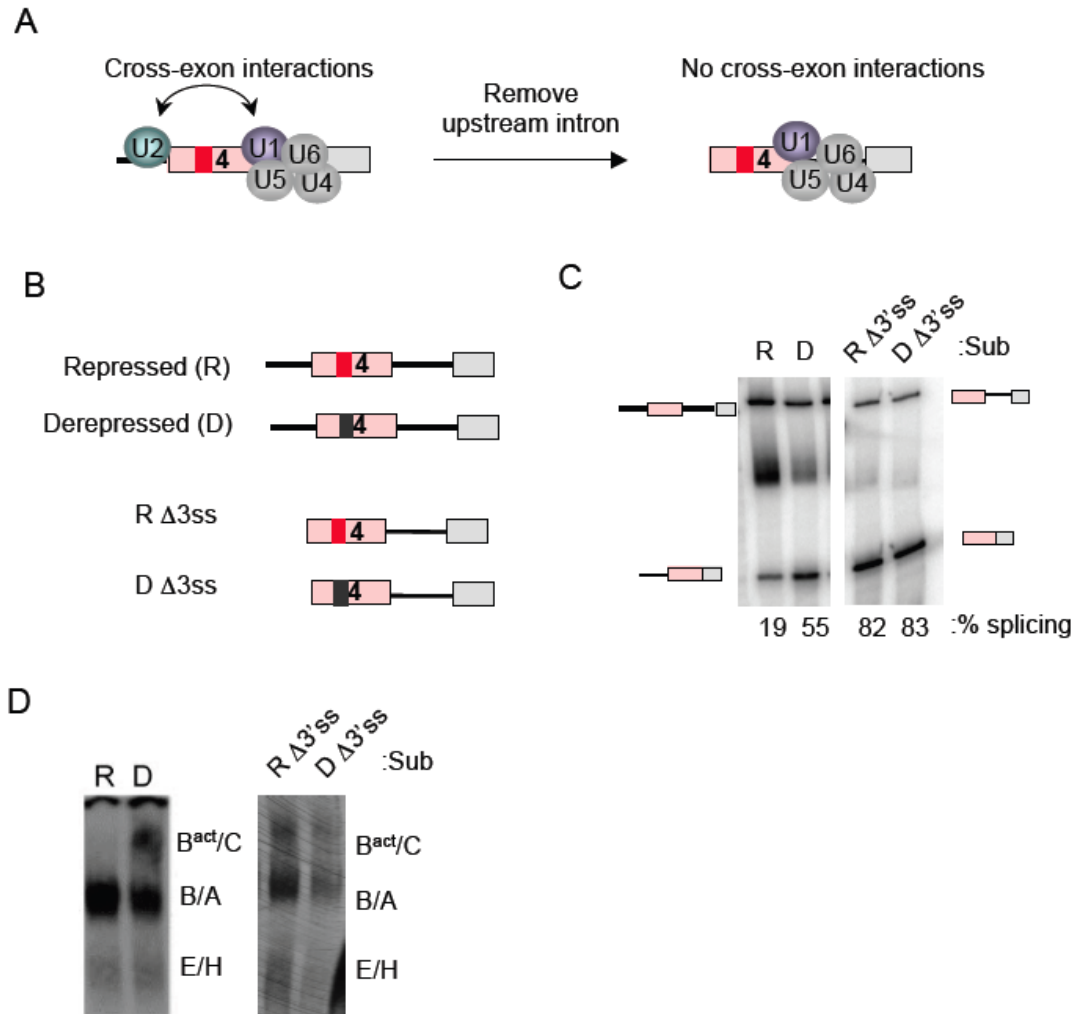
Figure 5.1 Exon-definition interactions are required for ESS1 to repress the splicing of CD45 exon 4 *in vitro*. (A) Comparison of exon-definition interactions between the substrates with upstream intron (left) and without the upstream intron (right). (B) Schematic of splicing substrates. In contrast to R and D substrate, RΔ3'ss and RΔ3'ss substrate have no upstream intorn. (C) RT-PCR analysis of the RNA in the *in vitro* splicing reactions containing the substrates as in panel B. (D) Native acrylamide gel electrophoresis of the spliceosome assembly reactions reconstituted with the indicated substrates.

It has been shown that binding of hnRNP A1 or the U1 snRNA at the C-15 region is also required for repressing the transition from the B to B^{act}/C complex (Figure 4.8). Thus, it is likely that exon-definition interactions are required for the ESS1-dependent recruitment of hnRNP A1 and the U1 snRNA into the C-15 region. It is also possible that the exon-definition interactions interferes other structural rearrangement events during the progression into the B^{act}/C complex. As the structures of U2 and tri-snRNP are flexible and they undergo the extensive structural changes during the catalytic activation, it is likely that the U2 snRNP bound in the intron upstream of CD45 exon 4 is extended to interact with the tri-snRNP in the intron downstream of exon 4 to interfere their rearrangement during the progression into the B^{act}/C complex. Future work will be to determine how the exon-definition interactions in the B complex interferes the U1 snRNP binding and tri-snRNP structural changes that are required for the B^{act}/C complex formation (Figure 5.2; question marks).
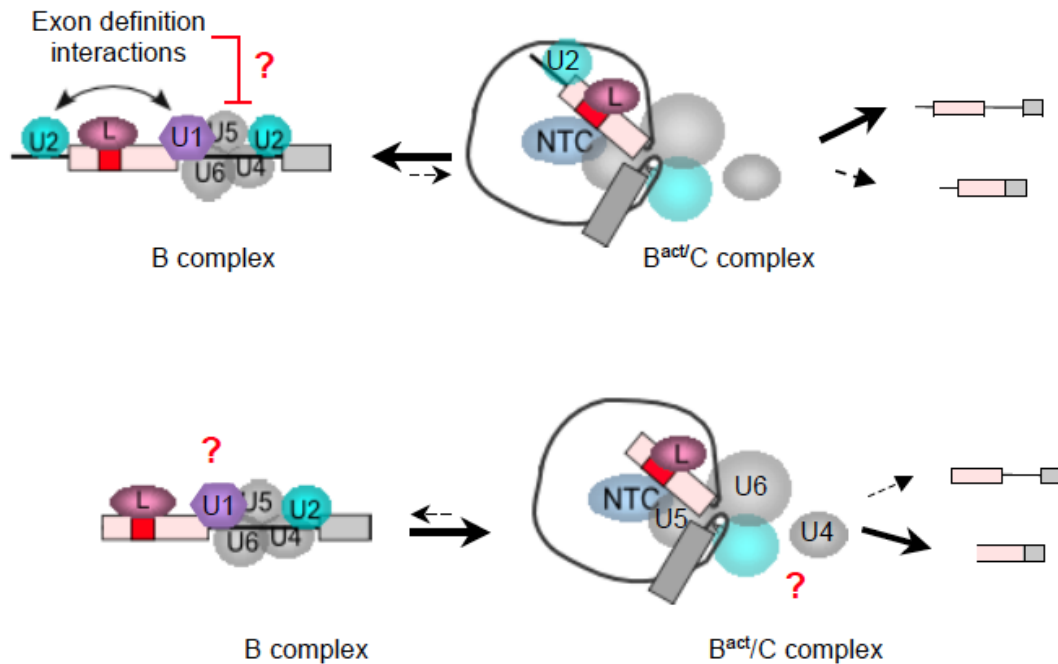
Figure 5.2 Exon-definition interactions within the repressed B complex may interfere U1 snRNP binding or rearrangements of the tri-snRNP. Exon-definition interactions formed across CD45 exon 4 are required for hnRNP L-repressed spliceosome assembly. It is unknown how exon-definition interactions function in hnRNP L-mediated repression of the B^{act}/C complex formation. It is possible that spliceosome components or interactions at the 5' splice site on the downstream intron are repressed by the U2 snRNP bound on the upstream intron.

5.2 Splicing regulators bound around the 5' ss interfere U1 snRNP binding or induce conformational change of U1 snRNP to regulate splicing

As mentioned in chapter 2, one of the novelties of my data is identification of extraneous spliceosome interaction within the exon that is involved in repressing use of the nearby 5'ss. Specifically, I showed that helix H in U1 snRNA unwinds to allow the 3' portion of helix H to basepair with the 3' end of CD45 exon 4. Additionally, this novel extraneous spliceosome interaction is extended from the 5' splice site-bound U1 snRNP

since reducing the recruitment of U1 snRNP to the 5' ss by cleaving the 5' end of the U1 snRNA abolishes the novel pairing interaction at C-15. Other studies also showed that the conformation of U1 snRNP binding at the 5' ss is altered such that the regions of the 5' ss that are protected against nucleases are changed upon repressing use of the 5' ss by splicing regulators (Sharma et al., 2011; Yu et al., 2008). Although the molecular basis and roles for such a conformational change are unknown, my findings suggest that unwinding helix H in U1 snRNA to make contacts with substrate is a possible way to change the conformation of U1 binding at the 5' ss.

The other novelty of my data is the demonstration that association of hnRNP A1 with a low-affinity binding site upstream of the 5' ss induces the extended U1 interaction. HnRNP A1 typically acts by competition with SR proteins and U1 snRNPs for binding to pre-mRNA in the presence of the high-affinity binding site (Eperon et al., 2000). Specifically, high affinity sites nucleate cooperative binding of hnRNP A1 that can displace other factors, such as the U1 snRNP, as it spreads along the RNA (Okunola and Krainer, 2009). Therefore, the low binding affinity of hnRNP A1 at the 3' end of exon 4 may allow hnRNP A1 to induce the extended conformation of U1 snRNP but limit its nucleation ability to spread along the 5'ss for displacing U1 snRNP from the 5' ss.

By contrast, TIA-1 has been shown to associate with the sequence downstream of the 5' ss to enhance U1 snRNP binding (Del Gatto-Konczak et al., 2000). Therefore, although the 5' ss is defined by the consensus sequence ranging from -3 to +6 relative to the 5' ss, the sequences flanking the -3 to +6 region of the 5'ss should also be considered when determining the usage or strength of the 5' ss.

5.3 Besides U1 snRNP, other spliceosome components that are associated with the 5'ss during catalytic activation may interfere with the use of the 5' ss for splicing

In chapter 4, I demonstrate the importance of association of hnRNP A1 and the U1 snRNA with the 3' end of exon 4 in repressing the subsequent U1/U6 switch at the 5' ss. This finding provides first example showing that a structural rearrangement during the transition into the B^{act}/C complex is a naturally occurring point for controlling alternative splicing decisions. Building the active site of the spliceosome involves a multitude of structural rearrangements, which are described in chapter 4.1. Since the ultimate goal of these rearrangements is to bring two splice sites together, the spliceosome components, such as U6 snRNA and Prp8, that are involved in these structural rearrangement events may interact with the regions around the splice site. Thus, it is possible that the sequences around the 5' ss that are involved in U6 snRNA pairing interactions or Prp8 binding are also important in determining the use of the 5' ss for splicing.

In chapter 4.4, the mutation downstream of the -3 to +6 region of the 5' ss increases the splicing of exon 4 by enhancing pairing interactions of U6 snRNA. In chapter 4.5, I showed that association of the U5 snRNP components, Prp8, could be repressed by hnRNP A1 or the U1 snRNA in the 3' end of exon 4. If the sequence downstream of the 5' ss could be mutated to enhance binding of Prp8, it would further demonstrate that even if U1 snRNP binding at the 5' ss is altered by hnRNP L and A1, enhancing the subsequent association of spliceosome components, such as U6 snRNP and Prp8, may restore the use of the 5' ss for splicing. Therefore, the binding affinity of U6 snRNP or Prp8 at the 5'ss is the other factor for considering when determining the splicing strength of a 5'ss.

5.4 Splicing regulators and spliceosome components are combined to regulate 5' ss selection

To rearrange the spliceosome structure for two transesterification steps, there are about 10 spliceosomal RNA helicases, which are involved in unwinding snRNA duplex, mediating pre-mRNA-snRNP interactions and the molecular and structural rearrangement. It has been shown that knockdown of these RNA helicases induces specific changes in the alternative splicing of some variable exons (Park et al., 2004). This suggests that modulations in the activity or concentration of RNA helicases would alter the kinetic equilibrium of one or more steps in the splicing reaction. Therefore, while most of studies focus on how the splicing regulators control alternative splicing, the intrinsic changes of the spliceosome core components could also be a critical point to be considered.

The skipping of CD45 exon 4 in the activated T-cells is also likely a good model to address the function of the phosphorylation of Prp28 in inducing the skipping of CD45 exon 4 (Lynch and Weiss, 2000; Rothrock et al., 2003). Although it has been shown that PSF and hnRNP L-like are recruited to CD45 exon 4 to induce its skipping in response to T-cell receptor signaling pathway (Melton et al., 2007; Oberdoerffer et al., 2008), the post-translation modification of spliceosome core components in activated T-cells could also play a role in the skipping of exon 4. A recent study showed that the activity of Prp28 can be regulated by SRPK2 phosphorylation (Mathew et al., 2008). Phosphorylation of Prp28 is required for integration of the tri-snRNP into the spliceosome. This indicates that the phosphorylation of prp28 could antagonize the effect of the repressed U6 binding at the 5' ss induced by hnRNP L. Future work will be to determine whether Prp28 associates differently with the tri-snRNP in the resting and

stimulated JSL1 nuclear extract. These studies will further demonstrate how spliceosome components and splicing regulators could be combined to regulate alternative splicing in response to the signaling transduction pathways.

5.5 Implications for predicting of 5' ss selection in alternative splicing

The canonical way to determine the strength of the 5' splice site is based on the pairing of the 5' end of U1 snRNA and the -3 to +6 region of the 5' splice site. However, the U1 snRNP extends its interactions with the pre-mRNA such that ~20 nt on either side of the 5' ss are protected against nucleases (Chabot and Steitz, 1987). Thus, the splicing regulators that associate with the regions ~20 nt on either side of the 5' ss could interfere U1 snRNP binding and should be considered an important factor for determining the use of the 5' ss for splicing. For example, when the sequence upstream of the 5' ss contains the AGU motif, it could be associated with hnRNP A1 and thus the use of the 5' ss could be reduced (Chiou et al., 2013). By contrast, when a 5'ss contains a U-rich tract that begins 5-9 nt downstream, the use of the 5' ss for splicing could be enhanced by TIA-1 (Del Gatto-Konczak et al., 2000). Moreover, when the sequence downstream of the +6 position of the 5' ss is complementary to the U6 snRNA, it probably enhances the strength of the 5'ss (Chiou et al., 2013). Investigations on the sequence specificity of other splicing regulators and spliceosome components on association with the regions around the 5' ss will bring further insights for determining the splicing patterns.

5.5 Conclusions

In conclusion, I set up a series of biochemical assays to show that hnRNP A1 and the U1 snRNA can cooperatively interact with the 3' end of CD45 exon 4 in a ESS1/hnRNP L-dependent manner, which represses the subsequent catalytic activation of the spliceosome. These biochemical approaches provides the framework to demonstrate the function of splicing regulators, spliceosome components and exon-defintion interactions in mediating splicing regulation, particularly the 5' ss selection. Future characterization of ESS1-repressed exon-defined complex, the U1-5'ss complex containing various sequences surrounding the 5'ss and complexes assembled in the stimulated JSL1 nuclear extract will provide insight into both the 5' ss selection for splicing and CD45 splicing regulation in response to TCR-signaling.

Chapter 6

Materials and Methods

6.1 Plasmids and RNA substrates

The DNA fragment containing CD45 exon 4 with either wild-type ESS1 or mutated ESS1 and its flanking introns was inserted into the upstream region of the AdML PPT and exon in pAdML (Rothrock et al., 2005). The pAdML was a kind gift from K.J. Hertel and the RNA generated from pAdML was described previously (Anderson and Moore, 1997; Hertel and Maniatis, 1999). To allow the splicing complexes assembled on the RNA substrates to be purified, three MS2 binding site was inserted to the 3' end of the 3' AdML exon.

The template for in vitro transcription was generated from the plasmid described above by PCR. The RNA was synthesized by T7 polymerase. The resultant RNA substrate contains a 150 nucleotide (nt) 5' intron, a 197 nt 5' exon 4, a 260 nt 3' intron and a 56 nt 3' AdML exon followed by a 120 nt MS2 binding site. The 60 nt ESS1 sequence is located at -110 to -170 of exon 4 (Figure 2.4A). PCR mutagenesis was used to introduce mutations into the -6 to -24 region of exon 4 to generate template for in vitro transcription of the substrates containing R, Q, A and U mutation. The sequences of Q, A and U mutation are shown in Figure 2.7A.

6.2 *In vitro* splicing and spliceosome assembly

Repressed (R), derepressed (D) RNA and the RNA substrates containing various mutations (Q, A and U) at the 3' end of exon 4 were transcribed from the PCR products

that contain a T7 promoter sequence (Figure 3.2). The downsteam AdML exon contains a stronger AdML polyprimidine tract, which enhances the formation of the splicing complexes on the RNA substrates. The 3' end of the RNA contains the three copies of MS2 hairpin sequence, which can be bound by MS2MBP fusion protein and functions as a tag for the splicing complex isolation.

In vitro splicing reactions and spliceosome assembly were carried out as described previously (House and Lynch, 2006),with some modifications as described in 6.2.1 and 6.2.2 For spliceosome assembly, the splicing reactions or the individual fractions from the gradient-fractionated splicing reaction were separated and visualized using native polyacrylamide gel in the presence or absence of heparin, as indicated in the figure.

6.2.1 *In vitro* splicing assays

Unlabeled RNA substrates (10 nM) were incubated with 60% JSL1 nuclear extract in a total volume of 12.5 μl under splicing condition, which contains (final concentration): 12 mM Tris-HCl, pH7.5, 3.2 mM $MgCl_2$, 4 mM ATP, 20 mM CP, 0.5 mM DTT, 0.125U RNasin (Promega), 60 mM KCl, 0.1 mM EDTA, and 12% glycerol. Reactions were incubated for 90 min at 30°C; then the RNA was recovered from the reactions by protease K treatment, phenol-chloroform extraction and EtOH precipitation. The recovered RNA was analyzed by RT-PCR as described previously (Rothrock et al., 2005). The primers for analyzing the repressed and derepressed substrates were within 5' intron and 3' exon.

6.2.2 Spliceosome assembly assays

12.5 μl splicing reactions containing uniformly ^{32}P-labeded RNA were incubated for 60 min and then treated with 1μl heparin (50μg/μl) to allow the complexes formed in the splicing reactions to be separated by the native gel. The 4% native polyacrylamide gel (Acrylamide/Bisacrylamide ratio of 80:1) was made and run in 25 mM Trsi-glyciune buffer at 250 V for 4 hour at room temperature. The gels were dried under vaccum and visualized by phoaphorimager.

For analyzing splicing complexes in gradient fractions, addition of heparin into fractions was not required for the complexes to be separated in a native but it affects the B and C complex assembly in a native gel. Of 215 μl gradient fraction, 10 μl was directly loaded into the native polyacrylamide gel or treated with 1μl heparin (5μg/μl) and then loaded into the gel.

6.3 Oligonucleotide-directed RNase H cleavage

To cleave the snRNA by the endogenous RNase H in JSL1 nuclear extract, 60% nuclear extract was incubated for 30 min at 30°C under splicing condition in the presence or absence of 8 μM oligonucleotide complementary to the target snRNA. The sequence of the oligonucleotides was described previously (House and Lynch, 2006). The RNA substrates were then added into the snRNA-inactivated nuclear extract under splicing condition, which then proceeded into spliceosome assembly or UV crosslinking assays.

For cleavage of U6 snRNA of the complexes purified from the spliceosome assembly reactions, the MS2MBP-affinity selected complexes were incubated for 5 min on ice in the presence of U6f oligonucleotide with the concentrations as indicated in

Figure 4.11 (Konforti and Konarska, 1994). The amount of the cleavage was determined by primer extension.

6.4 Gradient separation of splicing reactions and MSMBP affinity purification of splicing complexes

Standard splicing reactions containing the RNA substrate pre-bound by 10-fold excess of MS2-MBP fusion protein were incubated for 90 min at 30°C to allow the accumulation of the B and C complex. 250 μl splicing reaction was layered on a 15-35% (v/v) glycerol gradient containing buffer GS (20 mM Tris-HCl, pH 7.5, 100 mM NaCl, 4 mM $MgCl_2$ and 1 mM DTT). The gradients were centrifuged at 45000 rpm for 3 hours at 4°C in a SW50.1 rotor and then harvested manually in a 215-μl fractions from top into 21 aliquots. The splicing complexes in fractions were analyzed by native gel as described above. The early (E), middle (M), and late (L) fractions, which contain similar complexes, were pooled and passed once through a column containing 250 μl amylose beads (NEB) pre-equilibrate with buffer GSG (buffer GS containing 10% glycerol). The column was washed twice with 1 ml buffer GSG. Bound complexes were eluted three times with 125 μl elution buffer (buffer GSG containing 30 mM Maltose). The combined second and third elution contains approximately 0.1 pmole complexes, which is 10% of the input transcript in the L or M fractions. Because the substrate levels of the E fractions from the typical splicing reactions were much less, the E fractions from gradient separation of the ATP-depleted splicing reactions were pooled for the complex purification, which was used for the following western blot analysis.

6.5 Isolation and analysis of splicing complexes

The early (E), middle (M), and late (L) fractions were separated from the standard splicing reactions (Figure 1C). They were pooled for the following MS2MBP-affinity purification of splicing complexes as previously described (Schneider et al., 2010b; Sharma et al., 2005), with some modification as described in supplementary data.

The RNA recovered from the purified complexes was separated on 8% urea-PAGE gel followed by either silver-staining (Bio-rad) or exposure to phosphorimager to determine the levels of snRNAs or the ^{32}P-labeled splicing precursor, intermediates and product. The proteins from ~0.02 pmole of purified complexes were separated by SDS-PAGE and analyzed by western blot. The antibodies aganist hnRNP L, hnRNP A1, Prp19, CDC5L, SAP130, and Prp22, were all from Abcam; PLRG and SPF27 antibody were from bethyl laboratories; U2AF65 and MBP antibody were from Sigma.

6.6 Psoralen crosslinking

Pooled middle (M) fractions or the splicing reactions incubated for 30 min at 30°C were placed on ice. AMT-poralen was added to a final concentration of 24 μg/μl and the reactions were irradiated with 365 nm light for 10 min on ice (Sharma et al., 2005). The RNA-RNA cross-links were mapped by primer extension using the primer that was complementary to nucleotide 56-76 of the downstream intron.

6.7 UV crosslinking of complexes assembled on site-specifically labeled RNA substrate

Synthesis of RNA substrates containing a single ^{32}P-label was performed as described (Sharma et al., 2011). The standard splicing reactions containing the site-specific labeled RNA (5000 cpm) incubated for 30 min at 30°C were placed on ice, irradiated with 254 nm light for 20 min on ice and digested with RNase A and T1 for 20 min at 37°C. The crosslinked splicing reactions were separated by SDS-PAGA and analyzed by phosphorimager. The identities of the crosslinked proteins were determined by immuno-precipitaion of crosslinked splicing reactions (Rothrock et al., 2005).

6.8 SHAPE analysis of the purified U1-5'ss complex

The 5' ss RNA fragment containing the region ranging from -45 to +76 relative to 5' ss on the CD45 exon 4 is transcribed *in vitro*. The 5' ss RNA fragment was incubated with nuclear extract under the conditions as described in Chapter 6.2. 250μl of the assembled reactions was used for the MS2MBP-affinity selection. 30 μl of the purified complexes was incubated with BzCN to reach the concentrations as shown in Figure 2.9C at room temperature (Konforti and Konarska, 1994). The regions of U1 snRNA that react with BzCN were determined by primer extension. The sequence of the primer for primer extension was described previously (House and Lynch, 2006).

References

Abad, X., Vera, M., Jung, S. P., Oswald, E., Romero, I., Amin, V., Fortes, P., and Gunderson, S. I. (2008). Requirements for gene silencing mediated by U1 snRNA binding to a target sequence. Nucleic Acids Res *36*, 2338-2352.

Anderson, K., and Moore, M. J. (1997). Bimolecular exon ligation by the human spliceosome. Science *276*, 1712-1716.

Behzadnia, N., Golas, M. M., Hartmuth, K., Sander, B., Kastner, B., Deckert, J., Dube, P., Will, C. L., Urlaub, H., Stark, H., and Luhrmann, R. (2007). Composition and three-dimensional EM structure of double affinity-purified, human prespliceosomal A complexes. EMBO J *26*, 1737-1748.

Bessonov, S., Anokhina, M., Krasauskas, A., Golas, M. M., Sander, B., Will, C. L., Urlaub, H., Stark, H., and Luhrmann, R. (2010). Characterization of purified human Bact spliceosomal complexes reveals compositional and morphological changes during spliceosome activation and first step catalysis. RNA *16*, 2384-2403.

Black, D. L. (2003). Mechanisms of alternative pre-messenger RNA splicing. Annu Rev Biochem *72*, 291-336.

Bonnal, S., Martinez, C., Forch, P., Bachi, A., Wilm, M., and Valcarcel, J. (2008). RBM5/Luca-15/H37 regulates Fas alternative splice site pairing after exon definition. Mol Cell *32*, 81-95.

Burd, C. G., and Dreyfuss, G. (1994). RNA binding specificity of hnRNP A1: significance of hnRNP A1 high-affinity binding sites in pre-mRNA splicing. EMBO J *13*, 1197-1204.

Chabot, B., and Steitz, J. A. (1987). Multiple interactions between the splicing substrate and small nuclear ribonucleoproteins in spliceosomes. Mol Cell Biol *7*, 281-293.

Chan, S. P., and Cheng, S. C. (2005). The Prp19-associated complex is required for specifying interactions of U5 and U6 with pre-mRNA during spliceosome activation. J Biol Chem *280*, 31190-31199.

Chen, J. Y., Stands, L., Staley, J. P., Jackups, R. R., Jr., Latus, L. J., and Chang, T. H. (2001). Specific alterations of U1-C protein or U1 small nuclear RNA can eliminate the requirement of Prp28p, an essential DEAD box splicing factor. Mol Cell *7*, 227-232.

Chiou, N. T., Shankarling, G., and Lynch, K. W. (2013). hnRNP L and hnRNP A1 induce extended U1 snRNA interactions with an exon to repress spliceosome assembly. Mol Cell *49*, 972-982.

Consortium, I. H. G. S. (2004). Finishing the euchromatic sequence of the human genome. Nature *431*, 931-945.

Cooper, T. A., Wan, L., and Dreyfuss, G. (2009). RNA and disease. Cell *136*, 777-793.

David, C. J., and Manley, J. L. (2010). Alternative pre-mRNA splicing regulation in cancer: pathways and programs unhinged. Genes Dev *24*, 2343-2364.

Dawes, R., Hennig, B., Irving, W., Petrova, S., Boxall, S., Ward, V., Wallace, D., Macallan, D. C., Thursz, M., Hill, A.*, et al.* (2006). Altered CD45 expression in C77G carriers influences immune function and outcome of hepatitis C infection. J Med Genet *43*, 678-684.

Deckert, J., Hartmuth, K., Boehringer, D., Behzadnia, N., Will, C. L., Kastner, B., Stark, H., Urlaub, H., and Luhrmann, R. (2006). Protein composition and electron microscopy

structure of affinity-purified human spliceosomal B complexes isolated under physiological conditions. Mol Cell Biol *26*, 5528-5543.

Del Gatto-Konczak, F., Bourgeois, C. F., Le Guiner, C., Kister, L., Gesnel, M. C., Stevenin, J., and Breathnach, R. (2000). The RNA-binding protein TIA-1 is a novel mammalian splicing regulator acting through intron sequences adjacent to a 5' splice site. Mol Cell Biol *20*, 6287-6299.

Eperon, I. C., Makarova, O. V., Mayeda, A., Munroe, S. H., Caceres, J. F., Hayward, D. G., and Krainer, A. R. (2000). Selection of alternative 5' splice sites: role of U1 snRNP and models for the antagonistic effects of SF2/ASF and hnRNP A1. Mol Cell Biol *20*, 8303-8318.

Grainger, R. J., and Beggs, J. D. (2005). Prp8 protein: at the heart of the spliceosome. RNA *11*, 533-557.

Grohman, J. K., Gorelick, R. J., Lickwar, C. R., Lieb, J. D., Bower, B. D., Znosko, B. M., and Weeks, K. M. (2013). A guanosine-centric mechanism for RNA chaperone function. Science *340*, 190-195.

Grote, M., Wolf, E., Will, C. L., Lemm, I., Agafonov, D. E., Schomburg, A., Fischle, W., Urlaub, H., and Luhrmann, R. (2010). Molecular architecture of the human Prp19/CDC5L complex. Mol Cell Biol *30*, 2105-2119.

Guthrie, C., and Patterson, B. (1988). Spliceosomal snRNAs. Annu Rev Genet *22*, 387-419.

Hartmuth, K., Vornlocher, H. P., and Luhrmann, R. (2004). Tobramycin affinity tag purification of spliceosomes. Methods Mol Biol *257*, 47-64.

Hermiston, M. L., Xu, Z., Majeti, R., and Weiss, A. (2002). Reciprocal regulation of lymphocyte activation by tyrosine kinases and phosphatases. J Clin Invest *109*, 9-14.

Hertel, K. J., and Maniatis, T. (1999). Serine-arginine (SR)-rich splicing factors have an exon-independent function in pre-mRNA splicing. Proc Natl Acad Sci U S A *96*, 2651-2655.

Heyd, F., and Lynch, K. W. (2010). Phosphorylation-dependent regulation of PSF by GSK3 controls CD45 alternative splicing. Mol Cell *40*, 126-137.

Hoffman, B. E., and Grabowski, P. J. (1992). U1 snRNP targets an essential splicing factor, U2AF65, to the 3' splice site by a network of interactions spanning the exon. Genes Dev *6*, 2554-2568.

House, A. E., and Lynch, K. W. (2006). An exonic splicing silencer represses spliceosome assembly after ATP-dependent exon recognition. Nat Struct Mol Biol *13*, 937-944.

House, A. E., and Lynch, K. W. (2008). Regulation of alternative splicing: more than just the ABCs. J Biol Chem *283*, 1217-1221.

Huelga, S. C., Vu, A. Q., Arnold, J. D., Liang, T. Y., Liu, P. P., Yan, B. Y., Donohue, J. P., Shiue, L., Hoon, S., Brenner, S.*, et al.* (2012). Integrative genome-wide analysis reveals cooperative regulation of alternative splicing by hnRNP proteins. Cell Rep *1*, 167-178.

Hui, J., Hung, L. H., Heiner, M., Schreiner, S., Neumuller, N., Reither, G., Haas, S. A., and Bindereif, A. (2005). Intronic CA-repeat and CA-rich elements: a new class of regulators of mammalian alternative splicing. EMBO J *24*, 1988-1998.

Jurica, M. S., Licklider, L. J., Gygi, S. R., Grigorieff, N., and Moore, M. J. (2002). Purification and characterization of native spliceosomes suitable for three-dimensional structural analysis. RNA *8*, 426-439.

Jurica, M. S., and Moore, M. J. (2003). Pre-mRNA splicing: awash in a sea of proteins. Mol Cell *12*, 5-14.

Kaida, D., Berg, M. G., Younis, I., Kasim, M., Singh, L. N., Wan, L., and Dreyfuss, G. (2010). U1 snRNP protects pre-mRNAs from premature cleavage and polyadenylation. Nature *468*, 664-668.

Konarska, M. M., Vilardell, J., and Query, C. C. (2006). Repositioning of the reaction intermediate within the catalytic center of the spliceosome. Mol Cell *21*, 543-553.

Konforti, B. B., and Konarska, M. M. (1994). U4/U5/U6 snRNP recognizes the 5' splice site in the absence of U2 snRNP. Genes Dev *8*, 1962-1973.

Kumar, A., and Wilson, S. H. (1990). Studies of the strand-annealing activity of mammalian hnRNP complex protein A1. Biochemistry *29*, 10717-10722.

Labourier, E., Adams, M. D., and Rio, D. C. (2001). Modulation of P-element pre-mRNA splicing by a direct interaction between PSI and U1 snRNP 70K protein. Mol Cell *8*, 363-373.

Lynch, K. W. (2004). Consequences of regulated pre-mRNA splicing in the immune system. Nat Rev Immunol *4*, 931-940.

Lynch, K. W., and Weiss, A. (2000). A model system for activation-induced alternative splicing of CD45 pre-mRNA in T cells implicates protein kinase C and Ras. Mol Cell Biol *20*, 70-80.

Lynch, K. W., and Weiss, A. (2001). A CD45 polymorphism associated with multiple sclerosis disrupts an exonic splicing silencer. J Biol Chem *276*, 24341-24347.

Madhani, H. D., and Guthrie, C. (1992). A novel base-pairing interaction between U2 and U6 snRNAs suggests a mechanism for the catalytic activation of the spliceosome. Cell *71*, 803-817.

Makarova, O. V., Makarov, E. M., Urlaub, H., Will, C. L., Gentzel, M., Wilm, M., and Luhrmann, R. (2004). A subset of human 35S U5 proteins, including Prp19, function prior to catalytic step 1 of splicing. EMBO J *23*, 2381-2391.

Martinez, N. M., Pan, Q., Cole, B. S., Yarosh, C. A., Babcock, G. A., Heyd, F., Zhu, W., Ajith, S., Blencowe, B. J., and Lynch, K. W. (2012). Alternative splicing networks regulated by signaling in human T cells. RNA *18*, 1029-1040.

Mathew, R., Hartmuth, K., Mohlmann, S., Urlaub, H., Ficner, R., and Luhrmann, R. (2008). Phosphorylation of human PRP28 by SRPK2 is required for integration of the U4/U6-U5 tri-snRNP into the spliceosome. Nat Struct Mol Biol *15*, 435-443.

Matlin, A. J., Clark, F., and Smith, C. W. (2005). Understanding alternative splicing: towards a cellular code. Nat Rev Mol Cell Biol *6*, 386-398.

Melton, A. A., Jackson, J., Wang, J., and Lynch, K. W. (2007). Combinatorial control of signal-induced exon repression by hnRNP L and PSF. Mol Cell Biol *27*, 6972-6984.

Mortimer, S. A., and Weeks, K. M. (2009). Time-resolved RNA SHAPE chemistry: quantitative RNA structure analysis in one-second snapshots and at single-nucleotide resolution. Nat Protoc *4*, 1413-1421.

Mozaffari-Jovin, S., Santos, K. F., Hsiao, H. H., Will, C. L., Urlaub, H., Wahl, M. C., and Luhrmann, R. (2012). The Prp8 RNase H-like domain inhibits Brr2-mediated U4/U6

snRNA unwinding by blocking Brr2 loading onto the U4 snRNA. Genes Dev *26*, 2422-2434.

Oberdoerffer, S., Moita, L. F., Neems, D., Freitas, R. P., Hacohen, N., and Rao, A. (2008). Regulation of CD45 alternative splicing by heterogeneous ribonucleoprotein, hnRNPLL. Science *321*, 686-691.

Okunola, H. L., and Krainer, A. R. (2009). Cooperative-binding and splicing-repressive properties of hnRNP A1. Mol Cell Biol *29*, 5620-5631.

Pan, Q., Shai, O., Lee, L. J., Frey, B. J., and Blencowe, B. J. (2008). Deep surveying of alternative splicing complexity in the human transcriptome by high-throughput sequencing. Nat Genet *40*, 1413-1415.

Park, J. W., Parisky, K., Celotto, A. M., Reenan, R. A., and Graveley, B. R. (2004). Identification of alternative splicing regulators by RNA interference in Drosophila. Proc Natl Acad Sci U S A *101*, 15974-15979.

Pomeranz Krummel, D. A., Oubridge, C., Leung, A. K., Li, J., and Nagai, K. (2009). Crystal structure of human spliceosomal U1 snRNP at 5.5 A resolution. Nature *458*, 475-480.

Pontius, B. W., and Berg, P. (1990). Renaturation of complementary DNA strands mediated by purified mammalian heterogeneous nuclear ribonucleoprotein A1 protein: implications for a mechanism for rapid molecular assembly. Proc Natl Acad Sci U S A *87*, 8403-8407.

Query, C. C., and Konarska, M. M. (2013). Structural biology: Spliceosome's core exposed. Nature *493*, 615-616.

Reed, R. (2000). Mechanisms of fidelity in pre-mRNA splicing. Curr Opin Cell Biol *12*, 340-345.

Roca, X., and Krainer, A. R. (2009). Recognition of atypical 5' splice sites by shifted base-pairing to U1 snRNA. Nat Struct Mol Biol *16*, 176-182.

Roca, X., Krainer, A. R., and Eperon, I. C. (2013). Pick one, but be quick: 5' splice sites and the problems of too many choices. Genes Dev *27*, 129-144.

Rothrock, C., Cannon, B., Hahm, B., and Lynch, K. W. (2003). A conserved signal-responsive sequence mediates activation-induced alternative splicing of CD45. Mol Cell *12*, 1317-1324.

Rothrock, C. R., House, A. E., and Lynch, K. W. (2005). HnRNP L represses exon splicing via a regulated exonic splicing silencer. EMBO J *24*, 2792-2802.

Roybal, G. A., and Jurica, M. S. (2010). Spliceostatin A inhibits spliceosome assembly subsequent to prespliceosome formation. Nucleic Acids Res *38*, 6664-6672.

Ruby, S. W., and Abelson, J. (1988). An early hierarchic role of U1 small nuclear ribonucleoprotein in spliceosome assembly. Science *242*, 1028-1035.

Schneider, M., Hsiao, H. H., Will, C. L., Giet, R., Urlaub, H., and Luhrmann, R. (2010a). Human PRP4 kinase is required for stable tri-snRNP association during spliceosomal B complex formation. Nat Struct Mol Biol *17*, 216-221.

Schneider, M., Will, C. L., Anokhina, M., Tazi, J., Urlaub, H., and Luhrmann, R. (2010b). Exon definition complexes contain the tri-snRNP and can be directly converted into B-like precatalytic splicing complexes. Mol Cell *38*, 223-235.

Sharma, S., Falick, A. M., and Black, D. L. (2005). Polypyrimidine tract binding protein blocks the 5' splice site-dependent assembly of U2AF and the prespliceosomal E complex. Mol Cell *19*, 485-496.

Sharma, S., Kohlstaedt, L. A., Damianov, A., Rio, D. C., and Black, D. L. (2008). Polypyrimidine tract binding protein controls the transition from exon definition to an intron defined spliceosome. Nat Struct Mol Biol *15*, 183-191.

Sharma, S., Maris, C., Allain, F. H., and Black, D. L. (2011). U1 snRNA directly interacts with polypyrimidine tract-binding protein during splicing repression. Mol Cell *41*, 579-588.

Siebel, C. W., Fresco, L. D., and Rio, D. C. (1992). The mechanism of somatic inhibition of Drosophila P-element pre-mRNA splicing: multiprotein complexes at an exon pseudo-5' splice site control U1 snRNP binding. Genes Dev *6*, 1386-1401.

Siebel, C. W., Kanaar, R., and Rio, D. C. (1994). Regulation of tissue-specific P-element pre-mRNA splicing requires the RNA-binding protein PSI. Genes Dev *8*, 1713-1725.

Smith, D. J., Query, C. C., and Konarska, M. M. (2008). "Nought may endure but mutability": spliceosome dynamics and the regulation of splicing. Mol Cell *30*, 657-666.

Staley, J. P., and Guthrie, C. (1998). Mechanical devices of the spliceosome: motors, clocks, springs, and things. Cell *92*, 315-326.

Staley, J. P., and Guthrie, C. (1999). An RNA switch at the 5' splice site requires ATP and the DEAD box protein Prp28p. Mol Cell *3*, 55-64.

Tackenberg, B., Nitschke, M., Willcox, N., Ziegler, A., Nessler, S., Schumm, F., Oertel, W. H., Hemmer, B., and Sommer, N. (2003). CD45 isoform expression in autoimmune myasthenia gravis. Autoimmunity *36*, 117-121.

Tong, A., Nguyen, J., and Lynch, K. W. (2005). Differential expression of CD45 isoforms is controlled by the combined activity of basal and inducible splicing-regulatory elements in each of the variable exons. J Biol Chem *280*, 38297-38304.

Topp, J. D., Jackson, J., Melton, A. A., and Lynch, K. W. (2008). A cell-based screen for splicing regulators identifies hnRNP LL as a distinct signal-induced repressor of CD45 variable exon 4. RNA *14*, 2038-2049.

Tseng, C. K., and Cheng, S. C. (2008). Both catalytic steps of nuclear pre-mRNA splicing are reversible. Science *320*, 1782-1784.

van der Feltz, C., Anthony, K., Brilot, A., and Pomeranz Krummel, D. A. (2012). Architecture of the spliceosome. Biochemistry *51*, 3321-3333.

Villa, T., Pleiss, J. A., and Guthrie, C. (2002). Spliceosomal snRNAs: Mg(2+)-dependent chemistry at the catalytic core? Cell *109*, 149-152.

Wahl, M. C., Will, C. L., and Luhrmann, R. (2009). The spliceosome: design principles of a dynamic RNP machine. Cell *136*, 701-718.

Wang, E. T., Sandberg, R., Luo, S., Khrebtukova, I., Zhang, L., Mayr, C., Kingsmore, S. F., Schroth, G. P., and Burge, C. B. (2008). Alternative isoform regulation in human tissue transcriptomes. Nature *456*, 470-476.

Wang, G. S., and Cooper, T. A. (2007). Splicing in disease: disruption of the splicing code and the decoding machinery. Nat Rev Genet *8*, 749-761.

Warkocki, Z., Odenwalder, P., Schmitzova, J., Platzmann, F., Stark, H., Urlaub, H., Ficner, R., Fabrizio, P., and Luhrmann, R. (2009). Reconstitution of both steps of Saccharomyces cerevisiae splicing with purified spliceosomal components. Nat Struct Mol Biol *16*, 1237-1243.

Xu, Z., and Weiss, A. (2002). Negative regulation of CD45 by differential homodimerization of the alternatively spliced isoforms. Nat Immunol *3*, 764-771.

Yu, Y., Maroney, P. A., Denker, J. A., Zhang, X. H., Dybkov, O., Luhrmann, R., Jankowsky, E., Chasin, L. A., and Nilsen, T. W. (2008). Dynamic regulation of alternative splicing by silencers that modulate 5' splice site competition. Cell *135*, 1224-1236.

Zahler, A. M., Damgaard, C. K., Kjems, J., and Caputi, M. (2004). SC35 and heterogeneous nuclear ribonucleoprotein A/B proteins bind to a juxtaposed exonic splicing enhancer/exonic splicing silencer element to regulate HIV-1 tat exon 2 splicing. J Biol Chem *279*, 10077-10084.

Zhou, Z., Licklider, L. J., Gygi, S. P., and Reed, R. (2002). Comprehensive proteomic analysis of the human spliceosome. Nature *419*, 182-185.

Zhuang, Y., and Weiner, A. M. (1986). A compensatory base change in U1 snRNA suppresses a 5' splice site mutation. Cell *46*, 827-835.